CENTRO DE CIENCIAS BÁSICAS

DEPARTAMENTO DE MATEMÁTICAS Y FÍSICA

TESIS

NUMERICAL METHODS TO APPROXIMATE TRAVELING WAVE SOLUTIONS OF NONLINEAR ADVECTION-DIFFUSION-REACTION EQUATIONS — SEMILINEAR DISCRETIZATIONS

PRESENTA

Javier Ruiz Ramírez

PARA OBTENER EL GRADO DE MAESTRO EN CIENCIAS

TUTOR

Dr. Jorge Eduardo Macías Díaz

COMITÉ TUTORAL

Dr. José Villa Morales
Dr. Hugo Rodríguez Ordóñez

Aguascalientes, Ags, 16 de Agosto de 2013

UNIVERSIDAD AUTONOMA DE AGUASCALIENTES
Centro de Ciencias Básicas

ANIVERSARIO UAA

I.B.Q. JAVIER RUIZ RAMÍREZ,
ALUMNO (A) DE LA MAESTRÍA EN CIENCIAS CON OPCIÓN A LA COMPUTACIÓN, MATEMÁTICAS APLICADAS,
P R E S E N T E .

Estimado (a) alumno (a) Ruiz:

Por medio de este conducto me permito comunicar a Usted que habiendo recibido el voto aprobatorio de su tutor de tesis titulada: "Numerical methods to aprproximate traveling-wave solutions of nonlinear advection-diffusion-reaction equations—Semilinear discretizations", hago de su conocimiento que puede imprimir dicho documento y continuar con los trámites para la presentación de su examen de grado.

Sin otro particular me permito saludarle muy afectuosamente.

A T E N T A M E N T E
Aguascalientes, Ags., 2 de agosto de 2013
"SE LUMEN PROFERRE"
EL DECANO SUSTITUTO

M. en C. JOSÉ DE JESÚS RUIZ GALLEGOS

Universidad Autonoma de Aguascalientes
CENTRO DE CIENCIAS BÁSICAS

c.c.p.- Archivo
JJRG,mjda

UNIVERSIDAD AUTONOMA DE AGUASCALIENTES

FORMATO DE CARTA DE VOTO APROBATORIO

M. en C. José de Jesús Ruiz Gallegos
DECANO DEL CENTRO DE CIENCIAS BÁSICAS
PRESENTE

Por medio de la presente, en mi calidad de tutor designado del estudiante **Javier Ruiz Ramírez** con ID 98347 quien realizó la tesis titulada: **Numerical methods to approximate traveling-wave solutions of nonlinear advection-diffusion-reaction equations — Semilinear discretizations**, y con fundamento en el Artículo 175, Apartado II del Reglamento General de Docencia, me permito emitir el **VOTO APROBATORIO**, para que él pueda proceder a imprimirla, y así continuar con el procedimiento administrativo para la obtención del grado.

Pongo lo anterior a su digna consideración y, sin otro particular por el momento, me permito enviarle un cordial saludo.

ATENTAMENTE
"Se Lumen Proferre"
Aguascalientes, Ags., a 2 de Agosto de 2013

Dr. Jorge Eduardo Macías Díaz

c.c.p.- Interesado
c.c.p.- Secretaría de Investigación y Posgrado
c.c.p.- Jefatura del Depto. de Matemáticas y Física
c.c.p.- Consejero Académico
c.c.p.- Minuta Secretario Técnico

Acknowledgments

First, I would like to thank my advisor Dr. Jorge Eduardo Macías Díaz. It has been a privilege to be one of his students. The quality of his research, the love for his family and his passion for music are just examples of the great person he is. Without his guidance, I have no doubt this work would have never been completed.

I am also grateful to the Universidad Autónoma de Aguascalientes and CONACYT for their financial support which allowed me to pursue this Masters degree.

For this dissertation I would like to thank the reading committee members: Dr. Hugo Rodríguez Ordóñez and Dr. José Villa Morales for their time and valuable comments.

Finally, I want to acknowledge my parents, who through great sacrifice have provided me the means to continue my education in an uninterrupted way.

Contents

List of Tables

List of Figures

Resumen

En el presente trabajo, se proponen métodos numéricos para aproximar las soluciones de formas generalizadas de dos modelos multidimensionales famosos de la física matemática, a saber, la ecuación de Fisher y la ecuación de Huxley. Los modelos que se investigan en este trabajo son ecuaciones con difusión que consideran la inclusión de varios términos genéricos, como coeficientes variables de advección/convección, reacción y amortiguamiento alineales. Así, por ejemplo, las leyes de reacción son generalizaciones o extensiones de los términos correspondientes en la ecuación clásica de dinámica poblacional de Fisher, mientras que los factores generalizados de advección/convección son extensiones de los términos de advección/convección de la famosa ecuación de Burgers. Por su parte, los modelos con amortiguamiento alineal aparecen como generalizaciones de las ecuaciones de Fisher y de Huxley al caso hiperbólico

En el caso unidimensional, la literatura especializada en el área reporta la existencia de soluciones analíticas para la mayoría de dichos modelos, en la forma de soluciones de onda viajera acotadas dentro de un intervalo I del conjunto de los números reales. Con esta motivación, se propone una metodología en diferencias finitas que garantiza que, bajo ciertas condiciones analíticas sobre los parámetros del modelo y las constantes computacionales, aproximaciones iniciales que se encuentran acotadas en I, producen nuevas aproximaciones que están también acotadas dentro de I. La conservación de las propiedades de positividad y acotación de las soluciones aproximadas se demuestra usando la teoría de M-matrices, las cuales son matrices cuadradas, reales, no singulares, en las que todas las entradas de sus matrices inversas son números reales positivos. Además, se demuestra la propiedad de conservación de la antisimetría en los modelos computacionales propuestos. La implementación computacional de nuestras técnicas confirma numéricamente que las propiedades de positividad y acotación son conservadas bajo las restricciones analíticas derivadas en la teoría. Las técnicas propuestas son métodos de dos pasos (tres pasos en el escenario hiperbólico), consistentes de primer orden en el tiempo, y de segundo orden en el espacio. En la práctica, las simulaciones muestran buenas aproximaciones a las soluciones analíticas empleadas en el presente trabajo.

Abstract

In this work, we propose numerical methods to approximate the solutions of generalized forms of two famous, multi-dimensional models of mathematical physics, namely, Fisher's and Huxley's equations. The diffusive models investigated in this thesis consider the inclusion of several, generalized terms, like nonlinear advection/convection, nonlinear reaction, and nonlinear damping. The reaction laws considered are generalizations or extensions of the corresponding term in the classical Fisher's equation from population dynamics, while the generalized advection/convection factors are extended forms of the corresponding advection/convection term in the famous Burgers equation. Meanwhile, the models with nonlinear damping appear as generalizations of Fisher's and Huxley's equation to the hyperbolic case.

In the one-dimensional scenario, the specialized literature in the area gives account of the existence of analytical solutions for most of these models, in the form of traveling-wave fronts bounded within an interval I of the real numbers. Motivated by this fact, we propose a finite-difference methodology that guarantees that, under certain analytical conditions on the model and computer parameters, estimates within I will evolve discretely into new estimates which are likewise bounded within I. The preservation of the properties of positivity and boundedness of the approximate solutions is carried out using the theory of M-matrices, which are non-singular, real, square matrices in which the entries of the inverses are positive numbers. Additionally, we establish the preservation in the discrete domain of the skew-symmetry of the solutions of the models under study. Our computational implementation of the method confirms numerically that the properties of positivity and boundedness are preserved under the analytical constraints derived theoretically. The techniques are two-step methods (three-step methods in the hyperbolic scenario), and they are consistent of first order in time and second order in space. In practice, our simulations evince a good agreement between the analytical solutions derived in the present work and the corresponding numerical approximations.

Chapter 1

Introduction

1.1 The Newell-Whitehead-Segel equation

1.1.1 Mathematical model

Let a, b and κ be real numbers with $\kappa > 0$, and let q be a positive integer. Let u be a function of the spatial variable x and the temporal variable t, with $x \in \mathbb{R}$ and $t \geq 0$. Consider the nonlinear, parabolic partial differential equation

$$\frac{\partial u}{\partial t} = \kappa \frac{\partial^2 u}{\partial x^2} + au - bu^q, \tag{1.1}$$

where the function u may be though of as the (nonlinear) distribution of heat in an infinitely thin and infinitely long rod, or as the flow velocity of a fluid in an infinitely thin and infinitely long pipe.

It is readily verified that this mathematical model is a generalization of the Newell-Whitehead-Segel equation which appeared historically in the investigation of fluid mechanics [75, 83]. Here, the constant κ is the coefficient of diffusion, the constants a and b are the coefficients of linear and nonlinear reaction, respectively, and q will assume the form $q = 2p + 1$, where p is a positive integer. In our manuscript, both a and b will be strictly positive real numbers.

It is important to notice that our mathematical model may be seen as a generalization or as a particular case of other meaningful partial differential equations of mathematical physics or biology. For instance, Eq. (1.1) is the classical heat equation with constant of diffusivity κ if both a and b are equal to zero; it is a modified Fisher-KPP equation (a model employed in population dynamics [27, 47] and nuclear reactor kinetics [45]) with reaction term of the form $au - bu^q$ if both a and b are positive; the model is a FitzHugh-Nagumo equation [78] (a model employed in the investigation of the transmission of electric impulses in the nervous system [28, 74]) with nonlinear reaction term given by $au(1-u)(u+1)$, in which case both parameters a and b in (1.1) are equal, and $q = 3$.

On the other hand, (1.1) assumes many interesting roles in the hyperbolic scenario. More precisely, let τ be a positive real number, and consider the partial differential equation

$$\tau \frac{\partial^2 u}{\partial t^2} + \frac{\partial u}{\partial t} = \kappa \frac{\partial^2 u}{\partial x^2} + au - bu^q. \tag{1.2}$$

For instance, if b is equal to zero, then the Telegraph equation (a linear partial differential equation studied by O. Heaviside in the investigation of electrical transmission lines) immediately appears [43]; if a and b are positive numbers, then the resulting equation is the Ginzburg-Landau equation in the investigation of ϕ^4-theories [49]; if both a and b are

equal to zero, then the resulting regime is the classical wave equation. Finally, if a and b are negative, then a damped, nonlinear Klein-Gordon equation emerges [57].

It is useful to notice that (1.1) may be simplified for its study, when a and b are both positive numbers, and q is of the form $2p+1$. Indeed, a simple non-dimensional analysis shows that it is enough to consider the model under investigation with all of κ, a and b being equal to 1. In our investigation, we will restrict our attention to the approximation of bounded solutions of the diffusive equation with nonlinear reaction

$$\frac{\partial u}{\partial t} = \frac{\partial^2 u}{\partial x^2} + u(1-u^{2p}), \tag{1.3}$$

where p is a positive integer number.

1.1.2 Particular solutions

The one-dimensional Newell-Whitehead-Segel equation (that is, Eq. (1.3) with p equal to 1) admits bounded solutions on the real line given by the formulas

$$u_1^{\pm}(x,t) = \pm \frac{C_1 \exp(\frac{1}{\sqrt{2}}x) - C_2 \exp(-\frac{1}{\sqrt{2}}x)}{C_1 \exp(\frac{1}{\sqrt{2}}x) + C_2 \exp(-\frac{1}{\sqrt{2}}x) + C_3 \exp(-\frac{3}{2}t)} \tag{1.4}$$

and

$$u_2^{\pm}(x,t) = \pm \left[\frac{2C_1 \exp(\sqrt{2}x) + C_2 \exp(\frac{1}{\sqrt{2}}x - \frac{3}{2}t)}{C_1 \exp(\sqrt{2}x) + C_2 \exp(\frac{1}{\sqrt{2}}x - \frac{3}{2}t) + C_3} - 1 \right], \tag{1.5}$$

where C_1, C_2 and C_3 are arbitrary real constants [78]. Throughout this work, we will restrict our attention to the case when the coefficients C_1, C_2 and C_3 are non-negative.

Under the considerations stated above, it is important to remark that both particular solutions satisfy the constraints $|u_1^{\pm}(x,t)| \leq 1$ and $|u_2^{\pm}(x,t)| \leq 1$, for every $x \in \mathbb{R}$ and every $t \geq 0$. Also, it is worthwhile to notice that the second solution satisfies $0 \leq u_2^{\pm}(x,t) \leq 1$ when C_3 is equal to zero; evidently, the expression $u_2^{\pm}$ represents a traveling wave solution in this particular case.

1.2 The FitzHugh-Nagumo equation

1.2.1 Mathematical model

Let u be a function of the spatial variable x and the temporal variable t, where $x \in \mathbb{R}$ and $t > 0$. Assume that a is a real number in the interval $[0, \frac{1}{2}]$, and let κ and m be positive, real numbers. In this work, we approximate non-negative and bounded solutions of the partial differential equation

$$\frac{\partial u}{\partial t} = \kappa \frac{\partial^2 u}{\partial x^2} + m^2 u f(u), \tag{1.6}$$

where

$$f(u) = (1-u)(u-a). \tag{1.7}$$

This model is called the *FitzHugh-Nagumo equation* or, for short, simply the *Nagumo equation*, and it is one of the simplest reaction-diffusion equations with nonlinear reaction. Evidently, it differs from the Fisher-KPP equation in the reaction term: In the Fisher-KPP model, $f(u) = 1-u$. Moreover, as we mentioned in the introductory section, (1.6) is a particular case of the Burgers-Huxley equation given.

Before closing this section of our study, we must point out that appropriate initial and boundary conditions must be imposed upon (1.6) in order to be able to numerically

approximate solutions to this model. As we will mention in time, we will consider non-negative Dirichlet conditions bounded from above by 1. At the same time, we will consider non-negative and bounded profiles satisfying (1.6) at any instant.

1.2.2 Particular solutions

For the rest of this manuscript, we tacitly let κ and m be both equal to 1 in (1.6). This assumption is fully justified by an elementary non-dimensional analysis of the equation (1.6). Under this convention, the FitzHugh-Nagumo equation presented in this work admits a solution in the form of a traveling wave front, namely, the function

$$u(x,t) = \frac{A\exp(z_1) + aB\exp(z_2)}{A\exp(z_1) + B\exp(z_2) + C}, \tag{1.8}$$

where

$$z_1 = \pm\frac{1}{\sqrt{2}}x + \left(\frac{1}{2} - a\right)t, \tag{1.9}$$

$$z_2 = \pm\frac{1}{\sqrt{2}}ax + a\left(\frac{1}{2}a - 1\right)t, \tag{1.10}$$

and A, B and C are arbitrary constants [78].

1.3 The Burgers-Huxley equation

1.3.1 Mathematical model

Let α be a non-negative real number, let β, κ and δ be positive numbers with $\delta \geq 1$, and let γ be a real number in $(0,1)$. Suppose that I is a (bounded or unbounded) interval in the set of real numbers. Throughout, u will be a function that depends on the spatial variable $x \in I$ and the temporal variable $t \geq 0$, which satisfies the advection-diffusion equation with nonlinear reaction term

$$\frac{\partial u}{\partial t} + \alpha u^{\delta}\frac{\partial u}{\partial x} - \kappa\frac{\partial^2 u}{\partial x^2} - \beta u f(u) = 0, \tag{1.11}$$

for every $x \in I$ and every $t \geq 0$, where

$$f(u) = (1-u^{\delta})(u^{\delta} - \gamma). \tag{1.12}$$

This model is called the *generalized Burgers-Huxley equation*, and it is a quantitative paradigm which describes the interaction between reaction mechanisms, convection effects and diffusion transport. We immediately identify here the constant κ as the coefficient of diffusivity, while α is the advection coefficient and β is the coefficient of reaction. The function (1.12) is the factor of (nonlinear) reaction, and it will be fixed throughout this work, unless stated otherwise.

It is worthwhile noticing that this mathematical model is actually a generalization of several important partial differential equations from mathematical physics. For instance, the partial differential equation (2.1) is the classical heat equation if α and β are equal to zero. If the advection coefficient is equal to zero, then our model becomes a generalization of the FitzHugh-Nagumo equation [28, 74, 85], which is a model employed in the study of the transmission of electric impulses in nervous systems. On the other hand, if α is equal to zero and the function f assumes the general form $f(u) = 1-u^{\delta}$, then the resulting equation is a generalized Fisher-KPP model [1], an equation that was investigated simultaneously

and independently by R. A. Fisher [27], and A. Kolmogorov, I. Petrovski and N. Piscounov [47], in the context of population dynamics. In the frame of the Fisher-KPP equation, the case when δ equals 2 is of particular interest in the investigation of fluid dynamics, the arising model being identified as the Newell-Whitehead-Segel equation [75, 83]. Finally, the partial differential equation (1.11) is a generalized Burgers-Fisher equation [93] if f is the reaction function of the generalized Fisher-KPP equation.

As we mentioned above, we will assume that κ and β are positive real numbers. It is pragmatically important to notice that the partial differential equation (1.11) may be conveniently simplified for its study. In fact, if we let $\xi = x\sqrt{\beta/\kappa}$ and $\tau = \beta t$, then the model (1.11) can be written in terms of the new independent variables as

$$\mathcal{L}(u) = 0, \tag{1.13}$$

where

$$\mathcal{L}(u) = \frac{\partial u}{\partial t} + \alpha u^{\delta}\frac{\partial u}{\partial x} - \frac{\partial^2 u}{\partial x^2} - uf(u), \tag{1.14}$$

for every $x \in I$ and every $t \geq 0$. Here, the new coefficient α and the variables x and t have replaced the constant $\alpha/\sqrt{\beta\kappa}$ and the variables ξ and τ, respectively. It is important to point out that this simplified model will be our equation of interest in Section 4.4, which will be the proper scenario to perform some numerical simulations in order to assess the validity of the method presented in this manuscript.

1.3.2 Particular solutions

Throughout this section, we will let κ be equal to 1. Moreover, for computational purposes, we may think of β as equal to 1, too, as it will be the case in Section 4.4.

Example 1. The generalized Burgers-Huxley equation under investigation has a particular solution in the interval $I = [a, b]$, which satisfies the set of initial-boundary conditions

$$\begin{cases} u(x,0) = \left(\frac{\gamma}{2} + \frac{\gamma}{2}\tanh(a_1 x)\right)^{1/\delta}, & \text{for every } x \in I, \\ u(a,t) = \left(\frac{\gamma}{2} + \frac{\gamma}{2}\tanh(a_1(a - a_2 t))\right)^{1/\delta}, & \text{for every } t \geq 0, \\ u(b,t) = \left(\frac{\gamma}{2} + \frac{\gamma}{2}\tanh(a_1(b - a_2 t))\right)^{1/\delta}, & \text{for every } t \geq 0, \end{cases} \tag{1.15}$$

where

$$a_1 = \frac{-\alpha\delta + \delta\sqrt{\alpha^2 + 4\beta(1+\delta)}}{4(1+\delta)}\gamma, \tag{1.16}$$

$$a_2 = \frac{\gamma\alpha}{1+\delta} - \frac{(1+\delta-\gamma)(-\alpha + \sqrt{\alpha^2 + 4\beta(1+\delta)})}{2(1+\delta)}. \tag{1.17}$$

Such particular solution is given by the expression

$$u(x,t) = \left(\frac{\gamma}{2} + \frac{\gamma}{2}\tanh(a_1(x - a_2 t))\right)^{1/\delta}, \tag{1.18}$$

for every $x \in I$ and every $t \geq 0$ (see [39]). Evidently, if we consider the entire set of real numbers as the interval I, then the function (1.18) is a traveling-wave solution of the parabolic partial differential equation (1.11). These remarks will be important in the investigation of the performance of the method presented in Section 4.3. □

Example 2. Let us consider once again the partial differential equation (1.11), with non-negative parameter α, a positive value of β, γ being a real number in the interval $(0, 1)$, and both κ and δ equal to 1. In this case, assume first that the spatial domain I is the entire real line. Then, the following function is a traveling-wave solution of the equation (1.11) which connects the two steady-state solutions $u = 0$ and $u = 1$, independently of the value of γ:

$$u(x,t) = \frac{1}{2} - \frac{1}{2}\tanh\left[\frac{\beta}{r-\alpha}(x - vt)\right], \tag{1.19}$$

where the constant r and the wave velocity v are given by

$$r = \sqrt{\alpha^2 + 8\beta}, \tag{1.20}$$

$$v = \frac{(\alpha - r)(2\gamma - 1) + 2\alpha}{4}. \tag{1.21}$$

These solutions are the result of employing symbolic computations and some relevant nonlinear transformations [50, 24, 92]. Evidently, the formula (1.19) is the particular solution in the interval $I = [a, b]$ of the associated initial-boundary-value problem

$$\begin{cases} u(x,0) = \dfrac{1}{2} - \dfrac{1}{2}\tanh\left(\dfrac{\beta x}{r-\alpha}\right), & \text{for every } x \in I, \\ u(a,t) = \dfrac{1}{2} - \dfrac{1}{2}\tanh\left[\dfrac{\beta}{r-\alpha}(a - vt)\right], & \text{for every } t \geq 0, \\ u(b,t) = \dfrac{1}{2} - \dfrac{1}{2}\tanh\left[\dfrac{\beta}{r-\alpha}(b - vt)\right], & \text{for every } t \geq 0. \end{cases} \tag{1.22}$$

□

Chapter 2

A generalized Newell-Whitehead-Segel equation

In this work, we propose a finite-difference scheme to approximate the solutions of a generalization of the classical, one-dimensional, Newell-Whitehead-Segel equation from fluid mechanics, which is an equation for which the existence of bounded solutions is a well-known fact. The numerical method preserves the skew-symmetry of the problem of interest, and it is a non-standard technique which consistently approximates the solutions of the equation under investigation, with a consistency of the first order in time and of the second order in space. We prove that, under relatively flexible conditions on the computational parameters of the method, our technique yields bounded numerical approximations for every set of bounded initial estimates. Some simulations are provided in order to verify the validity of our analytical results. In turn, the validity of the computational constraints under which the method guarantees the preservation of the boundedness of the approximations, is successfully tested by means of computational experiments in some particular instances.

2.1 Introduction

The class of non-standard numerical methods is a family of techniques that has been extensively used in the computational approximation of the solutions of many integral equations, as well as ordinary and partial differential equations. This family includes a wide range of non-traditional techniques to approximate linear and nonlinear terms in differential equations, and it has been satisfactorily applied, for instance, to the solution of Lotka-Volterra systems [65], wave equations with nonlinear reaction of the logistic type [56], linear wave equations with damping [68, 69], Gauss-type predator-prey models [71], nonlinear heat equations for thin, finite rods [41], among many other physically or mathematically interesting problems.

Some of the numerical techniques designed under the non-standard methodologies (methodologies which, by the way, have been popularized in the literature by R. E. Mickens [65, 68, 69, 64, 63, 66]) have been created in order to preserve certain physical characteristics which are of interest in the context of the mathematical problem under investigation. For instance, some non-standard techniques have been developed in order to preserve the non-negative character of the solutions of problems where the independent variable is measured in an absolute scale. Such problems arise naturally in population dynamics, where the population size is a non-negative function of time [36, 30, 29], or in those thermodynamical problems where the variable of interest is the temperature measured in

Kelvin [60, 61], or in problems involving the dynamics of the concentration of a chemical substance or of the biological colony on a certain substrate [22], in which the characteristic of interest is given as a percentage or, equivalently, as a real number in the interval $[0, 1]$.

In view of its physical relevance, it is not surprising to know that the study of the condition of non-negativity is important both mathematically and numerically [7, 37, 7, 44, 38, 14, 48]. However, several other preserved properties in physical systems are of mathematical and numerical interest. For example, many numerical methods have been built, having in mind the property of conservation of energy [32, 20, 12, 94, 25, 18] or, more generally, the property of preservation of the dissipation of energy [57, 55]. In the present work, we consider the property of preservation of the boundedness of solutions of a generalized Newell-Whitehead-Segel equation, which is a diffusive equation with a nonlinear reaction term, employed in the investigation of fluid mechanics [75, 83]. The present study is motivated by a previous work of the corresponding author, in which both non-negativity and boundedness were fundamental properties in the design of a non-standard, finite-difference scheme for a nonlinear wave equation [56]. In the present manuscript, non-negativity plays an important part in the design of a numerical method for the equation of interest, however, boundedness takes the central stage in our study. As we will see in this article, the concept of M-matrix exploited in [56] will take, once more, the main role in the problem of designing a non-standard, symmetry-preserving, boundedness-preserving, computational technique to approximate solutions of the generalized Newell-Whitehead-Segel model under study.

Section 2.2 of this work presents the nonlinear, parabolic partial differential equation under investigation in its general form. Here, we provide some particular solutions of our equation for comparison purposes, and we observe that a non-dimensional analysis leads to a parametric simplification of the model under investigation: In fact, when all coefficients are positive, solving the problem under study is equivalent to solving the same equation with all coefficients equal to 1. In Section 2.3, we propose a non-standard, finite-difference method to approximate solutions of the generalized Newell-Whitehead-Segel model of interest. Our numerical technique is seen to be explicit, and it is represented in matrix form after imposing discrete, homogeneous Neumann boundary conditions; this matrix representation is employed to establish conditions under which bounded initial conditions yield bounded new approximations. The most important result is presented as Proposition 5, and the numerical constraint derived is seen to be relatively flexible. Section 2.4 is devoted to show some numerical simulations to evidence that the method approximates well the solutions of our equation, and that the property of boundedness is preserved when the conditions of Proposition 5 are satisfied. In fact, we compute numerically the regions for which the numerical parameters of the method provide bounded approximations. It is worth mentioning beforehand that the region provided by Proposition 5 is a subset of the region obtained through our simulations, confirming thus the validity of the analytical apparatus.

2.2 Preliminaries

2.2.1 Mathematical model

Let a, b and κ be real numbers with $\kappa > 0$, and let q be a positive integer. Let u be a function of the spatial variable x and the temporal variable t, with $x \in \mathbb{R}$ and $t \geq 0$. In this work, we design a numerical method to approximate bounded solutions of the nonlinear, parabolic partial differential equation

$$\frac{\partial u}{\partial t} = \kappa \frac{\partial^2 u}{\partial x^2} + au - bu^q, \tag{2.1}$$

where the function u may be though of as the (nonlinear) distribution of heat in an infinitely thin and infinitely long rod, or as the flow velocity of a fluid in an infinitely thin and infinitely long pipe.

It is readily verified that this mathematical model is a generalization of the Newell-Whitehead-Segel equation which appeared historically in the investigation of fluid mechanics [75, 83]. Here, the constant κ is the coefficient of diffusion, the constants a and b are the coefficients of linear and nonlinear reaction, respectively, and q will assume the form $q = 2p + 1$, where p is a positive integer. In our manuscript, both a and b will be strictly positive real numbers.

It is important to notice that our mathematical model may be seen as a generalization or as a particular case of other meaningful partial differential equations of mathematical physics or biology. For instance, Eq. (2.1) is the classical heat equation with constant of diffusivity κ if both a and b are equal to zero; it is a modified Fisher-KPP equation (a model employed in population dynamics [27, 47] and nuclear reactor kinetics [45]) with reaction term of the form $au - bu^q$ if both a and b are positive; the model is a FitzHugh-Nagumo equation [78] (a model employed in the investigation of the transmission of electric impulses in the nervous system [28, 74]) with nonlinear reaction term given by $au(1-u)(u+1)$, in which case both parameters a and b in (2.1) are equal, and $q = 3$.

On the other hand, (2.1) assumes many interesting roles in the hyperbolic scenario. More precisely, let τ be a positive real number, and consider the partial differential equation

$$\tau\frac{\partial^2 u}{\partial t^2} + \frac{\partial u}{\partial t} = \kappa\frac{\partial^2 u}{\partial x^2} + au - bu^q. \tag{2.2}$$

For instance, if b is equal to zero, then the Telegraph equation (a linear partial differential equation studied by O. Heaviside in the investigation of electrical transmission lines) immediately appears [43]; if a and b are positive numbers, then the resulting equation is the Ginzburg-Landau equation in the investigation of ϕ^4-theories [49]; if both a and b are equal to zero, then the resulting regime is the classical wave equation. Finally, if a and b are negative, then a damped, nonlinear Klein-Gordon equation emerges [57].

Before closing this stage of our work, it is useful to notice that (2.1) may be simplified for its study, when a and b are both positive numbers, and q is of the form $2p+1$. Indeed, a simple non-dimensional analysis shows that it is enough to consider the model under investigation with all of κ, a and b being equal to 1. So, for the rest of this manuscript, we will restrict our attention to the approximation of bounded solutions of the diffusive equation with nonlinear reaction

$$\frac{\partial u}{\partial t} = \frac{\partial^2 u}{\partial x^2} + u(1 - u^{2p}), \tag{2.3}$$

where p is a positive integer number.

2.2.2 Particular solutions

The one-dimensional Newell-Whitehead-Segel equation (that is, Eq. (2.3) with p equal to 1) admits bounded solutions on the real line given by the formulas

$$u_1^{\pm}(x,t) = \pm\frac{C_1\exp(\frac{1}{\sqrt{2}}x) - C_2\exp(-\frac{1}{\sqrt{2}}x)}{C_1\exp(\frac{1}{\sqrt{2}}x) + C_2\exp(-\frac{1}{\sqrt{2}}x) + C_3\exp(-\frac{3}{2}t)} \tag{2.4}$$

and

$$u_2^{\pm}(x,t) = \pm\left[\frac{2C_1\exp(\sqrt{2}x) + C_2\exp(\frac{1}{\sqrt{2}}x - \frac{3}{2}t)}{C_1\exp(\sqrt{2}x) + C_2\exp(\frac{1}{\sqrt{2}}x - \frac{3}{2}t) + C_3} - 1\right], \tag{2.5}$$

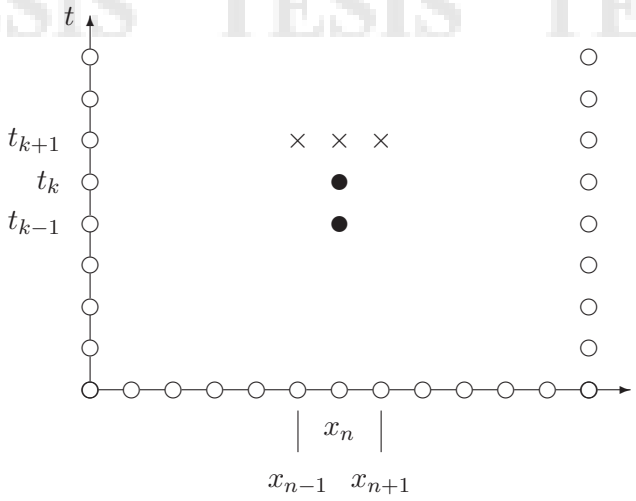

Figure 2.1: Forward-difference stencil for the approximation to the partial differential equation (2.3) at time t_k, using the finite-difference scheme (2.6). The black circles represent known approximations to the actual solutions at the times t_{k-1} and t_k, and the crosses denote the unknown approximations at the time t_{k+1}.

where C_1, C_2 and C_3 are arbitrary real constants [78]. Throughout this work, we will restrict our attention to the case when the coefficients C_1, C_2 and C_3 are non-negative.

Under the considerations stated above, it is important to remark that both particular solutions satisfy the constraints $|u_1^{\pm}(x,t)| \leq 1$ and $|u_2^{\pm}(x,t)| \leq 1$, for every $x \in \mathbb{R}$ and every $t \geq 0$. Also, it is worthwhile to notice that the second solution satisfies $0 \leq u_2^{\pm}(x,t) \leq 1$ when C_3 is equal to zero; evidently, the expression $u_2^{\pm}$ represents a traveling wave solution in this particular case.

2.3 Numerical method

2.3.1 Finite-difference scheme

Let M and N be positive integers, and fix a spatial domain $[a,b]$ and a temporal interval $[0,T]$, where $a < b$ and $T > 0$. Let $a = x_0 < x_1 < \ldots < x_N = b$ and $0 = t_0 < t_1 < \ldots < t_M = T$ be regular partitions of $[a,b]$ and $[0,T]$, respectively, and let $\Delta x = (b-a)/N$ and $\Delta t = T/M$ be their respective norms. For every $n \in \{0,1,\ldots,N\}$ and every $k \in \{0,1,\ldots,M\}$, let u_n^k be an approximation to the exact value of $u(x_n,t_k)$.

For every $k \in \{0,1,\ldots,M\}$, let $\mathbf{u}^k = (u_0^k, u_1^k, \ldots, u_N^k)^t$, where the symbol ^{t} indicates the matrix (and, in particular, the vector) operation of transposition. Assuming that the respective approximations $\mathbf{u}^k$ and $\mathbf{u}^{k-1}$ at times t_k and t_{k-1} are known, for some $k \in \{1,\ldots,M-1\}$, we approximate the exact solution $u(x_n,t_{k+1})$ of (2.3) by means of the finite-difference scheme

$$\delta_{t,\alpha} u_n^k = \delta_x^{(2)} u_n^{k+1} + u_n^{k+1}(1-(u_n^k)^{2p}), \tag{2.6}$$

where the following linear operators are employed:

$$\delta_{t,\alpha} u_n^k = (1-\alpha)\frac{u_n^{k+1}-u_n^k}{\Delta t} + \alpha\frac{u_n^{k+1}-u_n^{k-1}}{2\Delta t}, \tag{2.7}$$

$$\delta_x^{(2)} u_n^k = \frac{u_{n+1}^k - 2u_n^k + u_{n-1}^k}{(\Delta x)^2}. \tag{2.8}$$

It is clear that (2.7) is a weighted estimation of the exact value of $\frac{\partial u}{\partial t}$ at (x_n, t_k), formed by a linear combination of a first-order approximation and a second-order approximation. Meanwhile, (2.8) is the standard, second-order approximation to the value of $\frac{\partial^2 u}{\partial x^2}$ at (x_n, t_k). However, employing Taylor series approximations around the point (x_n, t_{k+1}), it is easy to show that (2.7) is a first order approximation of $\frac{\partial u}{\partial t}(x_n, t_{k+1})$. It follows that the linearized version of (2.3) is consistently estimated by the linearized version of the finite-difference scheme (2.6), with a consistency of the order of $\mathcal{O}(\Delta t + (\Delta x)^2)$.

2.3.2 Matrix representation

In order to conveniently represent the finite-difference scheme (2.6) in matrix form, it is important to notice first that our numerical method can be expressed explicitly as

$$k_1 u_{n+1}^{k+1} + k_2 u_n^{k+1} + k_1 u_{n-1}^{k+1} = k_3 u_n^k + k_4 u_n^{k-1}, \tag{2.9}$$

where the coefficients k_1, k_2, k_3 and k_4 are, in general, the functions of $\mathbf{u}^k$ given by

$$k_1 = -R, \tag{2.10}$$

$$k_2 = 1 - \frac{\alpha}{2} + 2R - \Delta t(1 - (u_n^k)^{2p}), \tag{2.11}$$

$$k_3 = 1 - \alpha, \tag{2.12}$$

$$k_4 = \frac{\alpha}{2}. \tag{2.13}$$

Here, we employ the auxiliary notation

$$R = \frac{\Delta t}{(\Delta x)^2}, \tag{2.14}$$

for the sake of convenience. As a corollary, the forward-difference stencil of the computational technique employed in this work is the one depicted in Fig. 2.1.

The explicit form of our numerical scheme, as provided by (2.9), yields a convenient matrix representation if we impose appropriate boundary conditions on the end points of the interval $[a, b]$. For practical reasons, we will consider discrete, homogeneous Neumann boundary data at the end points of the spatial interval, that is, we assume that, for every $k = 0, 1, \ldots, M$,

$$u_0^k - u_1^k = u_N^k - u_{N-1}^k = 0. \tag{2.15}$$

As a consequence, the numerical method (2.6) takes the matrix form

$$A_{\mathbf{u}^k} \mathbf{u}^{k+1} = B\mathbf{u}^k + C\mathbf{u}^{k-1}, \tag{2.16}$$

where $A_{\mathbf{u}^k}$, B and C are the real matrices of sizes $(N+1) \times (N+1)$, given by

$$A_{\mathbf{u}^k} = \begin{pmatrix} 1 & -1 & 0 & 0 & \cdots & 0 & 0 & 0 \\ k_1 & k_2 & k_1 & 0 & \cdots & 0 & 0 & 0 \\ 0 & k_1 & k_2 & k_1 & \cdots & 0 & 0 & 0 \\ \vdots & \vdots & \vdots & \vdots & \ddots & \vdots & \vdots & \vdots \\ 0 & 0 & 0 & 0 & \cdots & k_1 & k_2 & k_1 \\ 0 & 0 & 0 & 0 & \cdots & 0 & -1 & 1 \end{pmatrix}, \tag{2.17}$$

and

$$B = \begin{pmatrix} 0 & 0 & \cdots & 0 & 0 \\ 0 & k_3 & \cdots & 0 & 0 \\ \vdots & \vdots & \ddots & \vdots & \vdots \\ 0 & 0 & \cdots & k_3 & 0 \\ 0 & 0 & \cdots & 0 & 0 \end{pmatrix}, \quad C = \begin{pmatrix} 0 & 0 & \cdots & 0 & 0 \\ 0 & k_4 & \cdots & 0 & 0 \\ \vdots & \vdots & \ddots & \vdots & \vdots \\ 0 & 0 & \cdots & k_4 & 0 \\ 0 & 0 & \cdots & 0 & 0 \end{pmatrix}. \tag{2.18}$$

Let $\mathcal{V}$ be the real vector space $\mathbb{R}^{N+1}$. We must keep in mind that the matrix $A_{\mathbf{u}^k}$ is actually a function of $\mathbf{u}^k$, while B and C are constant matrices. Moreover, the finite-difference scheme (2.6) may be more accurately presented as the equation

$$\mathcal{L}(\mathbf{u}^{k+1}, \mathbf{u}^k, \mathbf{u}^{k-1}) = 0, \tag{2.19}$$

for every $k \in \{1, \ldots, M-1\}$, where $\mathcal{L} : \mathcal{V}^3 \to \mathcal{V}$ is the operator defined by

$$\mathcal{L}(\mathbf{x}, \mathbf{y}, \mathbf{z}) = A_{\mathbf{y}}\mathbf{x} - B\mathbf{y} - C\mathbf{z}. \tag{2.20}$$

Evidently, $\mathcal{V}^3 = \mathcal{V} \times \mathcal{V} \times \mathcal{V}$. We observe here that the function $\mathcal{L}$ is not a linear operator; however, it satisfies the following useful property, which is denominated *skew-symmetry* in the literature [90]. Here, we must mention that this symmetry condition arises naturally in many problems of turbulent flows where advection is present [90]. In mathematical physics, the Poisson manifolds (that is, smooth manifolds endowed with a Poisson bracket structure satisfying a skew-symmetry condition among other properties) are crucial in the foundation of the generalized Nabu mechanics [87]. Finally, skew-symmetry is of the utmost importance in the recognition of planar polygons [11] and surfaces [82].

Lemma 3. *If* $\mathbf{x}, \mathbf{y}, \mathbf{z} \in \mathcal{V}$, *then* $\mathcal{L}(-\mathbf{x}, -\mathbf{y}, -\mathbf{z}) = -\mathcal{L}(\mathbf{x}, \mathbf{y}, \mathbf{z})$.

Proof. The result is straight-forward. □

An easy consequence of this result indicates that $\mathcal{L}(\mathbf{u}^{k+1}, \mathbf{u}^k, \mathbf{u}^{k-1}) = 0$ if and only if $\mathcal{L}(-\mathbf{u}^{k+1}, -\mathbf{u}^k, -\mathbf{u}^{k-1}) = 0$. This statement is in agreement with the fact that a function u on the variables $x \in \mathbf{R}$ and $t \geq 0$ satisfies (2.3) if and only if $-u$ satisfies the same equation. Therefore, our numerical method preserves the skew-symmetry of solutions, among several other properties that we will derive in the subsequent discussions.

2.3.3 Boundedness preservation

Let A be a (non necessarily square) matrix over the field $\mathbb{R}$, and let s and t be real numbers with $s \leq t$. We employ the notation $A \leq t$ when every entry $a_{i,j}$ of A satisfies $a_{i,j} \leq t$. Similarly, $A \geq s$ holds when every $a_{i,j} \geq s$. Moreover, we convey that $s \leq A \leq t$ if and only if $A \geq s$ and $A \leq t$.

Recall that an *M-matrix* is a square matrix A with entries in the set of real numbers, which satisfies the following properties:

(i) the off-diagonal elements of A are non-positive,

(ii) the diagonal elements of A are positive, and

(iii) A is strictly diagonally dominant.

The M-matrices have been successfully used in some computational studies such as [56, 21], in view that they are non-singular, and the entries of their inverses are non-negative real numbers [33].

In the following, p will be a positive integer, Δt and Δx will be positive real numbers, and α will be a real number in the interval $(0, 1)$.

Lemma 4. *Let* $\mathbf{u}^k$ *be a vector in* $\mathbb{R}^{N+1}$ *satisfying* $-1 \leq \mathbf{u}^k \leq 1$. *The matrix* $A_{\mathbf{u}^k}$ *in* (2.17) *is an M-matrix if the following inequality is satisfied:*

$$\Delta t < 1 - \frac{\alpha}{2}. \tag{2.21}$$

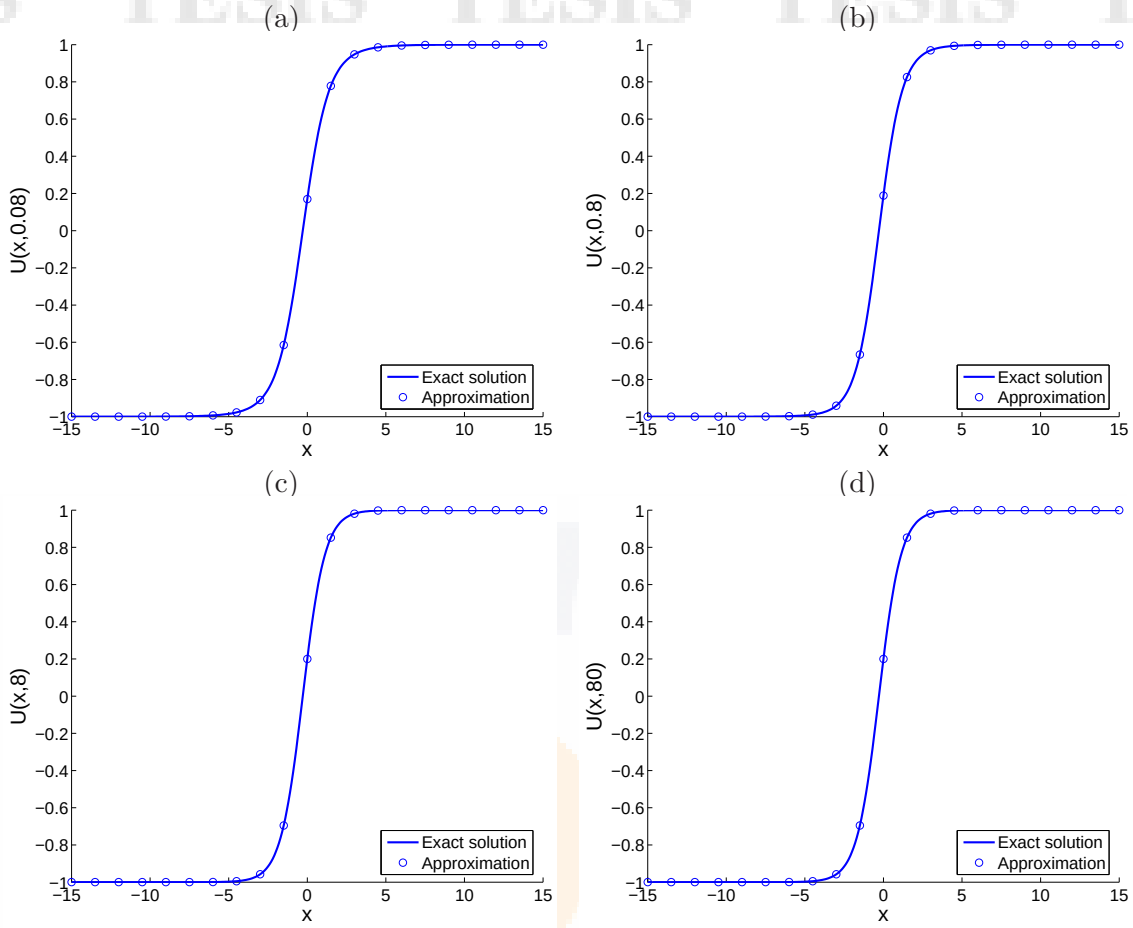

Figure 2.2: Graphs of the exact solution and the corresponding approximate solution versus the spatial variable x of a medium governed by (2.3) with $p = 1$, at four different times, namely, (a) $t = 0.08$, (b) $t = 0.8$, (c) $t = 8$ and (d) $t = 80$. The initial data were given by the function u_1^+ in (2.4) around the time $t = 0$, with the coefficients $C_1 = 30$, $C_2 = 20$ and $C_3 = 10$. Computationally, we fixed the spatial domain $[-15, 15]$, imposed discrete, homogeneous Neumann boundary conditions, and set $\alpha = 0.328$, $\Delta x = 0.1$ and $\Delta t = 0.001$.

Proof. We only need to establish properties (ii) and (iii) in the definition of an M-matrix. Observe that the constraint (2.21) implies that

$$\Delta t(1 - (x_n)^{2p}) < 1 - \frac{\alpha}{2}. \tag{2.22}$$

Subtracting the term $\Delta t(1 - (u_n^k)^{2p})$ on both sides of this inequality, and adding then the term $2R$ on both sides, we establish the inequality $|k_1| + |k_1| < k_2$, for every $n = 2, \ldots, N$. This proves (iii), and the property (ii) follows from the fact that $|k_1| + |k_1| = 2R$ is a positive number. □

Next, we want to establish conditions under which the finite-difference scheme (2.6) preserves the boundedness of solutions. To that end, let $D = (-\infty, 1] \times (-\infty, 1]$, and define the function $G : D \to \mathbb{R}$ by means of the rule

$$G(x, y) = 1 - \frac{\alpha}{2} - \Delta t(1 - x^{2p}) - (1 - \alpha)x - \frac{\alpha}{2}y. \tag{2.23}$$

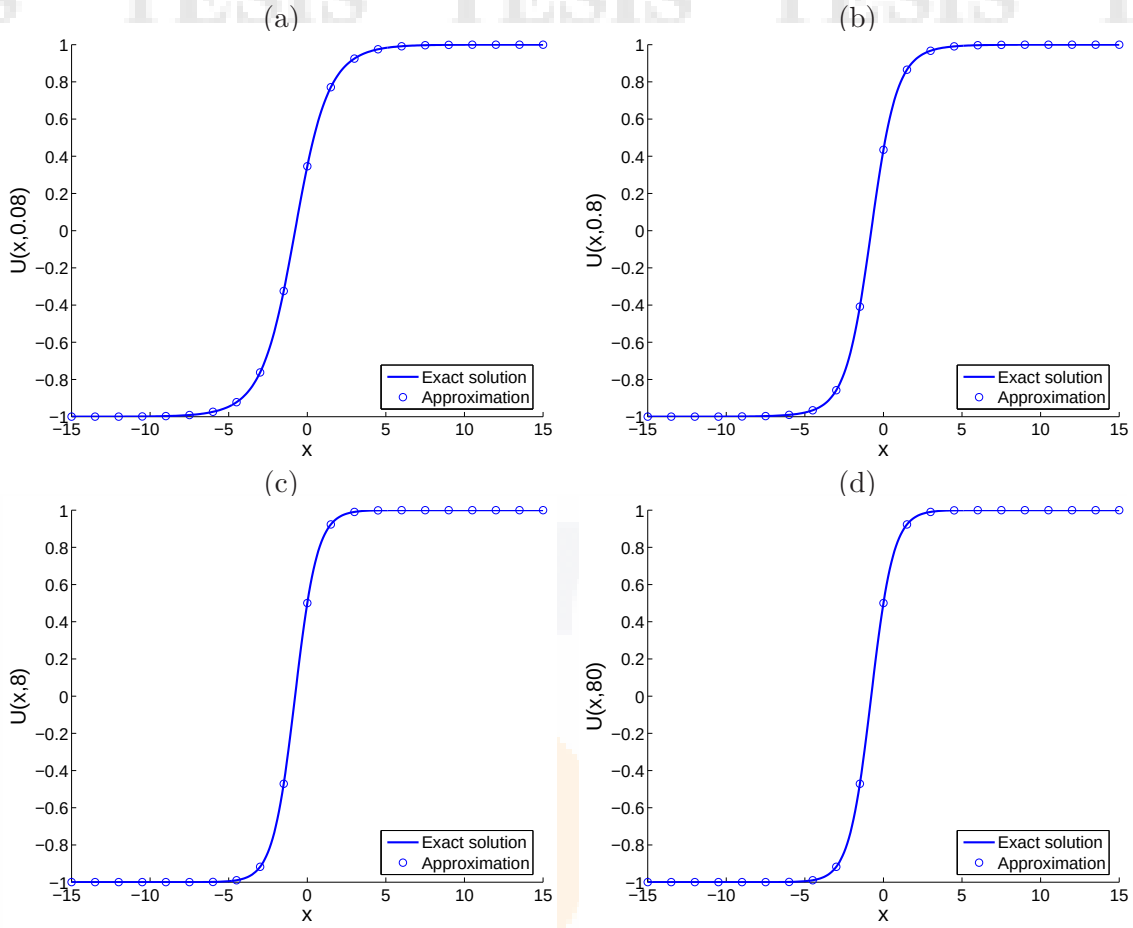

Figure 2.3: Graphs of the exact solution and the corresponding approximate solution versus the spatial variable x of a medium governed by (2.3) with $p = 1$, at four different times, namely, (a) $t = 0.08$, (b) $t = 0.8$, (c) $t = 8$ and (d) $t = 80$. The initial data were given by the function u_2^+ in (2.5) around the time $t = 0$, with the coefficients $C_1 = 30$, $C_2 = 20$ and $C_3 = 10$. Computationally, we fixed the spatial domain $[-15, 15]$, imposed discrete, homogeneous Neumann boundary conditions, and set $\alpha = 0.328$, $\Delta x = 0.1$ and $\Delta t = 0.001$.

Clearly, G is a continuous function on the set D, which satisfies $G(1, 1) = 0$. Moreover, it is an easy exercise of vector calculus to show that $\frac{\partial G}{\partial y}$ is negative in the interior of D, and that $\frac{\partial G}{\partial x}$ is likewise negative whenever the following inequality is satisfied:

$$\Delta t < \frac{1 - \alpha}{2p}. \tag{2.24}$$

As a consequence, the function G is nonnegative in D if the inequality (2.24) holds.

Proposition 5. *Let $k \in \{1, \ldots, M - 1\}$, and assume that $\mathbf{u}^k$ and $\mathbf{u}^{k-1}$ are vectors in $\mathbb{R}^{N+1}$ satisfying $-1 \leq \mathbf{u}^k \leq 1$ and $-1 \leq \mathbf{u}^{k-1} \leq 1$. Then, the vector $\mathbf{u}^{k+1}$ also satisfies $-1 \leq \mathbf{u}^{k+1} \leq 1$ if the inequality (2.24) holds.*

Proof. Beforehand, notice that the condition (2.21) holds whenever (2.24) is satisfied, so that the matrix $A_{\mathbf{u}^k}$ associated to the finite-difference scheme (2.6), is an M-matrix. Let

$\mathbf{w}^{k+1} = \mathbf{e} - \mathbf{u}^{k+1}$, where $\mathbf{e}$ is the $(N+1)$-dimensional vector whose components are all equal to 1. Substituting this representation of $\mathbf{u}^{k+1}$ in (2.16), we obtain the identity

$$A_{\mathbf{u}^k}\mathbf{w}^{k+1} = A\mathbf{e} - B\mathbf{u}^k - C\mathbf{u}^{k-1}. \tag{2.25}$$

Let $\mathbf{b}$ be the right-hand side of this expression. Clearly, the first and the last component of $\mathbf{b}$ are equal to zero. On the other hand, if $n = 1, \ldots, N-2$, then the $(n+1)$th component of $\mathbf{b}$ is given by $G(u_n^k, u_n^{k-1})$, where G is the function defined in (2.23). Since (2.24) holds, then $\mathbf{b}$ is a vector with nonnegative entries, whence it follows that $\mathbf{w}^{k+1} \geq 0$ or, equivalently, that $\mathbf{u}^{k+1} \leq 1$. It only remains to prove now that $\mathbf{u}^{k+1} \geq -1$.

By the hypotheses, $-1 \leq -\mathbf{u}^k \leq 1$ and $-1 \leq -\mathbf{u}^{k-1} \leq 1$. Lemma 3 implies that $A_{\mathbf{v}^k}\mathbf{v}^{k+1} = B\mathbf{v}^k + C\mathbf{v}^{k-1}$, where each $\mathbf{v}^j = -\mathbf{u}^j$, for $j = k-1, k, k+1$. By the first part of this proof, $\mathbf{v}^{k+1} \leq 1$ or, equivalently, $\mathbf{u}^{k+1} \geq -1$, as desired. □

Corollary 6. *Let $k \in \{1, \ldots, M-1\}$, and assume that $\mathbf{u}^k$ and $\mathbf{u}^{k-1}$ are vectors in $\mathbb{R}^{N+1}$ satisfying $0 \leq \mathbf{u}^k \leq 1$ and $0 \leq \mathbf{u}^{k-1} \leq 1$. The vector $\mathbf{u}^{k+1}$ satisfies $0 \leq \mathbf{u}^{k+1} \leq 1$ whenever the inequality (2.24) is satisfied.*

Proof. Proposition 5 assures that $-1 \leq \mathbf{u}^{k+1} \leq 1$. That $\mathbf{u}^{k+1} \geq 0$ follows from the fact that, under our assumptions, the right-hand side of (2.16) is a vector with non-negative entries, and that A is an M-matrix. □

In the context of kinematic waves, the solutions of (2.3) must be non-negative for the sake of physical meaningfulness. If our model is applied in the context of fluid mechanics, the condition of non-negativity on the solutions of (2.3) is of physical relevance in those cases when the flow velocity of the fluid in the pipe is likewise non-negative, that is, when the fluid moves in the same direction.

We must remark here that the inequality (2.24) is, indeed, a sufficient condition in order to guarantee the preservation of the boundedness of our method. We have conducted numerical experiments in order to determine the smallest value of Δt for which the boundedness is no longer preserved. In those simulations, our results (which are presented in the next section) establish the existence of a region wider than that prescribed by (2.24), confirming thus the validity of our analytical apparatus.

Finally, it is interesting to notice that the constraint (2.24) is relatively flexible. In fact, the dependency of the maximum value of Δt for which the boundedness of solutions of (2.1) is preserved, as given by (2.24) in terms of the parameters α and p, is a simple rule which guarantees the existence of sufficiently small values of Δt satisfying the condition. Moreover, the fact that the step-size Δx does not appear in that inequality, gives some indication of the robustness of our analytical results.

2.4 Simulations

2.4.1 Examples

In this stage of our work, we present some simulations in order to evidence the fact that our method approximates well the particular solutions (2.4) and (2.5) of the model (2.3), and that the boundedness of the corresponding approximations is kept when the constraint (2.24) is satisfied.

Example 7. Consider the partial differential equation (2.3) with p equal to 1, and fix initial data around $t = 0$ given by the particular solution u_1^+ in (2.4) at that instant of time, with $C_1 = 30$, $C_2 = 20$ and $C_3 = 10$. Computationally, we fix the values $\alpha = 0.328$,

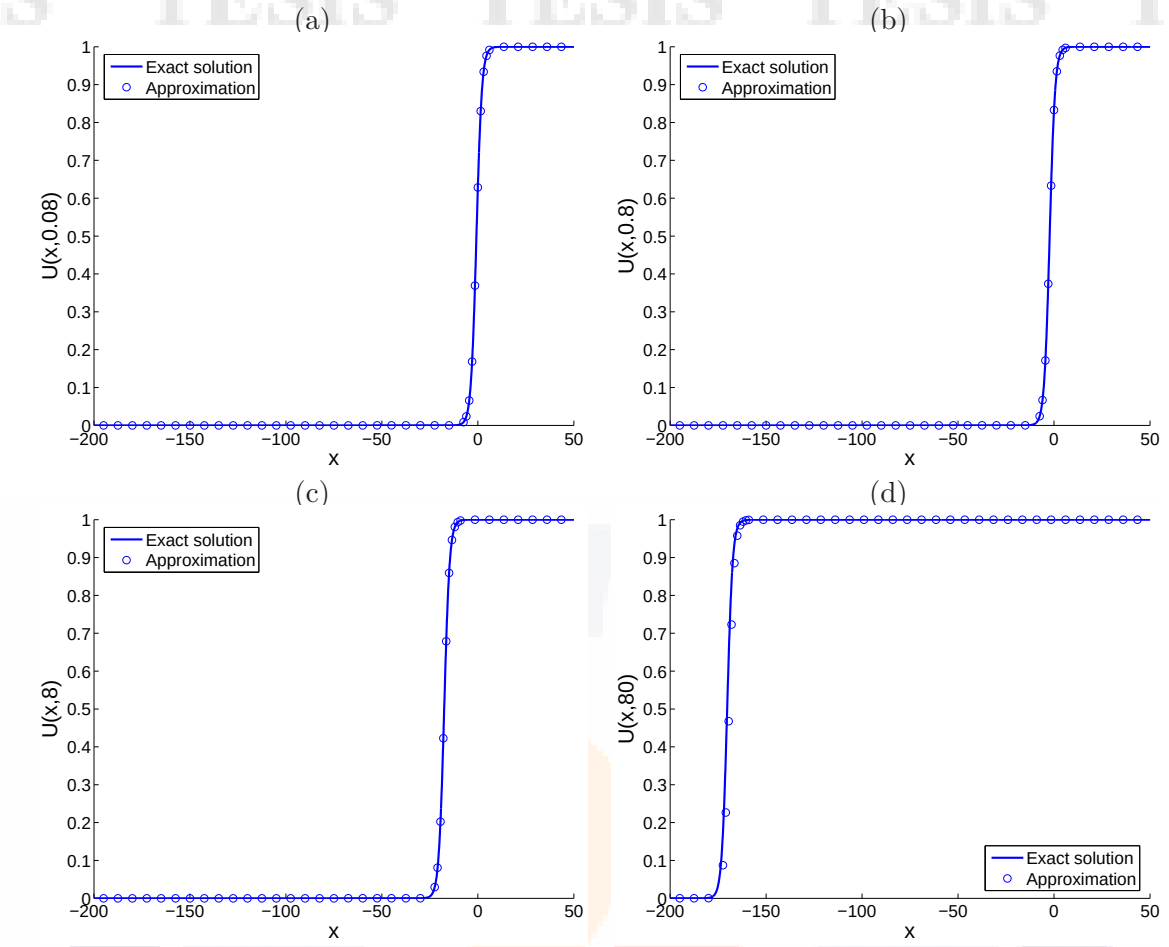

Figure 2.4: Graphs of the exact solution and the corresponding approximate solution versus the spatial variable x of a medium governed by (2.3) with $p = 1$, at four different times, namely, (a) $t = 0.08$, (b) $t = 0.8$, (c) $t = 8$ and (d) $t = 80$. The initial data were given by the function u_2^+ in (2.5) around the time $t = 0$, with the coefficients $C_1 = 30$, $C_2 = 20$ and $C_3 = 0$. Computationally, we fixed the spatial domain $[-200, 50]$, imposed discrete, homogeneous Neumann boundary conditions, and set $\alpha = 0.328$, $\Delta x = 0.1$ and $\Delta t = 0.001$.

$\Delta x = 0.1$ and $\Delta t = 0.001$, fix the spatial domain $[-15, 15]$ to perform simulations, and impose discrete, homogeneous Neumann boundary conditions. Under these conventions, we approximate the solution of the given initial-value problem at four different times, namely, $t = 0.08$, 0.8, 8 and 80. The exact solution and the approximations computed through (2.6) are presented in Fig. 2.2. The results evidence not only a good agreement between the numerical and theoretical values, but also that our finite-difference scheme is capable of preserving the boundedness of the solutions of the problem when the condition (2.24) is satisfied. *qed*

Example 8. We repeat the problem presented in the previous example with the same values of the model and computational parameters, changing the initial conditions for those given by the function u_2^+ in (2.5) around the time $t = 0$, using the constants $C_1 = 30$, $C_2 = 20$ and $C_3 = 10$. Under these conventions, Fig. 2.3 compares the exact solutions of our initial-value problem and the corresponding approximations given by our method at four different times, namely, $t = 0.08$, 0.8, 8 and 80. Again, we see that our method approximates well the solutions to the problem under consideration, and that the approx-

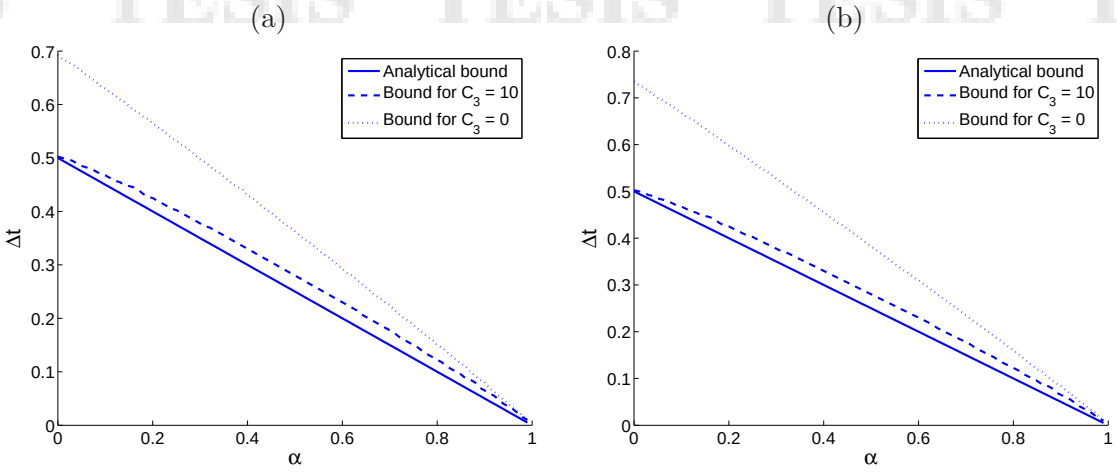

Figure 2.5: Graphs of minimum value of Δt for which the finite-difference scheme does not preserve the boundedness of the approximations versus the value of the parameter α, for a system governed by (2.3) with initial data provided by the particular solution u_1^+ around $t = 0$, $p = 1$, $C_1 = 30$, $C_2 = 20$, and two different values of C_3: 10 (dashed) and 0 (dotted). Two different values of Δx were used, namely, (a) 0.1 and (b) 0.05. In either case, a time period equal to 30 was used. The theoretical bound (2.24) is depicted in both graphs (solid).

imations remain bounded in the interval $[-1, 1]$. □

Example 9. Finally, we repeat the simulations of the Example 8 with $C_3 = 0$, over the spatial domain $[-200, 50]$. In this case, it is known that the exact solutions are bounded in the interval $[0, 1]$, and not in $[-1, 1]$. The comparison between the computational results and the exact solutions are shown in Fig. 2.4. Again, the same conclusions as before are drawn for this case, too. □

2.4.2 Boundedness condition

In this stage, we wish to show numerically that the condition (2.24) is, indeed, a sufficient condition to preserve the boundedness of the approximations given by (2.6). With this purpose in mind, we consider the equation (2.3) with $p = 1$, initial conditions prescribed by the function u_1^+ in (2.4) with parameters $C_1 = 30$, $C_2 = 20$, and two different values of C_3, namely, 0 and 10. Likewise, we choose the computational parameter Δx to be equal to 0.1, fix a time interval $[0, 30]$, and select the spatial domains $[-20, 20]$.

Using simple iterative procedures and letting α range in $[0, 1]$, we approximate numerically the smallest value of Δt for which the condition of boundedness is no longer preserved by the method. The results of our simulations are presented as Fig. 2.5(a), where the solid line corresponds to the analytical bound of Δt given by (2.24), and the dashed and the dotted lines represent the experimental bounds calculated through computer simulations, for $C_3 = 10$ and $C_3 = 0$, respectively. We conclude that the analytical bound is within the numerical bounds calculated by means of the finite-difference scheme (2.6).

Finally, Fig. 2.5(b) presents the results of the same experiments reported in Fig. 2.5(a), now with $\Delta x = 0.05$. Again, the theoretical bound that assures the boundedness-preservation of our method lies within the bounds computed by means of our method. We have performed more simulations for different values of the model and computer parameters; the results (not shown here in view of their redundancy) establish the same conclusions in every case.

Chapter 3

The FitzHugh-Nagumo equation

In this work, we present a finite-difference scheme that preserves the non-negativity and the boundedness of some solutions of a FitzHugh-Nagumo equation. The method is explicit, and it approximates the solutions of the nonlinear, parabolic partial differential equation under study with a consistency of order $\mathcal{O}(\Delta t + (\Delta x)^2)$ in the Dirichlet regime investigated. We give sufficient conditions in terms of the computational and the model parameters, in order to guarantee the non-negativity and the boundedness of the approximations. We also provide analyses of consistency, linear stability and convergence of the method. Our simulations establish that the properties of non-negativity and boundedness are actually preserved by the scheme when the proposed constraints are satisfied. Finally, a comparison against some second-order accurate methods reveals that our technique is easier to implement computationally, and it is better at preserving the properties of non-negativity and boundedness of the solutions of the FitzHugh-Nagumo equation under study.

3.1 Introduction

The conditions of non-negativity and boundedness of the solutions of some mathematical models are constraints which arise mostly from the physical context. For instance, in mathematical biology, it is interesting to understand the evolution of certain populations in which the growth is subjected to limited availability of resources [27]. In thermodynamics, the problem of describing the propagation of forest fires is a question of pragmatic relevance [61]. In chemistry, there exist many practical situations in which the temporal evolution of the concentration of a chemical or biological component in a medium is the topic of investigation, such as in the analysis of some chemical, kinetic systems [86] or in the mathematical modeling of the growth of bacterial films [22].

In the context of population dynamics with limited nutrients, the variable of interest is usually the quotient of the actual population at certain time, with respect to the maximum population size of the medium. In other words, in this scenario, the variable of interest is the population density, which is a function of time, bounded from below and from above by 0 and 1, respectively. In the case of the spread of forest fires, the variable under study is the temporal evolution of the temperature at each particular point in the forest, and the scale in which the measurements are handled are usually Kelvin: An absolute scale. Finally, in the case of the measurement of concentrations of chemical or biological components in a medium, the variable under investigation is a percentage which assumes real values between 0 and 100, only.

The problems described in the previous paragraph share many characteristics in com-

mon. First of all, meaningful solutions satisfy one or both of the properties of non-negativity and boundedness, which are conditions that are important in many other mathematical models governing the dynamics of realistic, physical situations [60, 36, 30, 29, 31, 6]. Secondly, the models describing these phenomena are relatively complicated and there is no exact solution for every possible problem associated to them, whence the need of employing reliable computational techniques to approximate the solutions is an obvious corollary. Finally, most of the numerical techniques available for these and other problems [70, 86, 62, 79, 16, 91, 13, 73], though powerful in their degrees of accuracy, do not guarantee the preservation of the properties of non-negativity and boundedness of solutions.

Another interesting example of a partial differential equation for which the existence of non-negative and bounded solutions is a well-known fact, is the FitzHugh-Nagumo model presented in [78]. This equation is a diffusive equation with a nonlinear reaction term, and it represents a particular case of the Burgers-Huxley equation [88], which is given in a general form by the advection-diffusion equation with nonlinear reaction

$$\frac{\partial u}{\partial t} + \alpha u^{\delta}\frac{\partial u}{\partial x} = \frac{\partial^2 u}{\partial x^2} + \beta u(1-u^{\delta})(u^{\delta}-a). \tag{3.1}$$

In our study, α is equal to zero, while β and δ are both equal to 1, and a is a real number in the interval $[0, \frac{1}{2}]$. As we will see, the model considered in this work has a solution in the form of a traveling wave front, which is bounded from below and from above by 0 and 1, respectively.

As the specialized literature indicates, some variations of this model appear in many physically relevant situations; however, no explicit form of the solution is known for every possible scenario, whence the need for developing reliable numerical methods to approximate solutions of this model in general, and non-negative and bounded solutions in particular, is an important motivation of investigation in the field of scientific computing. In fact, in the present work, we propose a finite-difference scheme to approximate non-negative and bounded solutions of the FitzHugh-Nagumo equation treated in [78]. As we will show below, the method presented here is consistent with the problem under study, with an order of consistency of $\mathcal{O}(\Delta t + (\Delta x)^2)$ when Dirichlet boundary data are considered; moreover, the computational simulations support our claim that our method performs well when approximating non-negative and bounded solutions of the FitzHugh-Nagumo equation under investigation. Additionally, our numerical technique is linearly stable under some flexible constraints of the computational parameters, whence Lax's equivalence theorem immediately yields the convergence of the method in the linear regime. Furthermore, our method is easier to implement computationally than Crank-Nicholson procedures.

In Section 3.2 of this work, we present the nonlinear, partial differential equation under investigation, together with a particular solution that we will employ in order to verify the performance of our numerical method. Section 3.3 introduces the computational technique to approximate solutions of the model under study; here we prove that the method preserves the non-negativity and the boundedness of solutions of the model under some relatively flexible constraints on the computational and the model parameters. Moreover, a brief study of consistency is presented here, along with a Neumann analysis of linear stability and convergence. In Section 3.4, we show some simulations in order to assess the convergence of the method, and the properties of preservation of the non-negativity and the boundedness of the approximations. We devote some time to compare the performance of our technique against some known standard methods available in the literature. As expected, we show that our method is able to preserve the non-negative and the bounded character of solutions of the FitzHugh-Nagumo equation under consideration, when the standard techniques may not. Section 3.5 is the section where we discuss our results.

3.2 Preliminaries

3.2.1 Mathematical model

Let u be a function of the spatial variable x and the temporal variable t, where $x \in \mathbb{R}$ and $t > 0$. Assume that a is a real number in the interval $[0, \frac{1}{2}]$, and let κ and m be positive, real numbers. In this work, we approximate non-negative and bounded solutions of the partial differential equation

$$\frac{\partial u}{\partial t} = \kappa \frac{\partial^2 u}{\partial x^2} + m^2 u f(u), \tag{3.2}$$

where

$$f(u) = (1-u)(u-a). \tag{3.3}$$

This model is called the *FitzHugh-Nagumo equation* or, for short, simply the *Nagumo equation*, and it is one of the simplest reaction-diffusion equations with nonlinear reaction. Evidently, it differs from the Fisher-KPP equation in the reaction term: In the Fisher-KPP model, $f(u) = 1 - u$. Moreover, as we mentioned in the introductory section, (3.2) is a particular case of the Burgers-Huxley equation given by (3.1).

Before closing this section of our study, we must point out that appropriate initial and boundary conditions must be imposed upon (3.2) in order to be able to numerically approximate solutions to this model. As we will mention in Section 3.3, we will consider non-negative Dirichlet conditions bounded from above by 1. At the same time, we will consider non-negative and bounded profiles satisfying (3.2) at any instant.

3.2.2 Particular solutions

For the rest of this manuscript, we tacitly let κ and m be both equal to 1 in (3.2). This assumption is fully justified by an elementary non-dimensional analysis of the equation (3.2). Under this convention, the FitzHugh-Nagumo equation presented in this work admits a solution in the form of a traveling wave front, namely, the function

$$u(x,t) = \frac{A\exp(z_1) + aB\exp(z_2)}{A\exp(z_1) + B\exp(z_2) + C}, \tag{3.4}$$

where

$$z_1 = \pm\frac{1}{\sqrt{2}}x + \left(\frac{1}{2} - a\right)t, \tag{3.5}$$

$$z_2 = \pm\frac{1}{\sqrt{2}}ax + a\left(\frac{1}{2}a - 1\right)t, \tag{3.6}$$

and A, B and C are arbitrary constants [78].

3.3 Numerical method

3.3.1 Finite-difference scheme

Let M and N be positive integers. In order to approximate solutions of (3.2) over the real line, we restrict our attention to a bounded spatial domain $[a_s, b_s]$, and impose appropriate boundary conditions. In order to approximate the solution of an initial-value problem associated to the FitzHugh-Nagumo problem under study over a temporal interval $[0, T]$, we fix regular partitions $a_s = x_0 < x_1 < \ldots < x_N = b_s$ and $0 = t_0 < t_1 < \ldots < t_M = T$ of $[a_s, b_s]$ and $[0, T]$, respectively, with norms $\Delta x = (b_s - a_s)/N$ and $\Delta t = T/M$, in each case.

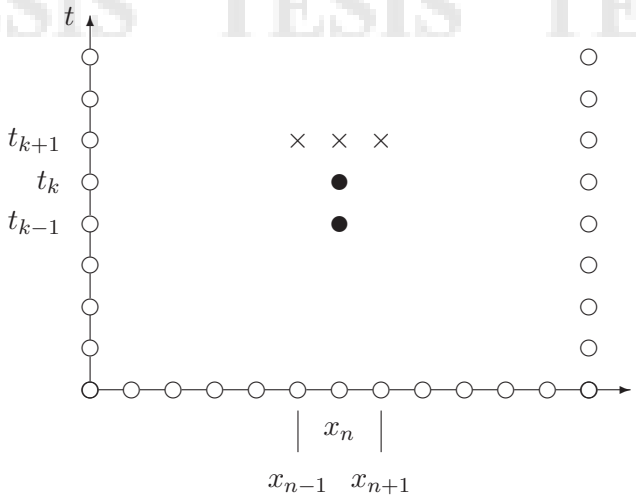

Figure 3.1: Forward-difference stencil for the approximation to the partial differential equation (3.2) at time t_k, using the finite-difference scheme (3.9). The black circles represent known approximations to the actual solutions at times t_{k-1} and t_k, and the crosses denote the unknown approximations at time t_{k+1}.

For every $n = 0, 1, \ldots, N$ and every $k = 0, 1, \ldots, M$, we denote by u_n^k the approximation provided by our method to the exact value of $u(x_n, t_k)$. Moreover, we introduce the following nomenclature in order to approximate, respectively, the first-order partial derivative of u with respect to t in (3.2), and the second-order partial derivative of u with respect to x (that is, the diffusion term), at the point (x_n, t_k):

$$\delta_{t,\alpha} u_n^k = (1-\alpha)\frac{u_n^{k+1} - u_n^k}{\Delta t} + \alpha \frac{u_n^{k+1} - u_n^{k-1}}{2\Delta t}, \tag{3.7}$$

$$\delta_x^{(2)} u_n^k = \frac{u_{n+1}^k - 2u_n^k + u_{n-1}^k}{(\Delta x)^2}. \tag{3.8}$$

Evidently, (3.7) is a weighted approximation of $\partial u/\partial t$ at (x_n, t_k), in the form of a linear combination of a first-order and a second-order estimations of this term. Meanwhile, (3.8) is the standard, second-order approximation to $\partial^2 u/\partial t^2$ at (x_n, t_k).

With these conventions at hand, we will approximate solutions of (3.2) in the spatial domain $[a_s, b_s]$ over the temporal interval $[0, T]$, through the finite-difference scheme

$$\delta_{t,\alpha} u_n^k = \delta_x^{(2)} u_n^{k+1} + u_n^{k+1} f(u_n^k) \tag{3.9}$$

(recall that both κ and m are equal to 1 in this study). It is readily checked that the forward-difference stencil of our method is the one shown in Fig. 3.1, which is similar to that reported in [59]. This assertion follows immediately from the fact that the finite-difference scheme (3.9) may be conveniently rewritten as

$$k_1 u_{n-1}^{k+1} + k_2 u_n^{k+1} + k_1 u_{n+1}^{k+1} = k_3 u_n^k + k_4 u_n^{k-1}, \tag{3.10}$$

where

$$R = \frac{\Delta t}{(\Delta x)^2} \tag{3.11}$$

is the Fourier number of the finite difference scheme (3.9), and the coefficients k_1, k_2, k_3 and k_4 are, in general, functions that depend on u_n^k, whose expressions are provided in Table 3.1.

Table 3.1: Expressions of the coefficients in (3.10).

k_1	k_2	k_3	k_4
$-R$	$1-\dfrac{\alpha}{2}+2R-f(u_n^k)\Delta t$	$1-\alpha$	$\dfrac{\alpha}{2}$

Before closing this section, it is important to notice that the numerical method (3.9) is not a self-starting technique as it is, for instance, a Crank-Nicholson procedure. So, in order to start the iterative process given by (3.9), one needs to know the approximations at times t_0 and t_1. In our simulations, we will employ the particular solutions presented in Section 3.2.2; these exact solutions at the times t_0 and t_1 will provide the initial approximations needed by the recursive method. More concretely, for every $n = 0, 1, \ldots, N$ and $k = 0, 1$, we will let $u_n^k = u(x_n, t_k)$, where u is the function given by (3.4), for previously fixed constants A, B and C. If no exact solution is available, an initial profile together with an initial velocity of the solution around the time $t = 0$ are required.

3.3.2 Matrix representation

The recursive process summarized by the finite-difference scheme (3.9) assumes that the approximations at times t_0 and t_1 are known. In addition, appropriate boundary conditions at the ends of the spatial interval $[a_s, b_s]$ need to be employed. In this work, we will impose constraints of the form

$$u(a_s, t) = a_0(t) \quad \text{and} \quad u(b_s, t) = a_1(t), \tag{3.12}$$

satisfied for every $t \geq 0$. Here, a_0 and a_1 are non-negative, real functions which are less than or equal to 1. In our simulations, the functions a_0 and a_1 will be the actual solutions of the problem under investigation, evaluated at each of the endpoints of the spatial interval $[a_s, b_s]$.

Let $\mathcal{M}_n$ be the vector space of all matrices over $\mathbb{R}$ of size $n \times n$, for each positive integer n. Clearly, the numerical method (3.9) can be presented in matrix form as

$$A\mathbf{u}^{k+1} = \mathbf{b}^k, \tag{3.13}$$

for $k \in \{1, \ldots, M-1\}$. Here, $\mathbf{u}^k$ is the $(N+1)$-dimensional vector $(u_0^k, u_1^k, \ldots, u_N^k)$, for every $k \in \{0, 1, \ldots, M\}$. Moreover, for every $k \in \{1, \ldots, M\}$, we let

$$\mathbf{b}^k = B\mathbf{u}^k + C\mathbf{u}^{k-1} + \mathbf{d}^k, \tag{3.14}$$

where B and C are the diagonal matrices of $\mathcal{M}_{N+1}$ given by

$$B = \begin{pmatrix} 0 & 0 & \cdots & 0 & 0 \\ 0 & k_3 & \cdots & 0 & 0 \\ \vdots & \vdots & \ddots & \vdots & \vdots \\ 0 & 0 & \cdots & k_3 & 0 \\ 0 & 0 & \cdots & 0 & 0 \end{pmatrix} \quad \text{and} \quad C = \begin{pmatrix} 0 & 0 & \cdots & 0 & 0 \\ 0 & k_4 & \cdots & 0 & 0 \\ \vdots & \vdots & \ddots & \vdots & \vdots \\ 0 & 0 & \cdots & k_4 & 0 \\ 0 & 0 & \cdots & 0 & 0 \end{pmatrix}. \tag{3.15}$$

Finally, the matrix A is a member of $\mathcal{M}_{N+1}$, and the vector $\mathbf{d}^k$ is an $(N+1)$-dimensional vector; their expressions depend on the type of boundary data imposed upon the FitzHugh-Nagumo equation under investigation. If the problem has Dirichlet boundary conditions

of the form (3.12), we employ discrete Dirichlet constraints in the form of the expressions $u_0^k = a_0(t_k)$ and $u_N^k = a_1(t_k)$, for every $k \in \{0, 1, \ldots, M\}$. These conditions clearly translate into the following definitions of A and $\mathbf{d}^k$:

$$A = \begin{pmatrix} 1 & 0 & 0 & 0 & \cdots & 0 & 0 & 0 \\ k_1 & k_2 & k_1 & 0 & \cdots & 0 & 0 & 0 \\ 0 & k_1 & k_2 & k_1 & \cdots & 0 & 0 & 0 \\ \vdots & \vdots & \vdots & \vdots & \ddots & \vdots & \vdots & \vdots \\ 0 & 0 & 0 & 0 & \cdots & k_1 & k_2 & k_1 \\ 0 & 0 & 0 & 0 & \cdots & 0 & 0 & 1 \end{pmatrix}, \quad \mathbf{d}^k = \begin{pmatrix} a_0(t_{k+1}) \\ 0 \\ 0 \\ \vdots \\ 0 \\ a_1(t_{k+1}) \end{pmatrix}. \tag{3.16}$$

3.3.3 Numerical properties

Non-negativity

Recall that the parameters κ and m of (3.2) are equal to 1, and we assume that a is a real number in the interval $[0, \frac{1}{2}]$. A squared matrix is an *M-matrix* if it is strictly diagonally dominant, its off-diagonal entries are non-positive, and its diagonal entries are positive. Every M-matrix is nonsingular, and its inverse has non-negative entries [33].

Lemma 10. *The matrix A in* (3.16) *is an M-matrix if α belongs to* $(0, 1)$ *and the inequality*

$$\Delta t < \left(\frac{2}{1-a}\right)^2 \left(1 - \frac{\alpha}{2}\right) \tag{3.17}$$

is satisfied.

Proof. The matrix A has non-positive, off-diagonal entries. Now, if (3.17) is satisfied, then

$$\Delta t f(u_n^k) + 2R \leq \Delta t \left(\frac{1-a}{2}\right)^2 + 2R < 1 - \frac{\alpha}{2} + 2R. \tag{3.18}$$

Subtracting $\Delta t f(u_n^k)$ in each link of this chain of inequalities, we obtain that $|k_1| + |k_1| < |k_2|$, which means that A is strictly diagonally dominant with positive entries in the diagonal. We conclude that A is an M-matrix. □

It is worth noticing that a simpler condition to guarantee that the matrix A in Lemma 10 be strictly diagonally dominant, is readily at hand. The fact that $f(u) \leq \frac{1}{4}$ for every $u \in [0, 1]$ and every $a \in [0, \frac{1}{2}]$, gives us the non-negativity constraint

$$\Delta t < 4\left(1 - \frac{\alpha}{2}\right). \tag{3.19}$$

Recall that a_0 and a_1 are non-negative functions of time which are less than or equal to 1. These facts will be employed in the following propositions.

Proposition 11. *Let $k \in \{1, \ldots, M-1\}$, and assume that $\mathbf{u}^k$ and $\mathbf{u}^{k-1}$ are vectors with non-negative entries. If α belongs to the set* $(0, 1)$ *and the inequality* (3.17) *is satisfied, then the vector $\mathbf{u}^{k+1}$ in* (3.13) *has non-negative entries.*

Proof. It follows from the previous lemma and the facts that M-matrices are non-singular matrices for which their inverses have non-negative entries, and that the right-hand side of (3.13) is a vector with non-negative entries. □

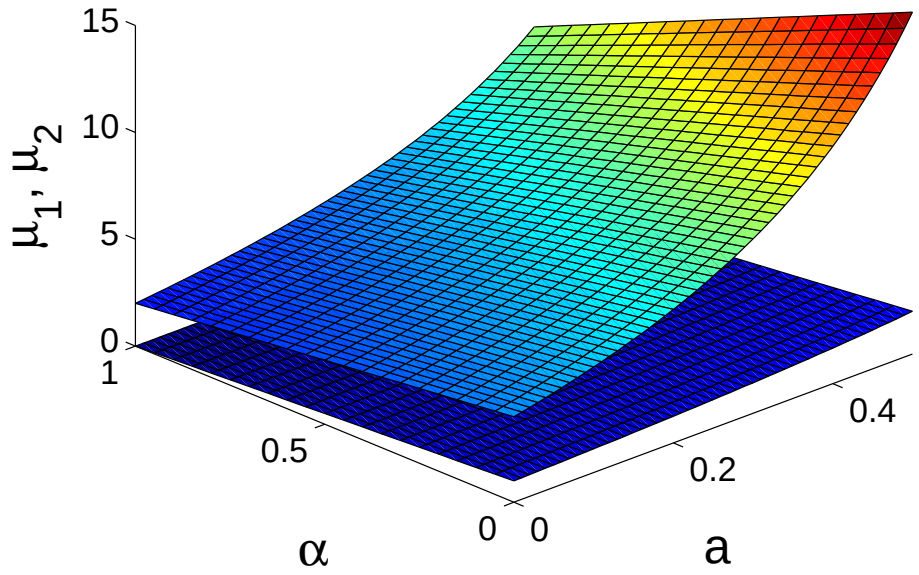

Figure 3.2: Graph of the functions $\mu_1 = (4-2\alpha)/(1-a)^2$ and $\mu_2 = (1-\alpha)/(1-a)$ as functions of a and α, for $0 \leq a \leq \frac{1}{2}$ and $0 \leq \alpha \leq 1$. The top surface is the graph of μ_1, while the bottom one represents the graph of μ_2.

Boundedness

We need the following result in order to establish conditions to guarantee the boundedness of our finite-difference scheme.

Lemma 12. *Let $D = \{(x,y) \in \mathbb{R}^2 : x, y \leq 1\}$, and let $G : D \to \mathbb{R}$ be the function given by $G(x,y) = 1 - \frac{\alpha}{2} - \Delta t f(x) - (1-\alpha)x - \frac{\alpha}{2}y$. If $0 < \alpha < 1$ and the inequality*

$$\Delta t(1-a) < 1 - \alpha \tag{3.20}$$

is satisfied, then $\frac{\partial G}{\partial x}(x,y)$ and $\frac{\partial G}{\partial y}(x,y)$ are negative, for every $(x,y) \in G$. Moreover, $G(1,1) = 0$.

Proof. The proof is an elementary application of vector calculus. □

Corollary 13. *Under the assumptions and the nomenclature of Lemma 12, the function G is positive in the interior of D.*

Proof. The conclusion is a consequence of the previous result and the continuity of G on the plane $\mathbb{R}^2$. □

We say that an n-dimensional, real vector $\mathbf{u}$ is *non-negative* if all of its components are non-negative; we represent this fact through the notation $\mathbf{u} \geq 0$. The vector $\mathbf{u}$ is *bounded from above* by 1 if all of its components are bounded from above by 1, and we denote this by $\mathbf{u} \leq 1$. Evidently, if $\mathbf{e}$ represents the n-dimensional vector whose components are all equal to 1, then $\mathbf{u} \leq 1$ if and only if $\mathbf{e} - \mathbf{u} \geq 0$. These conventions and remarks will be observed in the next result.

Proposition 14. *Suppose that α belongs to $(0,1)$, and let $k \in \{1,\dots,M-1\}$. Suppose that $\mathbf{u}^k$ and $\mathbf{u}^{k-1}$ are vectors bounded from above by 1. The vector $\mathbf{u}^{k+1}$ is likewise bounded from above by 1 if*

$$\Delta t < \min\left\{\frac{4-2\alpha}{(1-a)^2}, \frac{1-\alpha}{1-a}\right\}. \tag{3.21}$$

Proof. Let $\mathbf{w}^{k+1} = \mathbf{e} - \mathbf{u}^{k+1}$. Then (3.13) can be rewritten in terms of $\mathbf{w}^{k+1}$ as

$$A\mathbf{w}^{k+1} = A\mathbf{e} - B\mathbf{u}^k - C\mathbf{u}^{k-1} - \mathbf{d}^{k+1}, \tag{3.22}$$

where A is an M-matrix by virtue of the fact that the choice of Δt satisfies the conditions of Lemma 10. The vector in the right-hand side of (3.22) has non-negative first and last components. Now, if $n \in \{1,\dots,N-1\}$, then the expression of the $(n+1)$th component of the right-hand side of (3.22) is given by $G(u_n^k, u_n^{k-1})$, where G is the function defined in Lemma 12. The fact that the constraint (3.20) is satisfied, implies that the right-hand side of (3.22) is a non-negative vector. It follows that $\mathbf{w}^{k+1}$ is also non-negative or, equivalently, that $\mathbf{u}^{k+1} \leq 1$. □

Corollary 15. *Suppose that α belongs to $(0,1)$, and let $k \in \{1,\dots,M-1\}$. Assume that $\mathbf{u}^k$ and $\mathbf{u}^{k-1}$ are non-negative vectors bounded from above by 1. The vector $\mathbf{u}^{k+1}$ is likewise non-negative and bounded from above by 1 whenever (3.20) is satisfied.*

Proof. This result follows from the fact that the first bound for Δt in (3.21) is always greater than or equal to the second. This relation between the upper bounds for Δt can easily be established through simple algebraic manipulations, and it is depicted in Fig. 3.2. □

It is interesting to notice that the non-negativity and the boundedness constraints summarized in Proposition 14 do not depend on the value of the parameter Δx. This fact and Corollary 15 are our main evidences in favor of the flexibility of the finite-difference scheme (3.9), in order to guarantee the non-negative and the bounded characters of the approximate solutions.

Consistency

The method studied in this work approximates solutions to (3.2) with a consistency of the order of $\mathcal{O}(\Delta t + (\Delta x)^2)$ when Dirichlet conditions are imposed on the boundaries. This statement is evidenced by the following Taylor series approximations:

$$\frac{u_n^{k+1} - u_n^k}{\Delta t} \approx \frac{\partial u}{\partial t}(x_n, t_{k+1}) - \frac{\Delta t}{2}\frac{\partial^2 u}{\partial t^2}(x_n, t_{k+1}), \tag{3.23}$$

$$\frac{u_n^{k+1} - u_n^{k-1}}{2\Delta t} \approx \frac{\partial u}{\partial t}(x_n, t_{k+1}) - \Delta t\frac{\partial^2 u}{\partial t^2}(x_n, t_{k+1}), \tag{3.24}$$

$$\delta_x^{(2)} u_n^{k+1} \approx \frac{\partial^2 u}{\partial x^2}(x_n, t_{k+1}) + \frac{(\Delta x)^2}{12}\frac{\partial^4 u}{\partial x^4}(x_n, t_{k+1}). \tag{3.25}$$

As a consequence, $u(x_n, t_{k+1})$ is approximated by u_n^{k+1} with the stated order of consistency.

Stability and convergence

In this section, we establish the properties of linear stability and convergence of the finite-difference scheme (3.9). We state the main result of the section right away.

Proposition 16. *A sufficient condition for the finite-difference scheme (3.9) with reaction function f identically equal to 0 to be stable, is that $0 < \alpha < 1$.*

Proof. Let $u_n^k = c_k e^{in\theta}$, for every $n \in \{0, 1, \ldots, N\}$ and every $k \in \{0, 1, \ldots, M\}$. Substituting in (3.10) and simplifying, we obtain the identity

$$(2k_1 \cos\theta + k_2)c_{k+1} - k_3 c_k - k_4 c_{k-1} = 0. \tag{3.26}$$

The roots of the characteristic equation associated to (3.26) are given by

$$r_\pm = \frac{k_3 \pm \sqrt{k_3^2 + 4k_4(2k_1\cos\theta + k_2)}}{2(2k_1\cos\theta + k_2)} = \frac{1 - \alpha \pm \sqrt{1 + \alpha(8R\sin^2\frac{\theta}{2})}}{1 - \alpha + 1 + 8R\sin^2\frac{\theta}{2}}. \tag{3.27}$$

The inequality $|r_\pm| \leq r_+$ is satisfied by virtue of the fact that $\alpha < 1$. Moreover, it is clear that $r_+ \leq 1$, whence von Neumann stability follows. □

Corollary 17. *If $0 < \alpha < 1$ then the approximations given by the method* (3.9) *converge to the exact solutions of* (3.2)*, whenever f is identically equal to zero.*

Proof. The result follows from Proposition 16 and Lax's equivalence theorem. □

Before closing this section of our investigation, it is important to notice that the linear stability and convergence conditions summarized in Proposition 16 and Corollary 17, respectively, are in agreement with the non-negativity and boundedness constraints provided by Corollary 15. Also, we wish to mention that the numerical implementation of the finite-difference scheme (3.9) requires Thomas' technique for solving tridiagonal systems of linear equations [15].

3.4 Simulations

The purpose of this section is to show that the finite-difference scheme (3.9) approximates well the solutions of (3.2). In particular, we want to verify numerically that the method preserves the properties of non-negativity and boundedness of some solutions of the FitzHugh-Nagumo model under investigation, and that it converges to the solution. Throughout, the parameters κ and m in (3.2) will be equal to 1.

3.4.1 Preserved properties

We wish to verify computationally that our method preserves the properties of non-negativity and boundedness of solutions of (3.2). So, consider the partial differential equation of interest defined on the real line, with nonlinear reaction term (3.3) and a equal to 0.125. The data at the initial time $t = 0$ is given by the expression of the traveling wave solution (3.4) at that time, with constants A, B and C all equal to 1, with initial velocity being actually the velocity of the traveling wave (3.4) at $t = 0$. Computationally, we restrict our attention to the closed and bounded, spatial domain $[-80, 80]$, and impose Dirichlet boundary data given by the exact solution at the endpoints of this interval.

Example 18. *Let $\alpha = 0.543$, and let Δx be equal to 0.1. We let Δt be equal to 0.001, so that the non-negativity and the boundedness conditions of Proposition 14 are satisfied. Fig. 3.3 presents a comparison of the exact solution to the initial-boundary-value problem under study, and the corresponding approximate solution provided by our method, at four different times, namely, $t = 0.008$, 0.08, 0.8 and 8. The graphs evidence a good agreement between the theoretical and the numerical results, even for relatively longer periods of time, as Fig. 3.4 shows.*

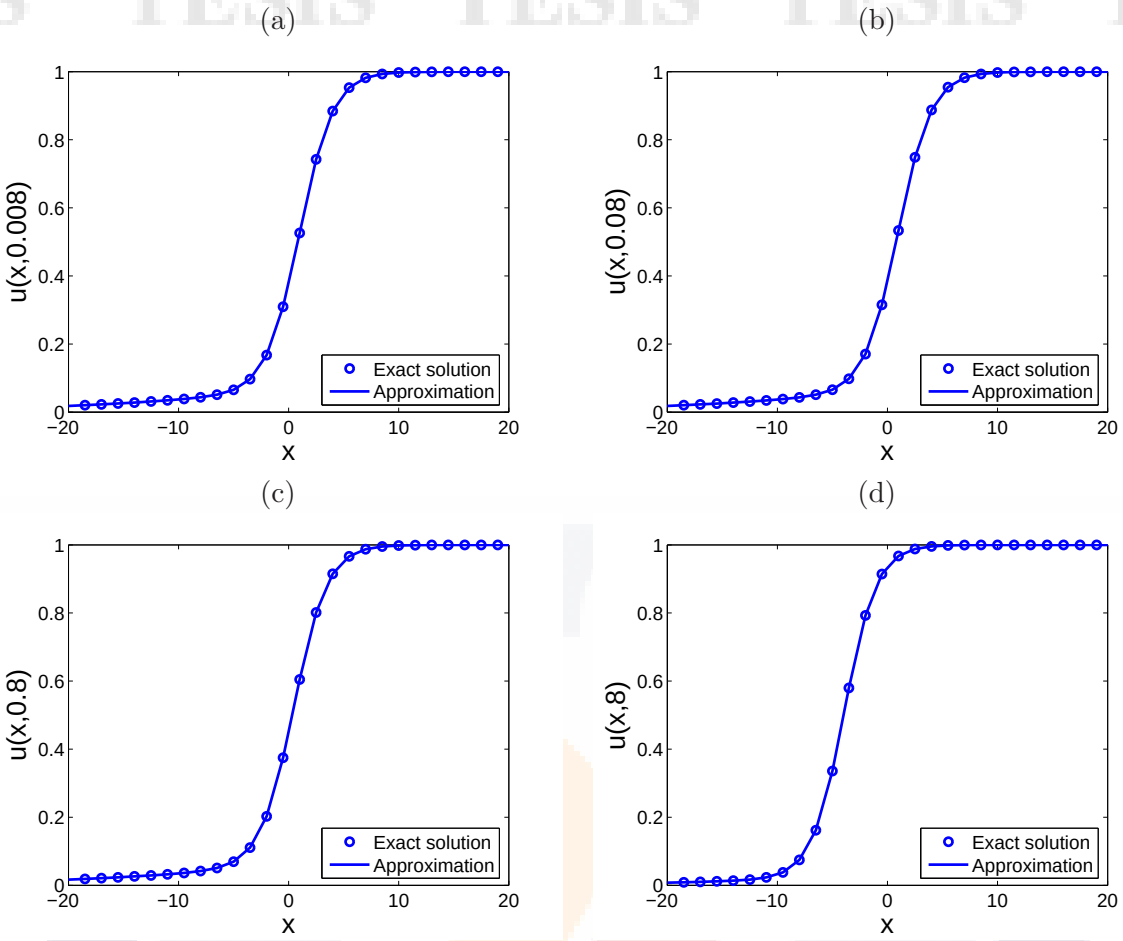

Figure 3.3: Graphs of the approximate and exact solutions of the partial differential equation (3.2) with reaction term (3.3) at several times, namely, (a) $t = 0.008$, (b) $t = 0.08$, (c) $t = 0.8$ and (d) $t = 8$. The initial data are the profile and the velocity associated to the particular solution (3.4) around the time $t = 0$, with $A = B = C = 1$. The model parameters $\kappa = m = 1$ and $a = 0.45$ were fixed, along with the discrete steps $\Delta x = 0.1$ and $\Delta t = 0.001$. Computationally, we restricted our attention to the spatial domain $[-80, 80]$, and imposed discrete, Dirichlet boundary conditions.

We must state that we have performed more simulations in order to verify that the finite-difference scheme (3.9) preserves the non-negativity and the boundedness of the solutions of (3.2), for values of the parameters satisfying the constraints in Proposition 14. The results (not included here for obvious reasons) show that the sufficient conditions of that proposition yield non-negative and bounded approximations to the non-negative and bounded solutions of the model under study.

3.4.2 Convergence

For the sake of numerical comparison, we associate the usual norms $\|\cdot\|_1$, $\|\cdot\|_2$ and $\|\cdot\|_\infty$ to the real vector space $\mathbb{R}^n$, for every positive integer n. For every such norm $\|\cdot\|_*$ and every pair of vectors $\mathbf{x}$ and $\mathbf{y}$ of $\mathbb{R}^n$, we define the *relative error* committed when approximating $\mathbf{y}$ by $\mathbf{x}$, by means of the expression

$$\rho_*(\mathbf{x}, \mathbf{y}) = \frac{\|\mathbf{x} - \mathbf{y}\|_*}{\|\mathbf{y}\|_*}. \tag{3.28}$$

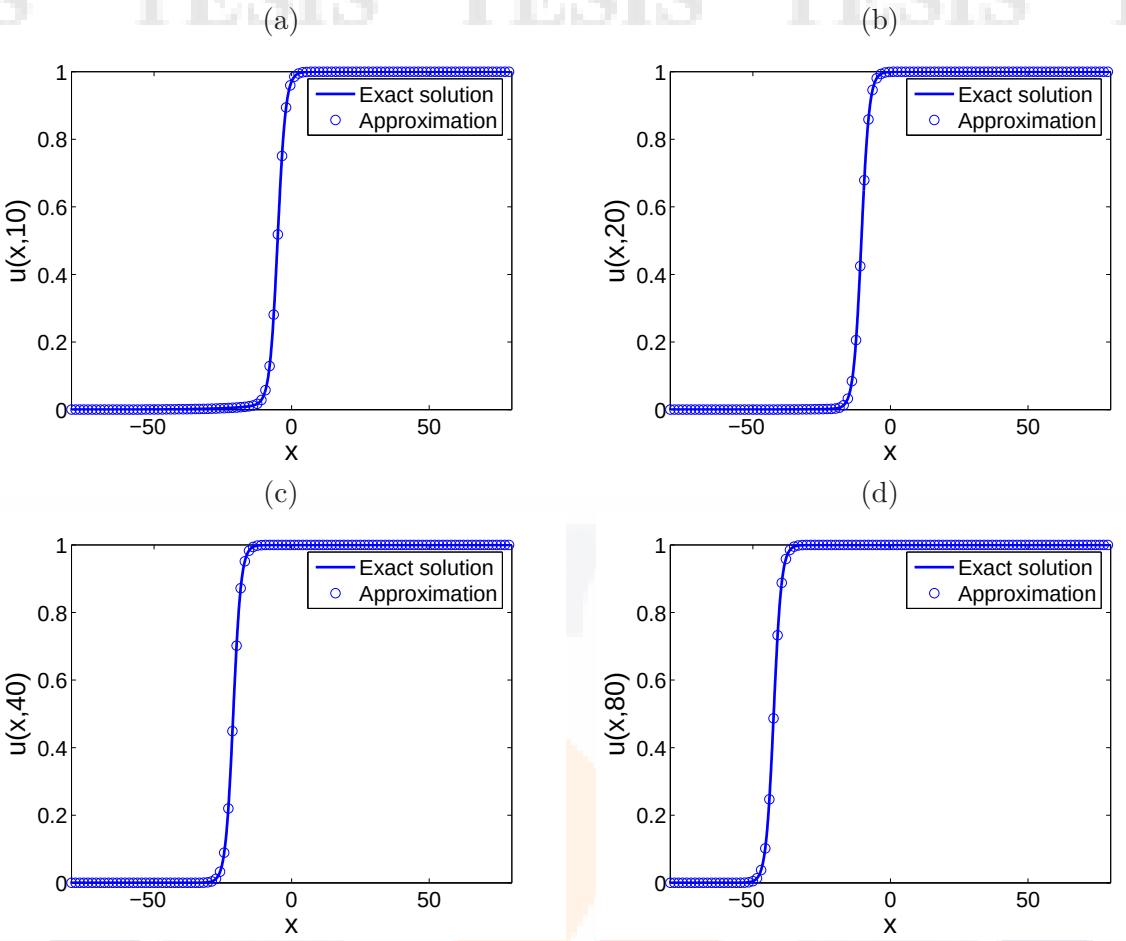

Figure 3.4: Graphs of the approximate and exact solutions of the partial differential equation (3.2) with reaction term (3.3) at several times, namely, (a) $t = 10$, (b) $t = 20$, (c) $t = 40$ and (d) $t = 80$. The initial data are the profile and the velocity associated to the particular solution (3.4) around the time $t = 0$, with $A = B = C = 1$. The model parameters $\kappa = m = 1$ and $a = 0.45$ were fixed, along with the discrete steps $\Delta x = 0.1$ and $\Delta t = 0.001$. Computationally, we restricted our attention to the spatial domain $[-80, 80]$, and imposed discrete, Dirichlet boundary conditions.

Evidently, this equation may not be numerically applicable when the denominator is close or equal to zero, in which case an *absolute error* formula of the form $\rho_*(\mathbf{x}, \mathbf{y}) = \|\mathbf{x} - \mathbf{y}\|_*$ may be more useful.

Example 19. *Consider now the problem presented in Example 18, with the same model and computational parameters. Under these circumstances, Fig. 3.5 presents the temporal behavior of the relative error when approximating the exact solution of the problem by means of* (3.9)*, using the three standard norms of* $\mathbb{R}^n$*.*

Example 20. *Once more, consider the initial-boundary-value problem studied in the previous section with the same values of the model parameters, over a time period of length* 50*. Several values of the computational parameters* Δt *and* Δx *were selected and, for each such pair of values and each of the usual norms in the previous paragraph, we computed the relative error of the final approximation at the time of interest with respect to the exact solution. The numerical results are presented in Table 3.2, and they agree with the fact that the linearized version of the method is convergent.*

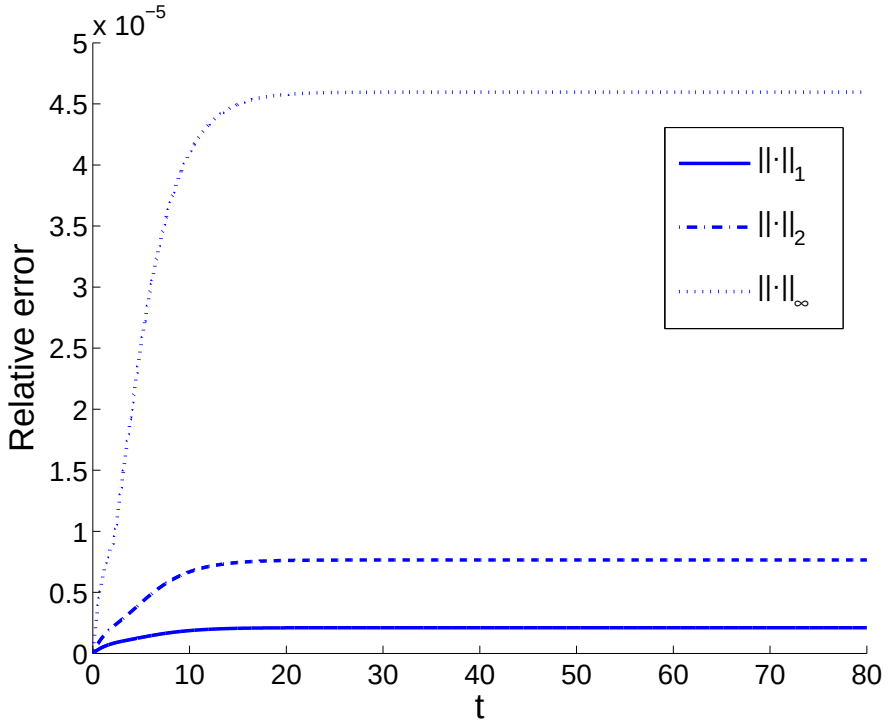

Figure 3.5: Temporal dynamics of the relative error (3.28) committed when approximating the exact solution of (3.2) through the finite-difference scheme (3.9). The reaction factor assumes the form (3.3), and the initial data are the profile and the velocity associated to the particular solution (3.4) around the time $t = 0$, with $A = B = C = 1$. The model parameters $\kappa = m = 1$ and $a = 0.45$ were fixed, along with the discrete steps $\Delta x = 0.1$ and $\Delta t = 0.001$. Computationally, we restricted our attention to the spatial domain $[-80, 80]$, and imposed Dirichlet boundary conditions. Three different norms were employed to compute the relative error, namely, the $\|\cdot\|_1$-norm (solid), the $\|\cdot\|_2$-norm (dash-dotted), and the $\|\cdot\|_\infty$-norm (dotted).

3.4.3 Comparisons

In this section of our work, we compare the performance of method (3.9) against some well-known, computational techniques of higher order of consistency. In particular, we are interested in comparing the properties of preservation of the non-negativity and the boundedness of the solutions of (3.2), against a nonlinear Crank-Nicholson procedure and a standard, three-time level, numerical technique. Both methods have a consistency of order $\mathcal{O}((\Delta t)^2 + (\Delta x)^2)$ in the linear regime. The first of them (that is, the Crank-Nicholson method) is given by

$$\frac{u_n^{k+1} - u_n^k}{\Delta t} = \frac{1}{2}\left(\delta_x^{(2)} u_n^{k+1} + \delta_x^{(2)} u_n^k\right) + \frac{1}{2}\left(u_n^{k+1} f(u_n^{k+1}) + u_n^k f(u_n^k)\right). \tag{3.29}$$

The second method considered for comparison purposes is the following standard, three-step technique:

$$\frac{u_n^{k+1} - u_n^{k-1}}{2\Delta t} = \delta_x^{(2)} u_n^k + u_n^k f(u_n^k). \tag{3.30}$$

Example 21. *Consider the problem* (3.2) *with* κ *and* m *both equal to* 1*, spatially defined on the interval* $[-100, 100]$*, with* a *equal to* 0.5*. We employ as initial profile the particular solution presented in Section 3.2.2, with* A*,* B *and* C *all equal to* 1*. As Dirichlet*

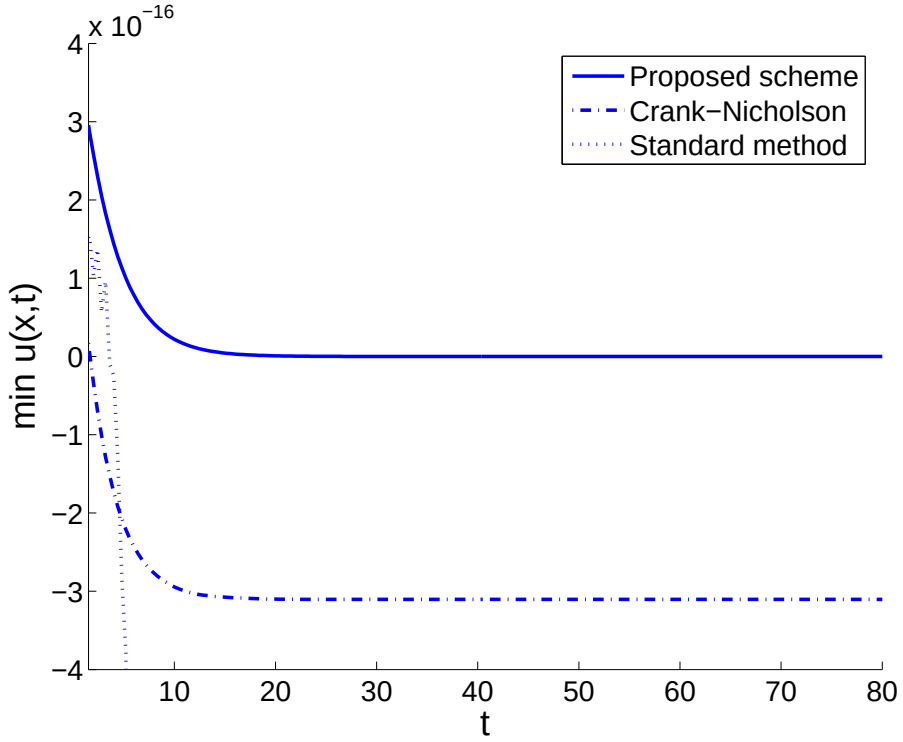

Figure 3.6: Graphs of the variable $\min\{u_n^k : n = 0, 1, \ldots, N\}$ versus t_k, where u_n^k represent the approximate solution of the partial differential equation (3.2), with $\kappa = m = 1$ and $a = 0.5$, over the spatial interval $[-100, 100]$, using the method (3.9) (solid), method (3.29) (dash-dotted), and method (3.30) (dotted). The initial conditions are given by (3.4) with $A = B = C = 1$, and the Dirichlet boundary conditions are given by the exact solution at the endpoints of the interval. Computationally, the parameters $\alpha = 0.543$, $\Delta x = 2$ and $\Delta t = 0.4$ were employed.

boundary conditions, we use the exact solution at the endpoints of the spatial interval, and we approximate the solutions on a period of time of length equal to 80. *Computationally, we use a parameter* α *equal to* 0.543, *and step sizes* $\Delta x = 2$ *and* $\Delta t = 0.4$, *so that the Fourier number* R, *as given by* (3.11), *is equal* 0.1*; in this way, the non-negativity and boundedness constraints summarized in Propositions 11 and 14 are satisfied. We employ the finite-difference scheme* (3.9), *as well as the methods* (3.29) *and* (3.30), *to approximate solutions of the initial-boundary-value problem. The results are presented in Fig. 3.6 as a time-dependent graph of the minimum value of the approximate solution obtained with each of the methods. In other words, Fig. 3.6 presents the dependence of the variable* $\min\{u_n^k : n = 0, 1, \ldots, N\}$ *on* t_k. *The results show that the Crank-Nicholson method and the standard technique (namely,* (3.29) *and* (3.30)*) may not be able to preserve the non-negativity of the solutions, even for relatively small, Fourier numbers* R. *On the other hand, scheme* (3.9) *is able to preserve the non-negative character of solutions.*

Table 3.2: Relative errors of the numerical approximation at time 50 obtained using (3.9), with respect to the exact solution[a] of the model (3.2)[b], for different values of the parameters Δx and Δt[b], and the three standard norms of $\mathbb{R}^n$.

	$\Delta x = 0.04$		
	Δt		
Norm	1×10^{-3}	5×10^{-4}	2.5×10^{-4}
$\|\cdot\|_1$	1.2283×10^{-5}	4.2456×10^{-6}	8.9076×10^{-7}
$\|\cdot\|_2$	3.3658×10^{-5}	1.0730×10^{-5}	1.9469×10^{-6}
$\|\cdot\|_\infty$	1.3767×10^{-4}	4.1846×10^{-5}	1.0084×10^{-5}
	$\Delta x = 0.02$		
	Δt		
Norm	5×10^{-4}	2.5×10^{-4}	1×10^{-4}
$\|\cdot\|_1$	7.2513×10^{-6}	3.2317×10^{-6}	8.1991×10^{-7}
$\|\cdot\|_2$	1.9949×10^{-5}	8.4534×10^{-6}	1.6687×10^{-6}
$\|\cdot\|_\infty$	8.3043×10^{-5}	3.4491×10^{-5}	6.0764×10^{-6}

[a]The exact solution is given by (3.4), with $A = B = C = 1$.
[b]The model parameters $\kappa = m = 1$, $a = 0.125$ were employed.
[c]Throughout, $\alpha = 0.543$.

3.5 Discussion

It is important to notice that the method presented in this work is consistent of order $\mathcal{O}(\Delta t + (\Delta x)^2)$ when Dirichlet conditions are imposed on the boundaries of the spatial domain. If discrete homogeneous Neumann boundary conditions of the form

$$u_N^k - u_{N-1}^k = u_1^k - u_0^k = 0 \tag{3.31}$$

are imposed at every discrete time-step, then it is possible to check that the non-negativity and the boundedness conditions derived in the present work are still valid for this case, however, the method becomes a first-order technique in both space and time. In order to possess a numerical technique consistent of second order in space when homogeneous Neumann conditions are imposed, a slight modification of the method must be implemented on the boundaries: For such case, one may employ the following second-order approximations of the partial derivatives with respect to x at every time t_k:

$$3u_0^k - 4u_1^k + u_2^k = 3u_N^k - 4u_{N-1}^k + u_{N-2}^k = 0. \tag{3.32}$$

In this case, the method is consistent of order $\mathcal{O}(\Delta t + (\Delta x)^2)$; however, the matrix A associated to the method is neither tridiagonal nor diagonally positive and, hence, the results presented in this work are not valid.

Of course, our method presents advantages and disadvantages with respect to other methods available in the standard literature. In terms of order of consistency, our method has a low accuracy when compared against methods like Crank-Nicholson. On the other hand, our results have shown that methods with higher order may be incapable of preserving the properties of non-negativity and boundedness of solutions of the FitzHugh-Nagumo

equation under investigation. From this point of view, the finite-difference scheme (3.9) has the advantage of possessing sufficient conditions on the computational parameters that guarantee that the approximations will be non-negative and bounded, a characteristic that, for instance, the Crank-Nicholson method may not possess.

On the other hand, the Crank-Nicholson procedure employed to approximate solutions of (3.2) is a two-time level method while, as depicted in Fig. 3.1, our technique is a three-time level procedure. However, the computational implementation of the Crank-Nicholson method requires an implementation of Newton's method together with Thomas' algorithm to solve tridiagonal systems of equations, while the implementation of (3.9) only demands the use of Thomas' method at each time level. From that point of view, our numerical technique is evidently more economic in terms of computational implementation and computer time.

Finally, it is important to notice that the condition for the matrix A —as given by (3.16)— to be an M-matrix depends on the discretization of the temporal derivative of u. Recall that Lemma 10 establishes conditions under which A is an M-matrix, and that such conditions involve the computational parameter α. The inclusion of such parameter in the discretization of the partial derivative of u with respect to t represents an advantage on the one hand, in view that it provides some flexibility to guarantee that the matrix A is an M-matrix and, ultimately, it gives flexibility in order to assure that the method preserves the non-negative character of solutions (see Proposition 11). Moreover, it is worth noticing that the simpler condition (3.19) for the preservation of the non-negativity of solution of (3.2) may be further simplified if α is equal to 1. In such case, the method (3.9) becomes a consistent method of second order in time, and the non-negativity constraint assumes the simpler form $\Delta t < 2$.

Chapter 4

A generalized Burgers-Huxley equation

In this article, we propose a non-standard, finite-difference scheme to approximate the solutions of a generalization of the Burgers-Huxley equation from fluid dynamics. Our numerical method preserves the skew-symmetry of the partial differential equation under study and, under some analytical constraints of the model constants and the computational parameters involved, it is capable of preserving the boundedness and the positivity of the solutions. In the linear regime, the scheme is consistent of first order in time (due partially to the inclusion of a tuning parameter in the approximation of a temporal derivative), and of second order in space. We compare the results of our computational technique against the exact solutions of some particular initial-boundary-value problems. Our simulations indicate that the method presented in this work approximates well the theoretical solutions and, moreover, that the method preserves the boundedness of solutions within the analytical constraints derived here. In the problem of approximating solitary-wave solutions of the model under consideration, we present numerical evidence on the existence of an optimum value of the tuning parameter of our technique, for which a minimum relative error is achieved. Finally, we linearly perturb a steady-state solution of the partial differential equation under investigation, and show that our simulations still converge to the same constant solution, establishing thus robustness of our method in this sense.

4.1 Introduction

In many particular situations, the numerical investigation of physical systems involves the simultaneous study of multiple domains of interest. For instance, a computational investigation of a medium where the energy is conserved throughout time requires the design of numerical methods to approximate not only the solutions of the problem, but also the local and the total energy of the system, in such way that the discrete energy of the medium be constant at all times. The idea behind this practice arises from two reasons at least: From a numerical perspective, the use of a numerical method that preserves the properties of a system in several scenarios is a positive sign of the validity of the technique and its implementation; from a physical point of view, the analysis of the dynamics of several physical characteristics may actually give more insight into the problem under investigation (as is the case, for example, in the analysis of the process of supratransmission in nonlinear media [55]). This avenue of computational research has proved to be fruitful,

indeed. In fact, many numerical techniques to approximate nonlinear wave equations have been designed specifically with this sole purpose in mind [35].

Nowadays, there are many numerical methods available in the specialized literature which guarantee the preservation of physical properties that are inherent to the exact solutions of the problems under investigation. For instance, some computational techniques have been designed to approximate consistently the solutions of dissipative media [34], while other methods have been developed with the property of mass conservation in mind [19]. The first problem is clearly a generalization of the avenue of research mentioned above, in which the property of conservation of the energy of a system is crucial to the design of appropriate computational techniques with physical relevance, while the second is an extension of the same departing problem to the conservation of mass in a system. As an imminent consequence, one may take this last direction of research further and design numerical techniques to approximate solutions of media with variable mass, with the time-dependent rate of change of the mass of the system as the motivating property.

On the other hand, several methods have been designed with the aim of preserving some mathematical characteristic of the solutions of the governing equation, like the properties of positivity, boundedness, symmetry or monotonicity. In the particular case of the properties of positivity and boundedness, the problems where these conditions play a central role are diverse in their physical nature. Thus, the condition of positivity is crucial in the investigation of the population dynamics of certain viruses in epidemiology [5], or in the study of the propagation of forest fires when the variable of interest is the temperature measured in an absolute scale [61]. In turn, the condition of boundedness assumes an important part in the study of the dynamics of populations with limited resources (such is the case for models in which a carrying capacity is considered), or in the investigation of the evolution of the concentration of a certain component in a chemical substance [86].

The problem of designing finite-difference schemes that preserve one or more of the properties of positivity, boundedness and symmetry of physical problems, has been attacked successfully in some particular cases by employing the family of non-standard methods popularized by R. Mickens [63]. This class of numerical techniques has allowed many computational methods to approximate solutions of epidemic models [5, 4], of the Lotka-Volterra system [65], of the linear wave equation with constant damping [68, 69], of bioremediation problems [17], of predator-prey models [71], of the nonlinear heat equation in a thin finite rod [41], among other problems of physical relevance. Motivated by this background, in the present work, we design a non-standard, finite-difference scheme that preserves the positivity, the boundedness and the symmetry of the solutions of a generalized Burgers-Huxley equation, under suitable, flexible conditions on the model and the computational parameters involved. We employ here the concept of M-matrices to establish the properties of the method. Our simulations evince not only a good agreement between the exact solutions and their numerical approximations, but also the method preserves in practice the properties of positivity and boundedness of the solutions.

Section 4.2 of this manuscript introduces the mathematical model under investigation in this work, namely, a nonlinear, parabolic partial differential equation that generalizes the Burgers-Huxley equation from fluid dynamics. At this stage, we provide some particular solutions of the differential equation under consideration, in the form of traveling-wave solutions. Additionally, we notice the skew-symmetry of the generalized Burgers-Huxley equation when the power in the nonlinear reaction term is an even, positive integer number. In Section 2.3, we present a finite-difference scheme to approximate solutions of our mathematical model. Then, we rewrite our method in matrix form for the sake of convenience, and establish that our technique is conditionally positivity- and boundedness-preserving and, moreover, that it preserves the skew-symmetry of the generalized Burgers-Huxley

equation. Most of the proofs of this section rely on the notion and the properties of the M-matrices from linear algebra. Section 4.4, in turn, presents some numerical results and contrasts them against the exact solutions presented previously, in order to assess the validity of the method. As a consequence, we notice that the numerical simulations are in good agreement with the expected results and, moreover, we observe that the properties of positivity and boundedness are preserved when the conditions derived in Section 4.3 hold.

4.2 Preliminaries

4.2.1 Mathematical model

Let α be a non-negative real number, let β, κ and δ be positive numbers with $\delta \geq 1$, and let γ be a real number in $(0, 1)$. Suppose that I is a (bounded or unbounded) interval in the set of real numbers. Throughout, u will be a function that depends on the spatial variable $x \in I$ and the temporal variable $t \geq 0$, which satisfies the advection-diffusion equation with nonlinear reaction term

$$\frac{\partial u}{\partial t} + \alpha u^{\delta} \frac{\partial u}{\partial x} - \kappa \frac{\partial^2 u}{\partial x^2} - \beta u f(u) = 0, \tag{4.1}$$

for every $x \in I$ and every $t \geq 0$, where

$$f(u) = (1 - u^{\delta})(u^{\delta} - \gamma). \tag{4.2}$$

In the present manuscript, this model is called the *generalized Burgers-Huxley equation*, and it is a quantitative paradigm which describes the interaction between reaction mechanisms, convection effects and diffusion transport. We immediately identify here the constant κ as the coefficient of diffusivity, while α is the advection coefficient and β is the coefficient of reaction. The function (4.2) is the factor of (nonlinear) reaction, and it will be fixed throughout this work, unless stated otherwise.

It is worthwhile noticing that our mathematical model is actually a generalization of several important partial differential equations from mathematical physics. For instance, the partial differential equation (2.1) is the classical heat equation if α and β are equal to zero. If the advection coefficient is equal to zero, then our model becomes a generalization of the FitzHugh-Nagumo equation [28, 74, 85], which is a model employed in the study of the transmission of electric impulses in nervous systems. On the other hand, if α is equal to zero and the function f assumes the general form $f(u) = 1-u^{\delta}$, then the resulting equation is a generalized Fisher-KPP model [1], an equation that was investigated simultaneously and independently by R. A. Fisher [27], and A. Kolmogorov, I. Petrovski and N. Piscounov [47], in the context of population dynamics. In the frame of the Fisher-KPP equation, the case when *delta* equals 2 is of particular interest in the investigation of fluid dynamics, the arising model being identified as the Newell-Whitehead-Segel equation [75, 83]. Finally, the partial differential equation (4.1) is a generalized Burgers-Fisher equation [93] if f is the reaction function of the generalized Fisher-KPP equation.

As we mentioned above, we will assume that κ and β are positive real numbers. It is pragmatically important to notice that the partial differential equation (4.1) may be conveniently simplified for its study. In fact, if we let $\xi = x\sqrt{\beta/\kappa}$ and $\tau = \beta t$, then the model (4.1) can be written in terms of the new independent variables as

$$\mathcal{L}(u) = 0, \tag{4.3}$$

where

$$\mathcal{L}(u) = \frac{\partial u}{\partial t} + \alpha u^{\delta}\frac{\partial u}{\partial x} - \frac{\partial^2 u}{\partial x^2} - uf(u), \tag{4.4}$$

for every $x \in I$ and every $t \geq 0$. Here, the new coefficient α and the variables x and t have replaced the constant $\alpha/\sqrt{\beta\kappa}$ and the variables ξ and τ, respectively. It is important to point out that this simplified model will be our equation of interest in Section 4.4, which will be the proper scenario to perform some numerical simulations in order to assess the validity of the method presented in this manuscript.

The proof of the following result is straight-forward. The statement is valid for arbitrary, even functions f.

Proposition 22. *If $f : \mathbb{R} \to \mathbb{R}$ is an even function, then $\mathcal{L}(-u) = -\mathcal{L}(u)$.* □

As a consequence of this result, if δ is an even positive integer, then the function u is a solution of (4.3) if and only if $-u$ is likewise a solution. This property of the operator $\mathcal{L}$ is referred to as the property of *skew-symmetry* [90]. One of the aims of this work is to design a finite-difference scheme that preserves the skew-symmetry of the problem under investigation.

4.2.2 Particular solutions

Throughout this section and for the rest of this work, we will let κ be equal to 1. Moreover, for computational purposes, we may think of β as equal to 1, too, as it will be the case in Section 4.4.

Particular solution 1. The generalized Burgers-Huxley equation under investigation has a particular solution in the interval $I = [a, b]$, which satisfies the set of initial-boundary conditions

$$\begin{cases} u(x,0) = \left(\dfrac{\gamma}{2} + \dfrac{\gamma}{2}\tanh(a_1 x)\right)^{1/\delta}, & \text{for every } x \in I, \\ u(a,t) = \left(\dfrac{\gamma}{2} + \dfrac{\gamma}{2}\tanh(a_1(a - a_2 t))\right)^{1/\delta}, & \text{for every } t \geq 0, \\ u(b,t) = \left(\dfrac{\gamma}{2} + \dfrac{\gamma}{2}\tanh(a_1(b - a_2 t))\right)^{1/\delta}, & \text{for every } t \geq 0, \end{cases} \tag{4.5}$$

where

$$a_1 = \frac{-\alpha\delta + \delta\sqrt{\alpha^2 + 4\beta(1+\delta)}}{4(1+\delta)}\gamma, \tag{4.6}$$

$$a_2 = \frac{\gamma\alpha}{1+\delta} - \frac{(1+\delta-\gamma)(-\alpha + \sqrt{\alpha^2 + 4\beta(1+\delta)})}{2(1+\delta)}. \tag{4.7}$$

Such particular solution is given by the expression

$$u(x,t) = \left(\frac{\gamma}{2} + \frac{\gamma}{2}\tanh(a_1(x - a_2 t))\right)^{1/\delta}, \tag{4.8}$$

for every $x \in I$ and every $t \geq 0$ (see [39]). Evidently, if we consider the entire set of real numbers as the interval I, then the function (4.8) is a traveling-wave solution of the parabolic partial differential equation (4.1). These remarks will be important in the investigation of the performance of the method presented in Section 4.3. □

Particular solution 2. Let us consider once again the partial differential equation (4.1), with non-negative parameter α, a positive value of β, γ being a real number in the interval

$(0,1)$, and both κ and δ equal to 1. In this case, assume first that the spatial domain I is the entire real line. Then, the following function is a traveling-wave solution of the equation (4.1) which connects the two steady-state solutions $u = 0$ and $u = 1$, independently of the value of γ:

$$u(x,t) = \frac{1}{2} - \frac{1}{2}\tanh\left[\frac{\beta}{r-\alpha}(x - vt)\right], \tag{4.9}$$

where the constant r and the wave velocity v are given by

$$r = \sqrt{\alpha^2 + 8\beta}, \tag{4.10}$$

$$v = \frac{(\alpha - r)(2\gamma - 1) + 2\alpha}{4}. \tag{4.11}$$

These solutions are the result of employing symbolic computations and some relevant nonlinear transformations [50, 24, 92]. Evidently, the formula (4.9) is the particular solution in the interval $I = [a, b]$ of the associated initial-boundary-value problem

$$\begin{cases} u(x,0) = \dfrac{1}{2} - \dfrac{1}{2}\tanh\left(\dfrac{\beta x}{r-\alpha}\right), & \text{for every } x \in I, \\ u(a,t) = \dfrac{1}{2} - \dfrac{1}{2}\tanh\left[\dfrac{\beta}{r-\alpha}(a - vt)\right], & \text{for every } t \geq 0, \\ u(b,t) = \dfrac{1}{2} - \dfrac{1}{2}\tanh\left[\dfrac{\beta}{r-\alpha}(b - vt)\right], & \text{for every } t \geq 0. \end{cases} \tag{4.12}$$

□

4.3 Numerical method

In the present section, we introduce a numerical method to approximate the solutions of (4.1). The presentation is sufficiently general to account for families of functions f which properly include the nonlinear reaction factor (4.2). Evidently, the problem on the existence of solutions for such families is a task outside the scope of the present work.

4.3.1 Finite-difference scheme

For the rest of this work, we will let M and N be positive integers, we will let a and b be real numbers such that $a < b$, and let T be a positive real number. In order to approximate the solutions of the partial differential equation (4.3) in the spatial interval $I = [a, b]$ over the time period T, we fix uniform partitions $a = x_0 < x_1 < \ldots < x_N = b$ and $0 = t_0 < t_1 < \ldots < t_M = T$ of $[a, b]$ and $[0, T]$, respectively, each of them having norm equal to $\Delta x = (b - a)/N$ and $\Delta t = T/M$.

For every $n = 0, 1, \ldots, N$ and every $k = 0, 1, \ldots, M$, let u_n^k be an approximation of the exact value of the function u at (x_n, t_k). With these conventions, we define the following discrete, linear operators, for every $n = 1, \ldots, N - 1$ and every $k = 1, \ldots, M - 1$:

$$\delta_t u_n^k = \frac{u_n^{k+1} - u_n^k}{\Delta t}, \tag{4.13}$$

$$\delta_t^{(1)} u_n^k = \frac{u_n^{k+1} - u_n^{k-1}}{2\Delta t}, \tag{4.14}$$

$$\delta_x^{(1)} u_n^k = \frac{u_{n+1}^k - u_{n-1}^k}{2\Delta x}, \tag{4.15}$$

$$\delta_x^{(2)} u_n^k = \frac{u_{n+1}^k - 2u_n^k + u_{n-1}^k}{(\Delta x)^2}. \tag{4.16}$$

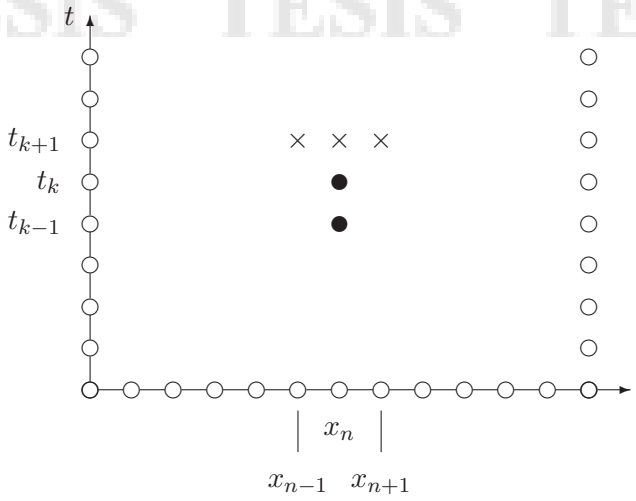

Figure 4.1: Forward-difference stencil for the approximation to the partial differential equation (4.3) at time t_k, using the finite-difference scheme (4.19). The black circles represent known approximations to the actual solutions at the times t_{k-1} and t_k, and the crosses denote the unknown approximations at the time t_{k+1}.

Notice that (4.13) and (4.14) provide consistent approximations of the exact value of $\frac{\partial u}{\partial t}$ at (x_n, t_k), of order $\mathcal{O}(\Delta t)$ and $\mathcal{O}((\Delta t)^2)$, respectively. In turn, the expressions (4.15) and (4.16) are consistent approximations of $\frac{\partial u}{\partial x}(x_n, t_k)$ and $\frac{\partial^2 u}{\partial x^2}(x_n, t_k)$, respectively, both of order $\mathcal{O}((\Delta x)^2)$. Meanwhile, for every real number λ in the set $(0, 1)$, the linear operator

$$\delta_{t,\lambda} u_n^k = \lambda \delta_t u_n^k + (1 - \lambda)\delta_t^{(1)} u_n^k \tag{4.17}$$

is evidently the weighted approximation of $\frac{\partial u}{\partial t}(x_n, t_k)$, formed by the linear combination of (4.13) and (4.14). Moreover, it is an easy task to establish that (4.17) is actually a consistent, first-order approximation in time, of the exact value of $\frac{\partial u}{\partial t}$ at (x_n, t_{k+1}).

For the sake of convenience, we define the computational parameter

$$R = \frac{\Delta t}{(\Delta x)^2}. \tag{4.18}$$

Under these circumstances, the finite-difference scheme employed to approximate the exact solutions of the simplified model (4.3) at the point x_n and the time t_{k+1}, is given by the discrete equation

$$\delta_{t,\lambda} u_n^k + \alpha (u_n^k)^\delta \delta_x^{(1)} u_n^{k+1} - \delta_x^{(2)} u_n^{k+1} - u_n^{k+1} f(u_n^k) = 0, \tag{4.19}$$

for every $n \in \{1, \ldots, N-1\}$ and every $k \in \{1, \ldots, M-1\}$. This method is clearly a non-standard, finite-difference technique that, in the linear regime, approximates the solutions of (4.3) with a consistency of order $\mathcal{O}(\Delta t + (\Delta x)^2)$. Moreover, some easy algebraic manipulations establish the following equivalent expression of the scheme (4.19), where the coefficients are those given in Table 4.1:

$$k_1 u_{n+1}^{k+1} + k_2 u_n^{k+1} + k_3 u_{n-1}^{k+1} = k_4 u_n^k + k_5 u_n^{k-1}. \tag{4.20}$$

In this expression, the coefficients k_4 and k_5 are constants, while k_1, k_2 and k_3 are functions of u_n^k, for every $n \in \{1, \ldots, N-1\}$. This dependency of k_1, k_2 and k_3 on u_n^k, however, is obviated for the sake of simplicity. As a corollary, the forward-difference stencil of the method (4.19) is the one depicted in Figure 4.1.

k_1	k_2	k_3	k_4	k_5
$\frac{\alpha(u_n^k)^\delta \Delta t}{2\Delta x} - R$	$1 - \frac{\lambda}{2} + 2R - \Delta t f(u_n^k)$	$-\frac{\alpha(u_n^k)^\delta \Delta t}{2\Delta x} - R$	$1 - \lambda$	$\frac{\lambda}{2}$

Table 4.1: Expressions of the coefficients in the explicit presentation of the finite-difference scheme (4.19), as given by Equation (4.20).

4.3.2 Matrix representation

For every $k = 0, 1, \ldots, M$, let $\mathbf{u}^k = (u_0^k, u_1^k, \ldots, u_N^k)$. The formula (4.20) readily induces a matrix representation of the finite-difference scheme (4.19) if we impose suitable, discrete boundary conditions on a bounded and closed interval I of $\mathbb{R}$. In our investigation, we will impose the discrete, Dirichlet boundary data

$$u_0^k = \phi(t_k), \quad u_N^k = \psi(t_k), \tag{4.21}$$

for every $k = 0, 1, \ldots, N$, where ϕ and ψ are suitable, real functions defined on the non-negative, real axis. Additionally, we suppose that ϕ and ψ satisfy the properties $\phi(t), \psi(t) \in (0, s^{1/\delta})$, for every $t \geq 0$, where s is a positive real number such that $s \leq 1$. Under these hypotheses, the numerical method (4.19) may be represented in vector form through

$$\mathbf{L}(\mathbf{u}^{k+1}, \mathbf{u}^k, \mathbf{u}^{k-1}) = \mathbf{0}, \tag{4.22}$$

where the function $\mathbf{L} : \mathbb{R}^{N+1} \times \mathbb{R}^{N+1} \times \mathbb{R}^{N+1} \to \mathbb{R}^{N+1}$ is prescribed by the rule

$$\mathbf{L}(\mathbf{u}^{k+1}, \mathbf{u}^k, \mathbf{u}^{k-1}) = A\mathbf{u}^{k+1} - B\mathbf{u}^k - C\mathbf{u}^{k-1} - \mathbf{b}^k. \tag{4.23}$$

Here, $\mathbf{0}$ is the zero vector of dimension $N+1$, A is the real matrix of size $(N+1) \times (N+1)$ given by

$$A = \begin{pmatrix} 1 & 0 & 0 & 0 & \cdots & 0 & 0 & 0 \\ k_1 & k_2 & k_3 & 0 & \cdots & 0 & 0 & 0 \\ 0 & k_1 & k_2 & k_3 & \cdots & 0 & 0 & 0 \\ \vdots & \vdots & \vdots & \vdots & \ddots & \vdots & \vdots & \vdots \\ 0 & 0 & 0 & 0 & \cdots & k_1 & k_2 & k_3 \\ 0 & 0 & 0 & 0 & \cdots & 0 & 0 & 1 \end{pmatrix}, \tag{4.24}$$

which is a function of the vector $\mathbf{u}^k$ in view of the fact that k_1, k_2 and k_3 are. In turn, the matrices B and C also have a size equal to $(N+1) \times (N+1)$ and are defined by

$$B = \begin{pmatrix} 0 & 0 & 0 & \cdots & 0 & 0 & 0 \\ 0 & k_4 & 0 & \cdots & 0 & 0 & 0 \\ 0 & 0 & k_4 & \cdots & 0 & 0 & 0 \\ \vdots & \vdots & \vdots & \ddots & \vdots & \vdots & \vdots \\ 0 & 0 & 0 & \cdots & k_4 & 0 & 0 \\ 0 & 0 & 0 & \cdots & 0 & k_4 & 0 \\ 0 & 0 & 0 & \cdots & 0 & 0 & 0 \end{pmatrix}, \quad C = \begin{pmatrix} 0 & 0 & 0 & \cdots & 0 & 0 & 0 \\ 0 & k_5 & 0 & \cdots & 0 & 0 & 0 \\ 0 & 0 & k_5 & \cdots & 0 & 0 & 0 \\ \vdots & \vdots & \vdots & \ddots & \vdots & \vdots & \vdots \\ 0 & 0 & 0 & \cdots & k_5 & 0 & 0 \\ 0 & 0 & 0 & \cdots & 0 & k_5 & 0 \\ 0 & 0 & 0 & \cdots & 0 & 0 & 0 \end{pmatrix}. \tag{4.25}$$

Additionally, $\mathbf{b}^k$ is the $(N+1)$-dimensional, real vector defined by

$$\mathbf{b}^k = (\phi(t_k), 0 \ldots, 0, \psi(t_k))^t. \tag{4.26}$$

Our next proposition is valid for a general class of functions f, which includes (4.2) when δ is an even, positive integer.

Proposition 23. *If $f : \mathbb{R} \to \mathbb{R}$ is an even function, then the identity $\mathbf{L}(-\mathbf{u}^{k+1}, -\mathbf{u}^k, -\mathbf{u}^{k-1}) = -\mathbf{L}(\mathbf{u}^{k+1}, \mathbf{u}^k, \mathbf{u}^{k-1})$ is satisfied for every $\mathbf{u}^{k+1}, \mathbf{u}^k, \mathbf{u}^{k-1} \in \mathbb{R}^{N+1}$.* □

As a consequence of this result and Proposition 22, we conclude that the finite-difference scheme (4.19) preserves the skew-symmetry of the model (4.3) under investigation, whenever δ is an even, positive integer number (we follow here the nomenclature found in [90]).

4.3.3 Numerical properties

In what follows, we will say that a (not necessarily square) matrix A is *positive* if every entry of A is a positive real number; such fact will be denoted by means of $A > 0$. On the other hand, if s is any real number, we will say that A is *bounded from above* by s if every entry of A is less than s, a fact that will be represented by $A < s$. Obviously, the n-dimensional, real vector $\mathbf{v}$ satisfies $\mathbf{v} < s$ if and only if $s\mathbf{e} - \mathbf{v} > 0$, where $\mathbf{e}$ is the n-dimensional vector all of whose components are equal to 1.

A square matrix A is a *Z-matrix* if all its off-diagonal entries are less than or equal to zero. We say that A is an *M-matrix* if the following three properties are satisfied:

(i) A is a Z-matrix,

(ii) all the diagonal entries of A are positive, and

(iii) there exists a diagonal matrix D with positive diagonal elements, such that AD is strictly diagonally dominant.

Lemma 24 (Fujimoto and Ranade [33])**.** *Every M-matrix is non-singular, and its inverse is positive.* □

Let $f : [0, 1] \to \mathbb{R}$ be the function defined by the expression (4.2), where δ and γ are real numbers satisfying $\delta \geq 1$ and $\gamma \in (0, 1)$. It is an easy exercise of real analysis to verify that this function satisfies $-\gamma \leq f(x) \leq (1-\gamma)^2/4$, for every $x \in [0, 1]$, that it is increasing in the interval $(0, ((\gamma + 1)/2)^{1/\delta})$ and decreasing in $(((\gamma + 1)/2)^{1/\delta}, 1)$, that the maximum and minimum values are attained at 0 and $((\gamma + 1)/2)^{1/\delta}$, respectively, and that the roots of the function occur at $\gamma^{1/\delta}$ and 1.

Lemma 25. *Let $\mathbf{u}^k$ be a positive vector of $\mathbb{R}^{N+1}$ satisfying $\mathbf{u}^k < s^{1/\delta}$, for some positive number $s \leq 1$, let α be a non-negative number, let λ belong to $(0, 1)$, and let $f : [0, s^{1/\delta}] \to \mathbb{R}$ be bounded from above by the positive number K. Then the matrix A of (4.24) is an M-matrix if the following conditions are satisfied:*

(a) $\alpha s \Delta x \leq 2$,

(b) $K\Delta t < 1 - \lambda/2$.

Proof. On the one hand, the positivity condition on $\mathbf{u}^k$ guarantees that k_3 is a non-positive function, while the assumption on the upper boundedness of the same vector and the inequality (a) assure the same conclusion for the coefficient k_1, whence it follows that A has non-positive, off-diagonal entries. On the other hand, inequality (a) gives $|k_1| + |k_3| = 2R$. Using the hypothesis (b), we obtain the chain of inequalities

$$|k_1| + |k_3| < 2R + 1 - \frac{\lambda}{2} - K\Delta t \leq k_2. \tag{4.27}$$

This means that the matrix A is strictly diagonally dominant, and that its diagonal entries are positive. We conclude that A is an M-matrix. □

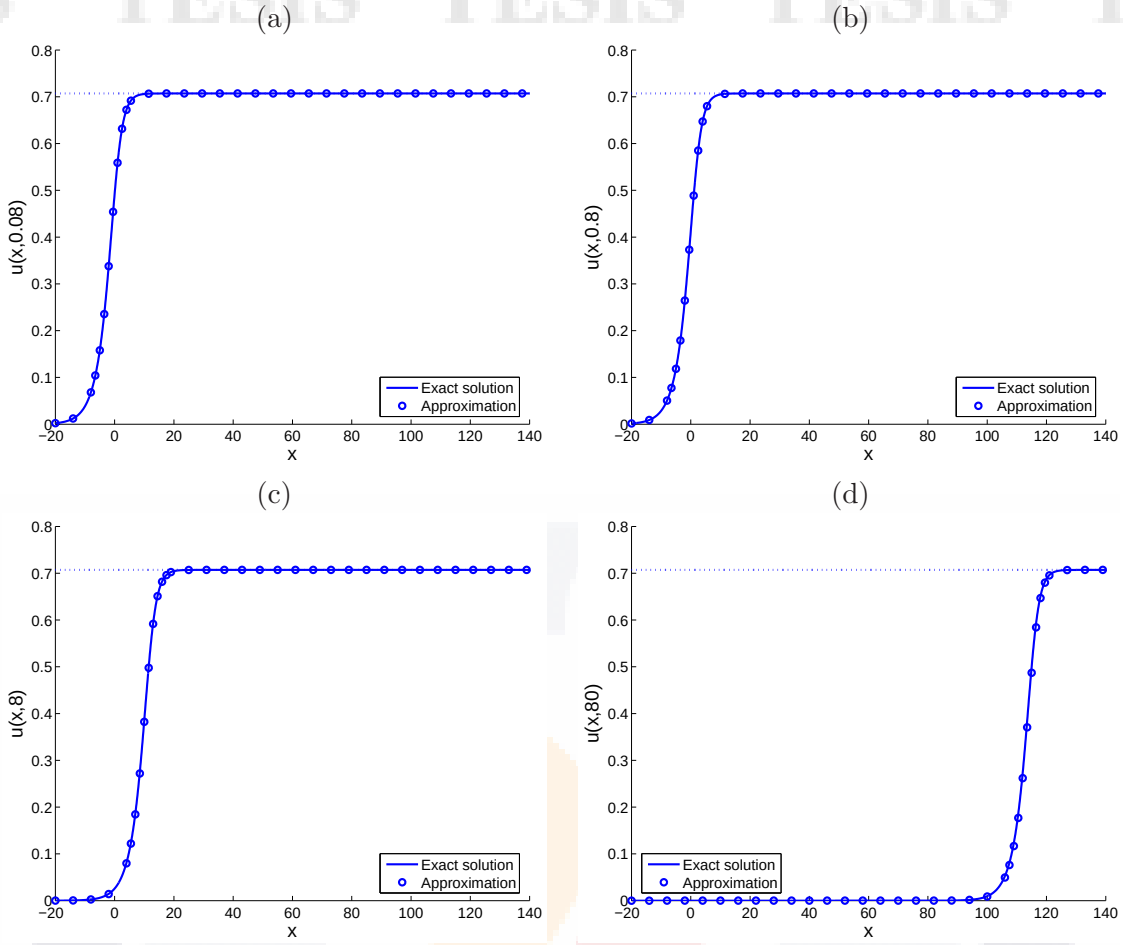

Figure 4.2: Graphs of the exact solution (continuous line) and the approximations (circles) computed through the numerical method (4.19) versus x, of the partial differential equation (4.3) subject to the initial-boundary conditions (4.5) on the interval $[-20, 140]$, with parameters $\alpha = 0.01$, $\gamma = 0.5$ and $\delta = 2$. The computational parameters $\Delta x = 0.1$, $\Delta t = 0.001$ and $\lambda = 0.9$ were employed, and four times were considered, namely, (a) $t = 0.08$, (b) $t = 0.8$, (c) $t = 8$ and (d) $t = 80$. The dotted line is the constant $\gamma^{1/\delta}$.

Let γ be a real number in $(0, 1)$, and let $\delta \geq 1$. It is worth noticing that Lemma 25 is valid in particular for the function f introduced in (4.2), for every positive, real number $s \leq 1$.

Proposition 26 (Positivity)**.** *Let* $\mathbf{u}^k$ *and* $\mathbf{u}^{k-1}$ *be positive vectors of* $\mathbb{R}^{N+1}$ *with* $\mathbf{u}^k < s^{1/\delta}$*, where* s *is a positive number with* $s \leq 1$*. Let* $f : [0, s^{1/\delta}] \to \mathbb{R}$ *be bounded from above by the positive number* K*. Suppose that* α *is a non-negative real number, and that* λ *belongs to* $(0, 1)$*. Then the vector* $\mathbf{u}^{k+1}$ *obtained by means of* (4.22) *is positive if the inequalities (a) and (b) of Lemma 25 hold.*

Proof. After Lemmas 24 and 25, the proof is immediate: The matrix A in (4.24) has a positive inverse, and the $(N+1)$-dimensional vector $B\mathbf{u}^k + C\mathbf{u}^k + \mathbf{b}^k$ of (4.22) is positive, whence the result follows. □

Let δ be a real number with $\delta \geq 1$, let s be a positive, real number such that $s \leq 1$, let λ belong in $(0, 1)$, and assume that the function $f : [0, s^{1/\delta}] \to \mathbb{R}$ is differentiable in the

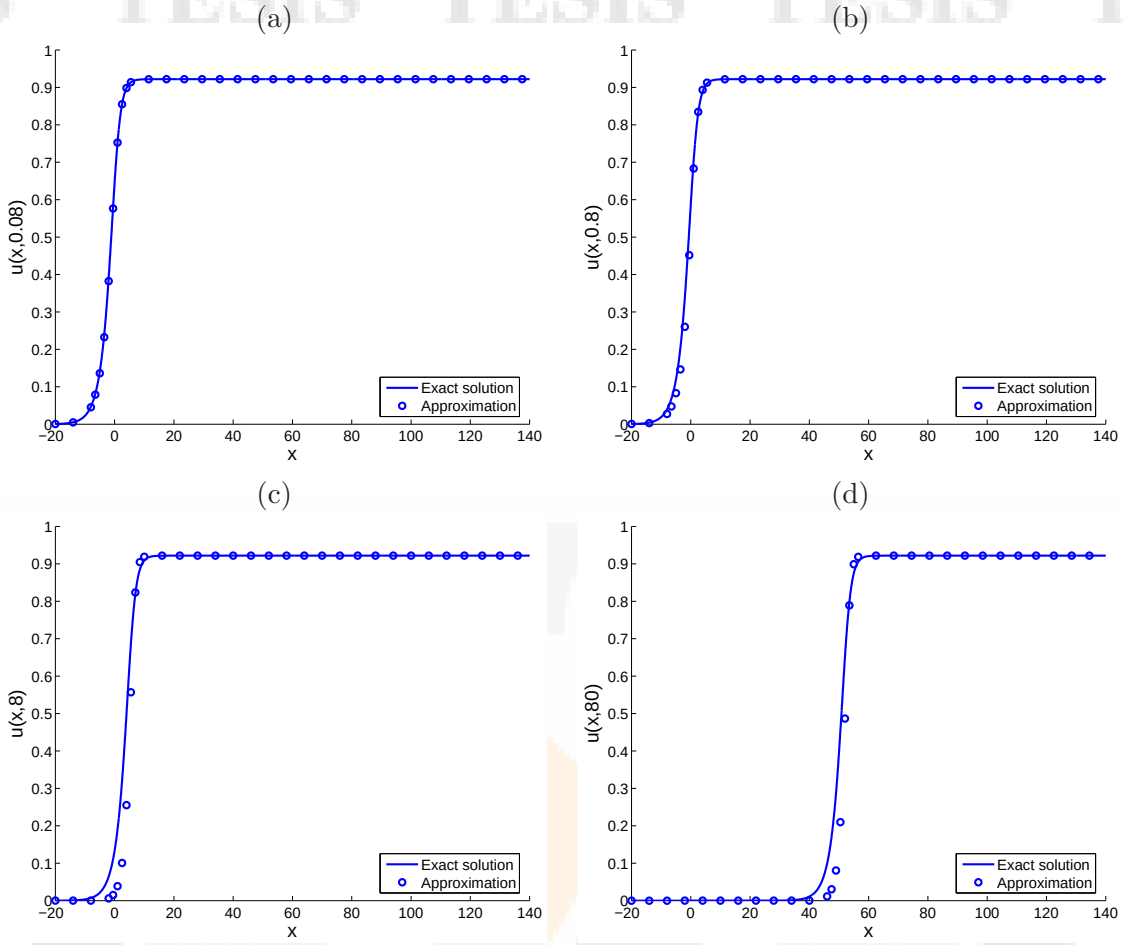

Figure 4.3: Graphs of the exact solution (continuous line) and the approximations (circles) computed through the numerical method (4.19) versus x, of the partial differential equation (4.3) subject to the initial-boundary conditions (4.5) on the interval $[-20, 140]$, with parameters $\alpha = 1$, $\gamma = 0.85$ and $\delta = 2$. The computational parameters $\Delta x = 0.1$, $\Delta t = 0.001$ and $\lambda = 0.9$ were employed, and four times were considered, namely, (a) $t = 0.08$, (b) $t = 0.8$, (c) $t = 8$ and (d) $t = 80$. The dotted line is the constant $\gamma^{1/\delta}$.

interior of its domain. Then the function $G : [0, s^{1/\delta}] \times [0, s^{1/\delta}] \to \mathbb{R}$ given by

$$G(x, y) = s^{1/\delta}\left[1 - \frac{\lambda}{2} - f(x)\Delta t\right] - (1 - \lambda)x - \frac{\lambda}{2}y, \tag{4.28}$$

is differentiable in the interior of its domain. Moreover, the first-order partial derivatives of G are provided by

$$\frac{\partial G}{\partial x}(x, y) = -s^{1/\delta} f'(x)\Delta t - (1 - \lambda), \tag{4.29}$$

$$\frac{\partial G}{\partial y}(x, y) = -\frac{\lambda}{2}. \tag{4.30}$$

Evidently, the function (4.30) is always negative, and in order for (4.29) to be likewise negative in $(0, s^{1/\delta}) \times (0, s^{1/\delta})$, we require that the inequality $s^{1/\delta} f'(x)\Delta t + 1 - \lambda > 0$ be satisfied for every $x \in (0, s^{1/\delta})$. Moreover, if $G(s^{1/\delta}, s^{1/\delta}) \geq 0$, then G will be positive in the interior of its domain. This last inequality holds if and only if $f(s^{1/\delta}) \leq 0$.

The function G and its properties are essential tools in the proof of the following result.

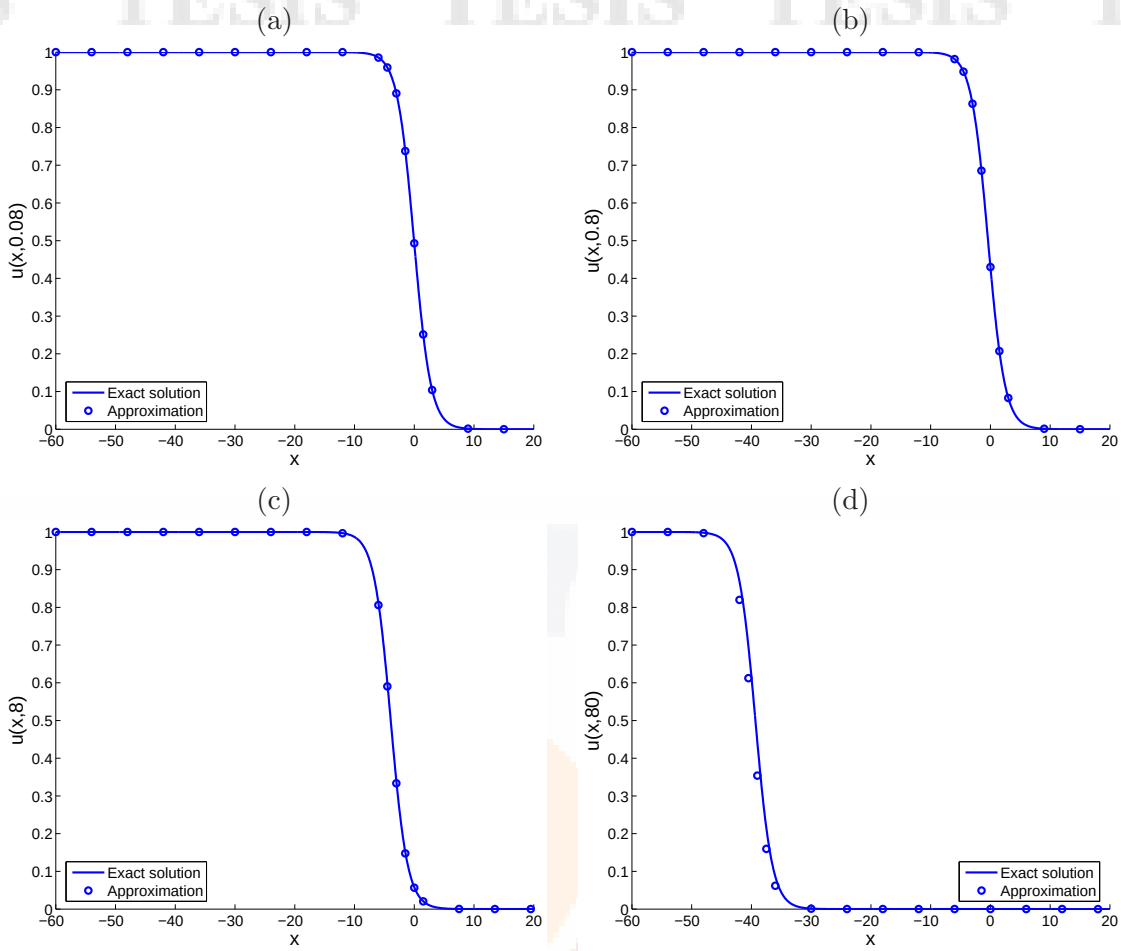

Figure 4.4: Graphs of the exact solution (continuous line) and the approximations (circles) computed through the numerical method (4.19) versus x, of the partial differential equation (4.3) subject to the initial-boundary conditions (4.12) on the interval $[-60, 20]$, with parameters $\alpha = 0.005$, $\gamma = 0.85$ and $\delta = 1$. The computational parameters $\Delta x = 0.1$, $\Delta t = 0.001$ and $\lambda = 0.5$ were employed, and four times were considered, namely, (a) $t = 0.08$, (b) $t = 0.8$, (c) $t = 8$ and (d) $t = 80$.

Proposition 27 (Boundedness)**.** *Suppose that α is a non-negative number, and that λ belongs to $(0, 1)$. Let $\mathbf{u}^k$ and $\mathbf{u}^{k-1}$ be positive vectors of $\mathbb{R}^{N+1}$ which are bounded from above by $s^{1/\delta}$, for some positive number $s \leq 1$, and let $f : [0, s^{1/\delta}] \to \mathbb{R}$ be bounded from above by $K > 0$. If (a) and (b) in Lemma 25 are satisfied and if, additionally, the inequalities*

(c) $s^{1/\delta} f'(x)\Delta t + 1 - \lambda > 0$,

(d) $f(s^{1/\delta}) \leq 0$,

hold, then the vector $\mathbf{u}^{k+1}$ obtained through (4.22) is a positive vector which is bounded from above by $s^{1/\delta}$.

Proof. Proposition 26 and the hypotheses (a) and (b) of Lemma 25 guarantee that $\mathbf{u}^{k+1}$ is positive. In order to verify the boundedness condition, let $\mathbf{w}^{k+1} = s^{1/\delta}\mathbf{e} - \mathbf{u}^{k+1}$. A simple substitution in (4.22) gives the identity

$$A\mathbf{w}^{k+1} = As^{1/\delta}\mathbf{e} - B\mathbf{u}^k - C\mathbf{u}^{k-1} - \mathbf{b}^k. \tag{4.31}$$

$\Delta x = 1$				
	Δt			
Time	0.1	0.01	0.001	0.0001
2.5	1.7894×10^{-3}	1.9409×10^{-4}	3.6169×10^{-4}	3.8037×10^{-4}
5	2.5870×10^{-3}	3.6822×10^{-4}	5.7714×10^{-4}	6.0146×10^{-4}
10	2.9225×10^{-3}	1.4146×10^{-3}	1.4548×10^{-3}	1.4615×10^{-3}
20	1.1326×10^{-2}	5.3108×10^{-3}	4.6949×10^{-3}	4.6337×10^{-3}
40	4.2899×10^{-2}	1.7318×10^{-2}	1.4650×10^{-2}	1.4401×10^{-2}
80	1.9397×10^{-1}	7.4834×10^{-2}	6.3295×10^{-2}	7.1182×10^{-2}
$\Delta x = 0.5$				
	Δt			
Time	0.1	0.01	0.001	0.0001
2.5	1.7619×10^{-3}	1.8348×10^{-4}	3.7242×10^{-4}	3.9214×10^{-4}
5	2.5117×10^{-3}	3.9200×10^{-4}	6.2890×10^{-4}	6.5471×10^{-4}
10	2.6978×10^{-3}	1.0673×10^{-3}	1.1448×10^{-3}	1.1557×10^{-3}
20	9.2589×10^{-3}	3.0891×10^{-3}	2.4825×10^{-3}	2.4237×10^{-3}
40	3.4839×10^{-2}	8.8806×10^{-3}	6.1919×10^{-3}	6.0123×10^{-3}
80	1.7476×10^{-1}	3.4782×10^{-2}	2.1314×10^{-2}	9.1006×10^{-1}
$\Delta x = 0.1$				
	Δt			
Time	0.1	0.01	0.001	0.0001
2.5	1.7551×10^{-3}	1.9422×10^{-4}	3.8304×10^{-4}	4.0275×10^{-4}
5	2.4898×10^{-3}	4.1062×10^{-4}	6.5193×10^{-4}	6.7796×10^{-4}
10	2.6327×10^{-3}	9.6300×10^{-4}	1.0576×10^{-3}	1.0703×10^{-3}
20	8.5959×10^{-3}	2.3720×10^{-3}	1.7811×10^{-3}	1.7256×10^{-3}
40	3.2233×10^{-2}	6.1413×10^{-3}	3.4550×10^{-3}	3.2040×10^{-3}
80	9.4971×10^{-1}	9.1541×10^{-1}	9.8005×10^{-3}	1.6896×10^{-2}

Table 4.2: Relative errors committed when approximating the exact solution of (4.3) subject to the initial-boundary conditions (4.5) on the interval $[-20, 140]$, with parameters $\alpha = 0.01$, $\gamma = 0.5$ and $\delta = 2$, by means of the finite-difference scheme (4.19). Computationally, $\lambda = 0.9$, and several values of Δx and Δt were employed. Six different times were considered for comparison purposes, namely, $t = 2.5$, 5, 10, 20, 40 and 80.

The first and the last components of the vector in the right-hand side of (4.31) are the numbers $s^{1/\delta} - \phi(t_k)$ and $s^{1/\delta} - \phi(t_k)$, respectively, which are positive. On the other hand, for every $n = 1, \ldots, N-2$, the $(n+1)$th component of the right-hand side of (4.31) has the form $G(u_n^k, u_n^{k-1})$, where both u_n^k and u_n^{k-1} belong to $(0, s^{1/\delta})$, and G is given by (4.28). The hypotheses (c) and (d), together with the discussion which precedes this proposition, imply that $G(u_n^k, u_n^{k-1})$ is positive. Summarizing, the right-hand side of (4.31) is a positive vector, and the matrix A is an M-matrix by Lemma 25. We conclude that the vector $\mathbf{w}^{k+1}$ is positive or, equivalently, that $\mathbf{u}^{k+1} < s^{1/\delta}$. □

It is interesting to notice that the function G may be negative in $[0, s^{1/\delta}] \times [0, s^{1/\delta}]$ if f assumes the expression (4.2) and $\gamma < s < 1$. However, if s is equal to 1 or if $s \leq \gamma$ then G is again positive in the interior of $[0, s^{1/\delta}] \times [0, s^{1/\delta}]$. As a consequence, we have the following result.

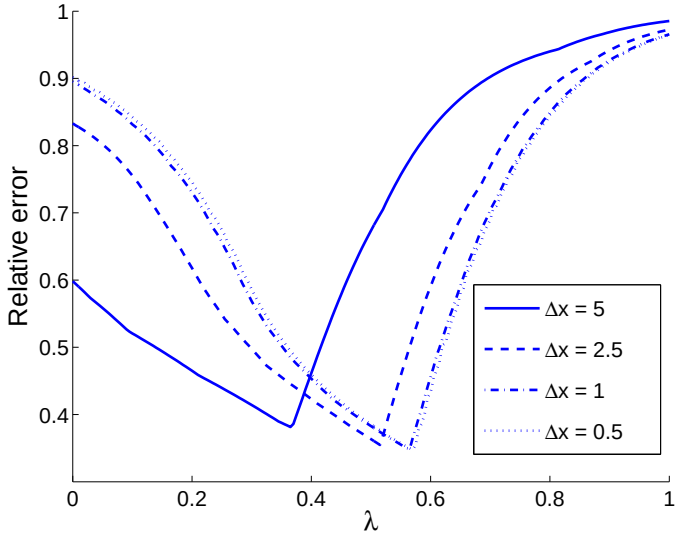

Figure 4.5: Graph of maximum relative error versus the computational parameter λ, obtained when approximating through (4.19) the exact solution of the partial differential equation (4.1) subject to the initial-boundary conditions (4.5) on the interval $[-20, 140]$, over a temporal period of length 80, with parameters $\alpha = 0.01$, $\gamma = 0.5$, and $\delta = 2$. Computationally, we employed $\Delta t = 2$, and four different values of Δx, namely, 5 (continuous), 2.5 (dashed), 1 (dash-dotted) and 0.5 (dotted).

Corollary 28. *Suppose that α is a non-negative number, and that γ and λ both belong to $(0, 1)$. Let $\mathbf{u}^k$ and $\mathbf{u}^{k-1}$ be positive vectors of $\mathbb{R}^{N+1}$ which are bounded from above by $s^{1/\delta}$, for some positive number s satisfying $s \leq \gamma$ or $s = 1$, and let f be given by (4.2). Then $\mathbf{u}^{k+1}$ obtained through (4.22) is a positive vector which is bounded from above by $s^{1/\delta}$ if*

(a) $\alpha s \Delta x \leq 2$,

(b) $(1-\gamma)^2 \Delta t < 2(2-\lambda)$,

(c) $s\delta\Delta t(2s - \gamma - 1) < 1 - \lambda$. □

Observe that (a) in Corollary 28 is trivially satisfied when the advection coefficient is equal to zero; otherwise, it is easy to choose Δx small enough in order for such constraint to hold. On the other hand, since γ and λ are positive numbers which are less than 1, then $(1-\gamma)^2 < 1 - \gamma < 2 < 2(2-\lambda)$, so that (b) holds by taking $\Delta t < 1$. Finally, part (c) is trivially satisfied if $2s \leq 1 + \gamma$ (as it happens when $s \leq \gamma$), in which case, the number in the parenthesis of (c) is non-positive; otherwise (as in the case when s is equal to 1), this condition is reached by taking Δt sufficiently small.

It is useful to mention that the simulations in the next section were obtained by means of an implementation of Thomas' technique for tridiagonal systems [15]. Additionally, it must be mentioned that a slight modification of our method can be easily done in order to account for homogeneous Neumann boundary conditions. In fact, one only needs to set $\mathbf{b}^k$ equal to zero, and do the following changes in the matrix $A = (a_{i,j})$ of (4.24): Redefine $a_{1,2} = a_{N+1,N} = -1$.

4.4 Numerical results

Throughout this section, the function f will be given by (4.2).

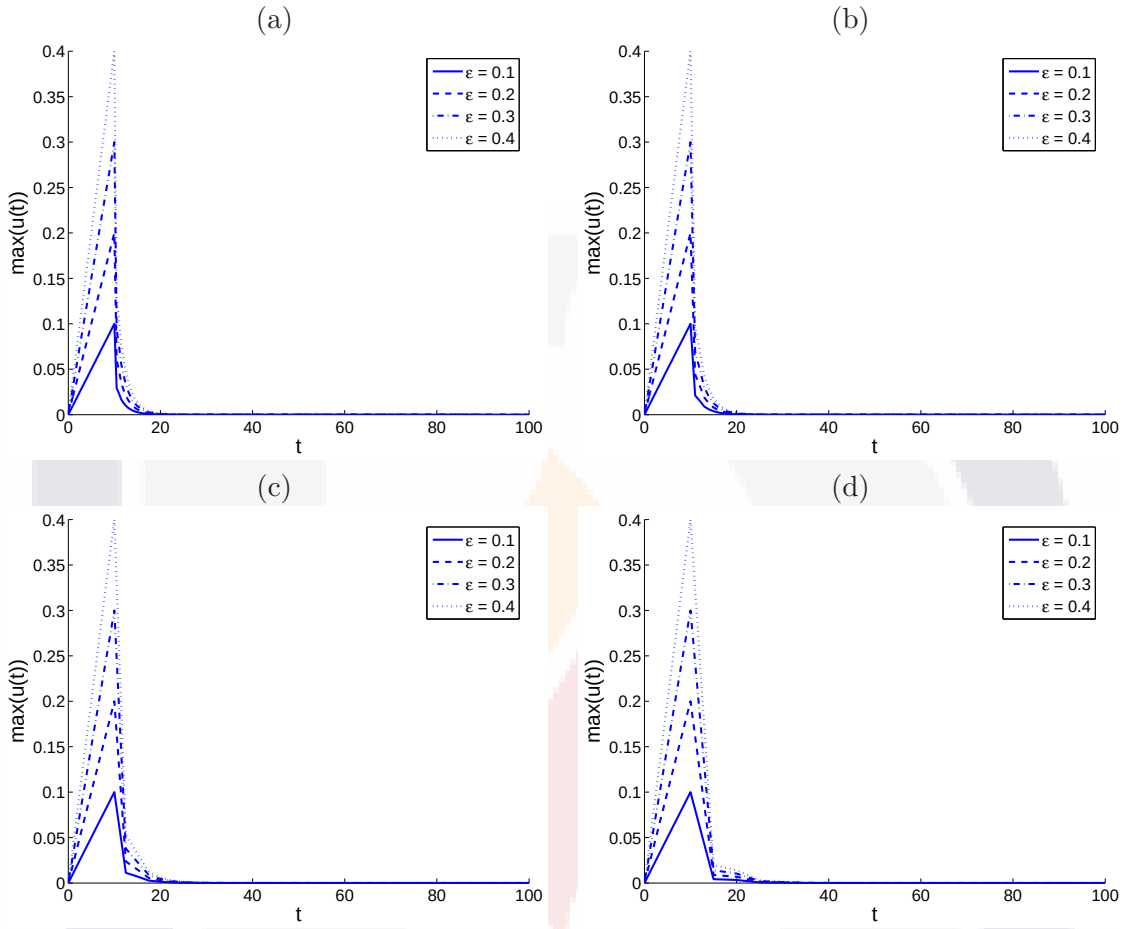

Figure 4.6: Time-dependent graph of the maximum value of the approximate solution of a system described by (4.1) over the spatial interval $I = [0, 100]$, with function f given by (4.2) and parameter values $\alpha = \beta = \kappa = \delta = 1$, $\gamma = 0.5$, $\Delta x = 1$ and $\lambda = 0.6$. Discrete, homogeneous Neumann conditions were imposed on the right endpoint of $[0, 100]$, while the left endpoint was linearly changed from 0 to ϵ during a period of time of length 10; afterwards, we impose discrete, homogeneous Neumann conditions. The system was initially given a constant profile $u = 0$, and several values of Δt were employed, namely, (a) 0.5, (b) 1, (c) 2.5 and (d) 5. In each case, several values of ϵ were also used.

Example 29. Let us consider the partial differential equation (4.3) with δ equal to 2, γ equal to 0.5, and an advection coefficient α equal to 0.01. Consider the initial-boundary data provided by (4.5) on the spatial domain $I = [-20, 140]$, in which case, the exact solution is given by (4.8). In order to approximate the solutions of this initial-boundary-value problem over the time period 80, we fix a uniform partition of the interval I, with norm Δx equal to 0.1, and a uniform partition of the temporal interval $[0, 80]$ with norm equal to 0.001. Computationally, the parameter λ will be equal to 0.9. Under these circumstances, Figure 4.2 presents a comparison between the actual solution of the initial-boundary-value problem under investigation against the approximations obtained by the numerical method (4.19), for four different times, namely, $t = 0.08$, 0.8, 8 and 80. We immediately notice that the results evidence a good agreement between the simulations and the exact solutions at the four times considered. Moreover, the approximate solutions are always bounded between 0 and $\gamma^{1/\delta}$. This last remark is in agreement with the fact that the boundedness conditions of Corollary 28 are satisfied. More precisely, we have compared the exact solutions and their corresponding approximations at different times, using several values of Δx and Δt, and employing the relative differences between the numerical and the theoretical solutions through the standard $\|\cdot\|_2$-norm in $\mathbb{R}^{N+1}$. The results are summarized in Table 4.2, and they show that the approximations tend to improve as the computational parameters Δx and Δt become smaller. □

Example 30. Consider the problem presented in the previous example, with the same model and computational parameters. In this case, however, we will let α be equal to 1, and let γ be equal to 0.85. The results of the simulations in this example are shown in Figure 4.3. Once again, the numerical approximations seem to be in good agreement with the exact solutions, even in this situation in which the value of α is relatively larger than the value used in the previous example. □

Example 31. Consider again the partial differential equation (4.3) with advection coefficient equal to 0.005, δ equal to 1, and γ equal to 0.85. We impose the initial-boundary conditions (4.12) on the spatial interval $I = [-60, 20]$; computationally, we choose Δx and Δt equal to 0.1 and 0.001, respectively, fix a time period of 80, and let λ be equal to 0.5. Figure 4.4 presents the exact solution of the problem as given by (4.9) and the corresponding approximations given by (4.19) versus $x \in I$, at four different times: 0.08, 0.8, 8 and 80. The theoretical and the numerical results are seen to be in good agreement and, moreover, the simulations are bounded in the interval $(0, 1)$. Evidently, the model and the computational parameters satisfy again the boundedness conditions of Corollary 28. □

Next, we analyze the role of λ in the approximation of one of the traveling-wave solutions considered above.

Example 32. Consider the problem studied in Example 29, with Δt equal to 2. We consider four decreasing values of Δx for which the boundedness conditions of Corollary 28 are satisfied (namely, 5, 2.5, 1 and 0.5), and compute the maximum relative error under the $\|\cdot\|_\infty$-norm of $\mathbb{R}^{N+1}$, over a temporal period of length 80, committed when we approximate the exact solution of the problem under investigation through our finite-difference method. In this example, the value of λ is varied in the interval $(0, 1)$. The results are presented in Figure 4.5, and they show the fact that the maximum relative error attains a minimum value for λ around the value 0.5. In fact, one can readily notice that, as the value of Δx is decreased within the region that guarantees the boundedness of solutions, the minimum value of the maximum relative errors is reached for a critical value of λ close to 0.6. This is in perfect agreement with the fact that the graphs of the solutions

to the problem under investigation show a sharp wave front, in which case, an appropriate linear combination of the approximations of orders 1 and 2 of the partial derivative of u with respect to time is recommended. □

We now carry out a study similar to that presented in [2], in which the behavior of the method around a bifurcation point is computationally investigated.

Example 33. We investigate now the effect of linearly perturbing the steady-state solution $u = 0$ of the partial differential equation (4.1) over the spatial interval $I = [0, 100]$; here, we set the parameters α, β, κ and δ all equal to 1, and let $\gamma = 0.5$. Computationally, we let Δx and λ be equal to 1 and 0.6, respectively. To that effect, we fix discrete, initial conditions of the form $u_n^0 = u_n^1 = 0$, for every $n \in \{1, \ldots, N-1\}$, and impose discrete, homogeneous Neumann boundary conditions on the right end of the spatial interval. On the left endpoint of I, we linearly change the value of u_0^k from 0 to ϵ over the time period $[0, 10]$, where ϵ is a positive, real number which is less than $\gamma^{1/\delta}$; afterwards, we impose discrete, homogeneous Neumann boundary conditions, too. Next, we determine computationally the value of the steady-state solution, letting the algorithm run for a period of time of length equal to 100. The results are displayed in Figure 4.6 as time-dependent graphs of the maximum value of the approximations over I, for several values of Δt and ϵ. In all cases, the results show that the solutions tend to the steady-state solution $u = 0$ as t increases. These graphical observations have been verified numerically by letting the algorithm run for periods of time of length 10000, and the results show that the solutions tend to the constant solution $u = 0$, indeed. □

Chapter 5

A time-delayed advection-diffusion-reaction equation

In this work, we consider a one-dimensional, time-delayed, advective version of the well-known Fisher-Kolmogorov-Petrovsky-Piscounov equation from population dynamics, which extends several models from mathematical physics, including the classical wave equation, the nonlinear Klein-Gordon equation, a FitzHugh-Nagumo equation from electrodynamics, and the Burgers-Huxley equation and the Newell-Whitehead-Segel equation from fluid mechanics. We propose a skew symmetry-preserving, finite-difference scheme to approximate the solutions of the model under investigation, and establish conditions on the model coefficients and the numerical parameters under which the method provides positive or bounded approximations for initial data which are likewise positive or bounded, respectively. The derivation of the conditions under which the positivity and the boundedness of the approximations is guaranteed, is based on the properties of the inverses of M-matrices; in fact, the conditions obtained here assure that the iterative method is described in vector form through the multiplication by a matrix of this type. We provide simulations in order to show that the technique is indeed conditionally positivity-preserving and boundedness-preserving.

5.1 Introduction

The class of problems in which variables measured in absolute scales appear is relatively large, indeed. For instance, some thermodynamical problems may require that the variable of interest be the dynamics of a temperature measured in Kelvin. In population dynamics, the amount of individuals in a discrete colony is a characteristic that must take on non-negative, integer values at any time; even in the continuous case scenario, the population density of a colony of bacteria is also a non-negative, real variable. In the investigation of thin-film and biofilm growth on rigid surfaces, the behavior of the film above any point on the surface is described by the time-evolution of its height, which can never be a negative number. Finally, in the investigation of some crack failures (for instance, in the study of cracks in airplane wings), the rate of change of the length of the cracks with respect to time is non-negative, that is, the length of the cracks is a non-decreasing function of time.

All of the above examples illustrate the physical importance of the condition of positivity. In fact, positivity is a characteristic of the solutions of many mathematical models

in the physical sciences, be it in the investigation of the population dynamics of certain viruses in epidemiology [5, 54], in the study of the propagation of forest fires when the variable of interest is the temperature measured in an absolute scale [61], in the investigation of the evolution of the concentration of a certain component in a chemical substance [86], in the study of biofilm growth on rigid surfaces [22, 21], or in the prediction of the crack failure of some materials [77, 51].

On the other hand, the condition of boundedness is also important in many models. For example, the dynamics of the concentration of a chemical component is a percentage [86], that is, a real function bounded between 0 and 1. Other examples where the variable of interest is a bounded function of time are the growth of microbial biofilms on a rectangular prism which is entirely closed [21, 10], the temporal evolution of the temperature in some thermomechanical models describing the phase transitions in terms of the entropy and order structure-balance laws [8], the cell density in some mathematical models governing the adhesion in cell aggregation in cancer invasion [84] and, in a more general setting, traveling wave solutions connecting asymptotically two constant solutions of a model [78]. Evidently, positivity and boundedness are conditions that go side by side in importance, in some of these instances.

The problem of designing finite-difference schemes that preserve one or more of the properties of positivity, boundedness and symmetry of physical models has been attacked successfully in some particular cases. Many computational methods have been proposed to approximate solutions of epidemic models [5, 4], of the Lotka-Volterra system [63, 65], of the linear wave equation with constant damping [68, 69], of bioremediation problems in aquifers [17], of predator-prey models [71], of the nonlinear heat equation in a thin, finite rod [41], of some mathematical models for the influenza disease [40], among other problems of physical relevance. In fact, many of these methods have been applied to the computational investigation of physical phenomena, from the epidemiological transmission of diseases [5], to the propagation of mechanical waves in nonlinear media [55, 52] and in nonlinear lattices [81, 53], where nonlinear processes such as the phenomena of supratransmission and infratransmission are studied through numerical integrators which preserve not only the positive character of the energy of the systems involved, but also the local energy density, the total energy of the systems, and the dissipation of the energy. Needless to mention that many methods have been designed with the property of the conservation of energy in mind [35, 34].

In the present work, we propose an implicit, finite-difference method to approximate solutions of a hyperbolic partial differential equation with nonlinear advection and nonlinear reaction, which generalizes many known models of mathematical physics, including the classical Fisher-Kolmogorov-Petrovsky-Piscounov equation [27, 47], a FitzHugh-Nagumo equation [78], the Newell-Whitehead-Segel equation [75, 83], the Burgers-Huxley equation [92], and the damped wave equation, just to mention some of them. Under certain conditions on the model constants and the computational parameters, positive and/or bounded initial approximations evolve into positive and/or bounded, new approximations. In these terms, our finite-difference scheme is conditionally positive and conditionally bounded; moreover, our method preserves the skew symmetry of the solutions of the equation studied in this work. We must state beforehand that the computational implementation of our technique yields good results when they are compared against known, exact solutions of some particular models.

In Section 5.2, we introduce the model under investigation in this work, namely, a hyperbolic version of a generalization of the Burgers-Huxley equation from fluid mechanics. We provide a non-dimensional analysis of the equation under study for simplification purposes, and present some particular solutions of this equation for validation purposes.

Section 5.3 is devoted to present the finite-difference scheme employed to approximate solutions of the problem under investigation. We restate here our numerical method in vector form; with this formulation in hand, we show in Section 5.4 that our technique is able to preserve the properties of positivity and boundedness of solutions under some constraints of the model and the computational parameters. Moreover, we show that the method is capable of preserving the skew symmetry of the equation that motivates our study. In this point, the concept of M-matrices and their properties will be a cornerstone. In Section 5.5, we present some computational evidence that the method introduced in the present manuscript yields good approximations to some of the exact solutions of our equation. To that effect, we will consider several particular models where some analytical solutions are available.

5.2 Preliminaries

5.2.1 Mathematical model

Let $\mathbb{R}^+$ represent the set of all non-negative, real numbers. Let I be a nonempty, closed interval of real numbers which is possibly unbounded, and let u be a real function of the ordered pair (x,t), where (x,t) denotes an arbitrary element of $I \times \mathbb{R}^+$. Let α, β κ, τ and m be non-negative, real numbers, let γ belong in $[-1,1]$, and assume that the real number δ satisfies $\delta \geq \frac{1}{2}$. Throughout this work, we consider the hyperbolic partial differential equation with nonlinear advection term

$$\tau \frac{\partial^2 u}{\partial t^2} + \beta \frac{\partial u}{\partial t} + \alpha u^{\delta} \frac{\partial u}{\partial x} - \kappa \frac{\partial^2 u}{\partial x^2} - mug(u) = 0, \quad (x,t) \in I \times \mathbb{R}^+, \tag{5.1}$$

where the reaction factor assumes the nonlinear form

$$g(u) = (1-u^{\delta})(u^{\delta} - \gamma). \tag{5.2}$$

On physical grounds, one immediately identifies the parameter τ as the time of relaxation or the lag constant. The parameter β is recognized as the damping coefficient, α is the coefficient of advection, κ the diffusivity constant, and m is the constant of nonlinearity or the coefficient of reaction. The nonlinear factor (5.2) is evidently a generalization of the logistic law, which has been expressed in this manner in order to generalize several parabolic and hyperbolic partial differential equations from mathematical physics. For instance, in the parabolic scenario (more precisely, when τ is equal to zero), this model is the classical Fisher-Kolmogorov-Petrovsky-Piscounov equation from population dynamics [27, 47] if α equals zero, δ is equal to $\frac{1}{2}$, and γ is equal to -1; our equation is the FitzHugh-Nagumo equation which appears in the study of the propagation of electric pulses in the nervous system [78] when α is equal to zero, δ is equal to 1, and γ belongs in $(0, \frac{1}{2})$; moreover, equation (5.1) becomes the Newell-Whitehead-Segel equation from fluid mechanics [75, 83] if α is equal to zero and γ is equal to -1.

For the sake of simplification, let us assume that m is a positive constant, and let a and b be positive, real numbers. Define the new variables $\xi = \frac{1}{a}x$ and $\zeta = \frac{1}{b}t$. If we consider u as a function of the ordered pair (ξ, ζ), then the partial differential equation (5.1) becomes

$$\frac{\tau}{mb^2} \frac{\partial^2 u}{\partial \zeta^2} + \frac{\beta}{mb} \frac{\partial u}{\partial \zeta} + \frac{\alpha}{ma} u^{\delta} \frac{\partial u}{\partial \xi} - \frac{\kappa}{ma^2} \frac{\partial^2 u}{\partial \xi^2} - ug(u) = 0. \tag{5.3}$$

Suppose now that β and κ are positive numbers, too. We may suitably define the constants a and b, to demonstrate that it is sufficient to study (5.1) when all of the coefficients β, κ

and m are equal to 1. Therefore, for most of what remains of the present document, we investigate the simplified equation

$$\tau\frac{\partial^2 u}{\partial t^2}+\frac{\partial u}{\partial t}+\alpha u^{\delta}\frac{\partial u}{\partial x}-\frac{\partial^2 u}{\partial x^2}-ug(u)=0. \tag{5.4}$$

For our next result, we let $\mathcal{L}(u)$ represent the left-hand side of (5.4), for every function u which is twice differentiable over the set $I\times\mathbb{R}^+$.

Proposition 34. *Let $u: I\times\mathbb{R}^+\to\mathbb{R}$ be a function which is twice differentiable. Then the identity $\mathcal{L}(-u)=-\mathcal{L}(u)$ is satisfied if either δ is a positive, even number, or if δ is a positive integer, α is equal to zero and γ is equal to -1.*

Proof. The proof is straightforward. □

Suppose that δ is a positive, even integer or, alternatively, that δ is a positive integer, α equals zero and γ is equal to -1. As a consequence of Proposition 34, the function u is a solution of (5.4) if and only if $-u$ is also a solution of (5.4). We refer to this characteristic of our model as the property of *skew symmetry*.

5.2.2 Particular solutions

In order to verify the validity of the method that we will introduce in Section 5.3, we will compare our simulations against known, analytical solutions. The present section is devoted to quote some particular solutions. Three specific, damped models are employed for validation purposes: The advectionless Newell-Whitehead-Segel equation, an advective Burgers-Huxley equation, and an advectionless Klein-Gordon equation.

A Newell-Whitehead-Segel equation An important, parabolic partial differential equation in this work is the generalization of the Newell-Whitehead-Segel equation from fluid mechanics [75, 83], derived from (5.4) by letting both τ and α be equal to zero, and setting γ equal to -1 in (5.2), where δ is any positive integer. The classical form of our equation appears when δ is equal to 1, and it has a family of exact solutions given by the formula

$$u_{\pm}(x,t)=\pm\left[\frac{2C_1\exp(\sqrt{2}x)+C_2\exp(\frac{1}{\sqrt{2}}x-\frac{3}{2}t)}{C_1\exp(\sqrt{2}x)+C_2\exp(\frac{1}{\sqrt{2}}x-\frac{3}{2}t)+C_3}-1\right],\quad (x,t)\in\mathbb{R}\times\mathbb{R}^+, \tag{5.5}$$

where C_1, C_2 and C_3 are, in general, arbitrary, real constants [78], and non-negative, real numbers for this particular investigation. It is readily checked that $|u_{\pm}(x,t)|<1$, for every $x\in\mathbb{R}$ and every $t\geq 0$. Moreover, the function $u_{\pm}$ represents a traveling wave solution satisfying $0<u_{\pm}(x,t)<1$ when C_3 is equal to zero.

A Burgers-Huxley equation A generalized form of the classical Burgers-Huxley equation results from (5.4) if τ is equal to zero, δ is a positive, integer number, and the reaction function takes on the form (5.2) with $\gamma\in(0,1)$. This equation possesses also exact solutions that we will employ in our simulations for comparison purposes. One such solution of this model is given by the formula

$$u(x,t)=\left(\frac{\gamma}{2}+\frac{\gamma}{2}\tanh(a_1(x-a_2t))\right)^{1/\delta},\quad (x,t)\in\mathbb{R}\times\mathbb{R}^+, \tag{5.6}$$

where the constants a_1 and a_2 are defined by

$$a_1=\frac{-\alpha\delta+\delta\sqrt{\alpha^2+4(1+\delta)}}{4(1+\delta)}\gamma,\quad a_2=\frac{\gamma\alpha}{1+\delta}-\frac{(1+\delta-\gamma)(-\alpha+\sqrt{\alpha^2+4(1+\delta)})}{2(1+\delta)}. \tag{5.7}$$

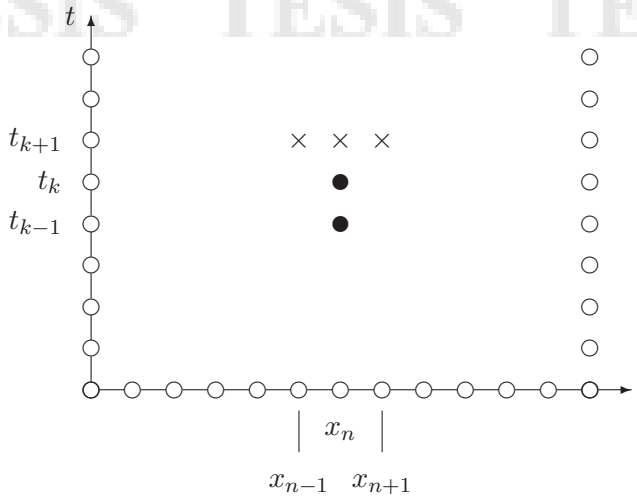

Figure 5.1: Forward-difference stencil for the approximation to the partial differential equation (5.4) at the time t_k, using the finite-difference scheme (5.15). The black circles represent known approximations to the exact solutions at the times t_{k-1} and t_k, and the crosses denote the unknown approximations at the time t_{k+1}.

Evidently, the function (5.6) is a traveling wave solution of the generalized Burgers-Huxley equation introduced here, which connects asymptotically the constant solutions $u = 0$ and $u = \gamma^{1/\delta}$. If δ is equal to 1 and γ belongs in $(0, 1)$, then the expression

$$u(x,t) = \frac{1}{2} - \frac{1}{2}\tanh\left[\frac{1}{r-\alpha}(x - vt)\right], \quad (x,t) \in \mathbb{R} \times \mathbb{R}^+, \tag{5.8}$$

also represents a traveling wave solution of our model which connects the two steady state solutions $u = 0$ and $u = 1$, independently of the value of γ. In this case, the constant r and the wave velocity v are given by

$$r = \sqrt{\alpha^2 + 8}, \quad v = \frac{(\alpha - r)(2\gamma - 1) + 2\alpha}{4}. \tag{5.9}$$

These solutions are the result of employing symbolic computations along with some non-linear transformations [50, 24, 92].

A Klein-Gordon equation Finally, in our comparisons, we will employ a hyperbolic version of (5.1), in the form of a nonlinear, damped Klein-Gordon equation. The Klein-Gordon model used in the present work is the advectionless expression derived from (5.1) by letting γ be -1, and letting δ, κ, τ and m be all equal to 1. Such equation has traveling wave solutions of the form

$$u_\pm(x,t) = \pm\left\{1 + C_0 \exp\left[\frac{\sqrt{9+2\beta^2}}{2\beta}\left(x - \frac{3}{\sqrt{9+2\beta^2}}t\right)\right]\right\}^{-1}, \quad (x,t) \in \mathbb{R}\times\mathbb{R}^+, \tag{5.10}$$

where C_0 is an arbitrary, positive number [26].

5.3 Numerical method

5.3.1 Finite-difference scheme

Let N and M be positive integers, and let T be a positive, real number. For computational purposes, we restrict our attention to closed and bounded, spatial intervals I of the form

$[a,b]$, and fix a regular partition $a = x_0 < x_1 < \ldots < x_N = b$ consists of N subintervals. We wish to approximate the solutions of (5.4) over a period of time of length T, so we select a regular partition of the temporal interval $[0,T]$, consisting of M subintervals, say $0 = t_0 < t_1 < \ldots < t_M = T$. For convenience, we let Δx and Δt be the norms of the spatial and the temporal partitions, respectively, that is, we let $\Delta x = (b-a)/N$ and $\Delta t = T/M$. Moreover, we let u_n^k represent an approximation of the exact value of the function u at (x_n, t_k).

Let λ be an arbitrary, real number. For the sake of convenience, we introduce the following standard, discrete, linear operators:

$$\delta_{t,\lambda} u_n^k = (1-\lambda)\frac{u_n^{k+1} - u_n^k}{\Delta t} + \lambda \frac{u_n^{k+1} - u_n^{k-1}}{2\Delta t}, \tag{5.11}$$

$$\delta_t^{(2)} u_n^k = \frac{u_n^{k+1} - 2u_n^k + u_n^{k-1}}{(\Delta t)^2}, \tag{5.12}$$

$$\delta_x^{(1)} u_n^k = \frac{u_{n+1}^k - u_{n-1}^k}{2\Delta x}, \tag{5.13}$$

$$\delta_x^{(2)} u_n^k = \frac{u_{n+1}^k - 2u_n^k + u_{n-1}^k}{(\Delta x)^2}. \tag{5.14}$$

Remark 35. *Several quick observations may be given in this point. First of all, one can notice that the symbol "δ" has been employed to denote the power of the nonlinear factors in the advection and the reaction terms of* (5.1) *and* (5.4)*, and also in the notations of the linear operators* (5.11)*,* (5.12)*,* (5.13) *and* (5.14)*. The use of this symbol will not turn ambiguous, in view that the linear operators require sub-indexes in order to accurately refer to them. On the other hand, a look at the definitions of those four operators leads us to some immediate remarks:*

- *The operator* (5.11) *is a linear and weighed combination of a first-order approximation to the partial derivative of u with respect to t at (x_n, t_k), and a second-order approximation to the same value. The weighed approximation* (5.11) *is consistent of the second order when λ is equal to* 1*.*
- *The functional* (5.12) *yields a consistent approximation of the second order in time, to the exact value of $\frac{\partial^2 u}{\partial t^2}$ at the point (x_n, t_k).*
- *Finally, it is readily checked that* (5.13) *and* (5.14) *approximate the exact values at the point (x_n, t_k) of $\frac{\partial u}{\partial x}$ and $\frac{\partial^2 u}{\partial x^2}$, respectively, with a consistency of the second order in x.*

With this nomenclature at hand, the finite-difference method employed to approximate solutions of the partial differential equation (5.4) over the spatial interval I through a temporal period of length T, is given by the system of equations

$$\tau \delta_t^{(2)} u_n^k + \delta_{t,\lambda} u_n^k + \alpha (u_n^k)^\delta \delta_x^{(1)} u_n^{k+1} - \delta_x^{(2)} u_n^{k+1} - u_n^{k+1} g(u_n^k) = 0, \tag{5.15}$$

where $n = 1, \ldots, N-1$, and $k = 1, \ldots, M-1$. Some algebraic manipulations of these equations may convince us that the forward-difference stencil of our method is the one presented in Figure 5.1. In fact, one can alternatively express the finite-difference scheme (5.15) through the set of identities

$$k_1 u_{n+1}^{k+1} + k_2 u_n^{k+1} + k_3 u_{n-1}^{k+1} = k_4 u_n^k + k_5 u_n^{k-1}, \tag{5.16}$$

k_1	k_2	k_3	k_4	k_5
$\frac{\alpha\Delta t}{2\Delta x}(u_n^k)^\delta - R$	$1 - \frac{\lambda}{2} + \frac{\tau}{\Delta t} + 2R - \Delta t g(u_n^k)$	$-\frac{\alpha\Delta t}{2\Delta x}(u_n^k)^\delta - R$	$1 - \lambda + \frac{2\tau}{\Delta t}$	$\frac{\lambda}{2} - \frac{\tau}{\Delta t}$

Table 5.1: Expressions of the coefficients in the implicit presentation (5.16) of the finite-difference method (5.15). The computational constant R is given in (5.17), and the non-linear reaction factor g is provided by (5.2).

valid for every $n = 1, \ldots, N-1$ and every $k = 1, \ldots, M-1$. The functions k_1, k_2 and k_3 of u_n^k, as well as the constants k_4 and k_5, are provided in Table 5.1 for the Fourier number

$$R = \frac{\Delta t}{(\Delta x)^2}. \tag{5.17}$$

5.3.2 Matrix representation

The finite-difference method presented in the previous stage requires boundary conditions to be imposed on the interval I. In this work, we will focus our attention mainly to the approximation of traveling wave solutions in relatively long, spatial intervals. In view of this, we will present the development for a set of homogeneous, Neumann boundary conditions, that is, boundary constraints of the form

$$\frac{\partial u}{\partial x}(a,t) = \frac{\partial u}{\partial x}(b,t) = 0, \quad t \geq 0, \tag{5.18}$$

the development for different boundary data being similarly treated. The constraints (5.18) will be translated to the discrete scenario as the following set of conditions, satisfied for every $k = 0, 1, \ldots, M$:

$$u_1^k - u_0^k = u_{N-1}^k - u_N^k = 0. \tag{5.19}$$

The numerical method (5.15) can be expressed now more conveniently in vector form. For every $k = 0, 1, \ldots, M$, let $\mathbf{u}^k$ be the $(N+1)$-dimensional vector $(u_0^k, u_1^k, \ldots, u_N^k)$. For each such integer k, we let $A = A_{\mathbf{u}^k}$ be the square matrix of size $(N+1)\times(N+1)$ provided by the formula

$$A = \begin{pmatrix} 1 & -1 & 0 & 0 & \cdots & 0 & 0 & 0 \\ k_1 & k_2 & k_3 & 0 & \cdots & 0 & 0 & 0 \\ 0 & k_1 & k_2 & k_3 & \cdots & 0 & 0 & 0 \\ \vdots & \vdots & \vdots & \vdots & \ddots & \vdots & \vdots & \vdots \\ 0 & 0 & 0 & 0 & \ldots & k_1 & k_2 & k_3 \\ 0 & 0 & 0 & 0 & \ldots & 0 & -1 & 1 \end{pmatrix}. \tag{5.20}$$

For each $n = 1, \ldots, N-1$, the constants k_1, k_2 and k_3 of the $(n+1)$th row of this matrix are the functions of u_n^k given in Table 5.1; however, these dependencies have been obviated for the sake of simplicity. Finally, for every real number c, we define the diagonal matrix of size $(N+1)\times(N+1)$

$$B_c = \begin{pmatrix} 0 & 0 & 0 & \cdots & 0 & 0 & 0 \\ 0 & c & 0 & \cdots & 0 & 0 & 0 \\ 0 & 0 & c & \cdots & 0 & 0 & 0 \\ \vdots & \vdots & \vdots & \ddots & \vdots & \vdots & \vdots \\ 0 & 0 & 0 & \cdots & c & 0 & 0 \\ 0 & 0 & 0 & \cdots & 0 & c & 0 \\ 0 & 0 & 0 & \cdots & 0 & 0 & 0 \end{pmatrix}. \tag{5.21}$$

Let $\mathbf{0}$ be the zero vector in $\mathbb{R}^{N+1}$. With this notation at hand, the numerical method (5.15) may be expressed as the following vector identity, valid for every $k = 1, \ldots, M-1$:

$$A\mathbf{u}^{k+1} - B_{k_4}\mathbf{u}^k - B_{k_5}\mathbf{u}^{k-1} = \mathbf{0}. \tag{5.22}$$

5.4 Preserved properties

Throughout this section, we follow the nomenclature employed in Sections 5.2 and 5.3. The present stage of our investigation is devoted to establish the symmetry-preserving property of our technique, as well as conditions under which positive or bounded, initial profiles evolve under (5.15) into positive or bounded approximations, respectively.

5.4.1 Symmetry

Notice first of all that the left-hand side of (5.22) is a function of the ordered triple $\mathbf{U}^k = (\mathbf{u}^{k+1}, \mathbf{u}^k, \mathbf{u}^{k-1})$, for every k in $\{1, \ldots, M-1\}$. For the sake of convenience, we define $-\mathbf{U}^k$ as the ordered triple $(-\mathbf{u}^{k+1}, -\mathbf{u}^k, -\mathbf{u}^{k-1})$, and let $\mathbf{L}(\mathbf{U}^k)$ be the left-hand side of (5.22).

The following result establishes the symmetry properties of the numerical method introduced in this work.

Proposition 36. *For every k in $\{2, \ldots, M-1\}$, the identity $\mathbf{L}(-\mathbf{U}^k) = -\mathbf{L}(\mathbf{U}^k)$ holds if either δ is any positive, even number, or if δ is a positive integer, α is equal to zero and γ equals -1.*

Proof. The matrix A in (5.22) satisfies the identity $A_{-\mathbf{u}^k} = A_{\mathbf{u}^k}$ under our hypotheses, whence the conclusion follows. □

Under the hypotheses of this result, the ordered triple $\mathbf{U}^k$ satisfies the identity (5.22) if and only if $-\mathbf{U}^k$ does. In view of this remark, Proposition 36 shows that our computational technique preserves the skew symmetry of the solutions of the equation under investigation.

5.4.2 Boundedness

We say that a square, real matrix is a *Z-matrix* if all its off-diagonal elements are non-positive. An *M-matrix* is a Z-matrix A for which the following conditions are satisfied:

(i) All the diagonal entries of A are positive, and

(ii) There exists a positive, diagonal matrix D such that AD is strictly diagonally dominant (evidently, this property is trivially satisfied if the matrix A itself is strictly diagonally dominant).

Remark 37. *There exist many characterizations of M-matrices, but the definition given above is good for our purposes. In fact, one of the properties of this type of matrices is that they are contained in the class of* inverse-positive matrices*, which is the collection of non-singular matrices for which all the entries of their inverses are positive, real numbers.*

Let J represent a bounded, open interval. We say that a matrix (or a vector) of any size is *bounded* in J if all of its entries belong in J. A matrix (or vector) is *positive* if all of its entries are positive, real numbers. Let s be a real number, and let $\mathbf{x}$ be a vector in $\mathbb{R}^n$. We employ the notation $\mathbf{x} < s$ (respectively, $\mathbf{x} > s$) to signify that every component of $\mathbf{x}$ is less than s (respectively, greater than s). Clearly, the inequality $\mathbf{x} < s$ holds if and

only if $s\mathbf{e} - \mathbf{x} > 0$ is satisfied for the n-dimensional, real vector $\mathbf{e}$ all of whose components are equal to 1.

For the sake of generality, we consider two possible scenarios in our search for general conditions under which the properties of positivity and boundedness are preserved, namely, the case of Newell-Whitehead-Segel-type equations, and the case of Burgers-Huxley-type equations.

Newell-Whitehead-Segel equations

Throughout, we assume that γ is equal to -1, and that δ is a positive, integer number in the case of a generalized Newell-Whitehead-Segel equation, or that δ is equal to $\frac{1}{2}$ in the case of a Fisher-Kolmogorov-Petrovsky-Piscounov-type equation. In other words, we suppose that the reaction factor takes on the form $g(u) = 1 - u^{2\delta}$. Clearly, the function g restricted to the domain $[-1, 1]$ is non-negative, and it is bounded from above by the number $c_0 = 1$ if δ is a positive integer, and by $c_0 = 2$ if δ is equal to $\frac{1}{2}$.

Lemma 38. *Let δ be a positive, real number which is either an integer or $\frac{1}{2}$, let λ be in $(0, 2)$, and let τ be a non-negative, real number. Suppose that the vector $\mathbf{u}^k$ is bounded in $(-1, 1)$, for some $k \in \{1, \ldots, M-1\}$. If the inequalities*

(a) $\alpha\Delta x < 2$ *and*

(b) $c_0\Delta t < 1 - \lambda/2 + \tau/\Delta t$

are satisfied, then the matrix A of (5.22) is an M-matrix.

Proof. The off-diagonal elements of A are non-positive by assumption (a). The paragraph preceding this lemma states that $g(u_n^k) \leq c_0$. This observation and the condition (b) imply that, for every $n = 1, \ldots, N-1$, the diagonal element of A in the $(n+1)$th row satisfies $k_2 > |k_1| + |k_2| = 2R$. The positivity of the diagonal elements of A and the strictly diagonal dominance of this matrix follow at once. □

Let δ be a positive, real number which is either an integer or $\frac{1}{2}$, and let τ be a non-negative, real number. Define the function $F : [-1, 1] \times [-1, 1] \to \mathbb{R}$ by the rule of correspondence

$$F(x, y) = 1 - \frac{\lambda}{2} + \frac{\tau}{\Delta t} - \Delta t(1 - x^{2\delta}) - \left(1 - \lambda + \frac{2\tau}{\Delta t}\right) x - \left(\frac{\lambda}{2} - \frac{\tau}{\Delta t}\right) y. \tag{5.23}$$

It is readily checked that $F(1, 1) = 0$, and that F is differentiable in the interior of its domain. Moreover, the first-order partial derivatives of F are given by

$$\frac{\partial F}{\partial x}(x, y) = 2\delta\Delta t x^{2\delta-1} - 1 + \lambda - \frac{2\tau}{\Delta t}, \tag{5.24}$$

$$\frac{\partial F}{\partial y}(x, y) = \frac{\tau}{\Delta t} - \frac{\lambda}{2}. \tag{5.25}$$

Clearly, the partial derivative of F with respect to y is negative if $2\tau/\Delta t < \lambda$. On the other hand, the partial derivative of F with respect to x is bounded from above in $(-1, 1) \times (-1, 1)$ by the number $2\delta\Delta t - 1 + \lambda - 2\tau/\Delta t$. Consequently, (5.24) and (5.25) are negative if the condition (c) of the following result holds.

Proposition 39 (Boundedness)**.** *Let δ be a positive integer, and that either δ is even or that α is equal to zero. Let λ be in $(0, 2)$, and let τ be a non-negative, real number. Suppose that $\mathbf{u}^k$ and $\mathbf{u}^{k-1}$ are bounded in $(-1, 1)$, for some $k \in \{1, \ldots, M-1\}$, and that (b) of Lemma 38 holds. The vector $\mathbf{u}^{k+1}$ is bounded in $(-1, 1)$ if*

(c) $2\tau/\Delta t < \lambda < 1 + 2\tau/\Delta t - 2\delta\Delta t$.

Proof. The matrix A is an M-matrix by Lemma 38, so that its inverse is positive. Introduce the vector $\mathbf{w}^{k+1} = \mathbf{e} - \mathbf{u}^{k+1}$ and substitute it in (5.22) to obtain the equation $A\mathbf{w}^{k+1} = \mathbf{b}$, where $\mathbf{b} = A\mathbf{e} - B_{k_4}\mathbf{u}^k - B_{k_5}\mathbf{u}^{k-1}$. The first and the last components of $\mathbf{b}$ are equal to zero, while for every $n \in \{1, \ldots, N-1\}$, the $(n+1)$th component of $\mathbf{b}$ is given by $F(u_n^k, u_n^{k-1})$, where F is provided by (5.23). Hypothesis (c) and the discussion preceding this result establish that $\mathbf{b}$ is a non-negative vector whose only zero components are the first and the last. It follows that the vector $\mathbf{w}^{k+1}$ is positive or, equivalently, that $\mathbf{u}^{k+1} < 1$. On the other hand, let $\mathbf{v}^j = -\mathbf{u}^j$, for every $j = k-1, k, k+1$. Proposition 36 implies that $A_{\mathbf{v}^k}\mathbf{v}^{k+1} = B_{k_4}\mathbf{v}^k + B_{k_5}\mathbf{v}^{k-1}$, and the first part of this result shows that $\mathbf{v}^{k+1} < 1$ or, equivalently, that $\mathbf{u}^{k+1} > -1$. □

Corollary 40 (Positivity)**.** *Let δ be a positive integer, and that either δ is even or that α is equal to zero. Let λ be in $(0,2)$, and let τ be a non-negative, real number. Suppose that $\mathbf{u}^k$ and $\mathbf{u}^{k-1}$ are bounded in $(0,1)$, for some $k \in \{1, \ldots, M-1\}$. If (b) of Lemma 38 and (c) of Proposition 39 hold, then $\mathbf{u}^{k+1}$ is bounded in $(0,1)$.*

Proof. Proposition 39 assures that $-1 < \mathbf{u}^{k+1} < 1$. The constraint (c) of Proposition 39 implies that $B_{k_4}\mathbf{u}^k + B_{k_5}\mathbf{u}^{k-1}$ is a vector all of whose components are positive except for the first and the last ones, which are zero. The conclusion is reached by virtue that A is an M-matrix. □

Burgers-Huxley equations

Let δ be a real number such that $\delta \geq 1$, and let γ be a real number in the interval $[-1, 1]$. Under these conditions, it is easy to show that the function defined by (5.2) satisfies $g(u) \leq \frac{1}{4}(1-\gamma)^2$, for every $u \in [0,1]$.

Lemma 41. *Let s be a real number such that $0 < s \leq 1$, let δ be a real number such that $\delta \geq 1$, let γ be a real number in $[-1,1]$, let λ be in $(0,2)$, let τ be a non-negative, real number, and assume that $\mathbf{u}^k$ is bounded in $(0, s^{1/\delta})$, for some $k \in \{1, \ldots, M-1\}$. The matrix A in (5.22) is an M-matrix if the following inequalities are satisfied:*

(a) $\alpha s \Delta x < 2$ *and*

(b) $\frac{1}{4}(1-\gamma)^2\Delta t < 1 - \lambda/2 + \tau/\Delta t$.

Proof. The positivity of $\mathbf{u}^k$ guarantees that the entry k_3 in the $(n+1)$th row of the matrix A is a negative, real number, for every $n \in \{1, \ldots, N-1\}$. Moreover, the assumption that $(u_n^k)^\delta < s$ and the hypothesis (a) yield that k_1 is likewise negative. The condition (b) and the observation preceding this result give that $g(u_n^k)\Delta t < 1 - \lambda/2 + \tau/\Delta t + 2R$ or, equivalently, that k_2 is positive. Finally, notice that the inequality $|k_1| + |k_3| = 2R < k_2$ holds for every n, which shows that A is strictly diagonally dominant. □

Proposition 42 (Positivity)**.** *Let s be a real number such that $0 < s \leq 1$, let δ be a real number such that $\delta \geq 1$, let γ belong in $[-1,1]$, let λ be in $(0,2)$, let τ be a non-negative, real number, and suppose that $\mathbf{u}^{k-1}$ and $\mathbf{u}^k$ are bounded in $(0, s^{1/\delta})$, for some $k \in \{1, \ldots, M-1\}$. If the inequalities (a) and (b) of Lemma 41 hold and the constraint*

(c) $2\tau/\Delta t < \lambda < 1 + 2\tau/\Delta t$

is satisfied, then $\mathbf{u}^{k+1}$ is a positive vector.

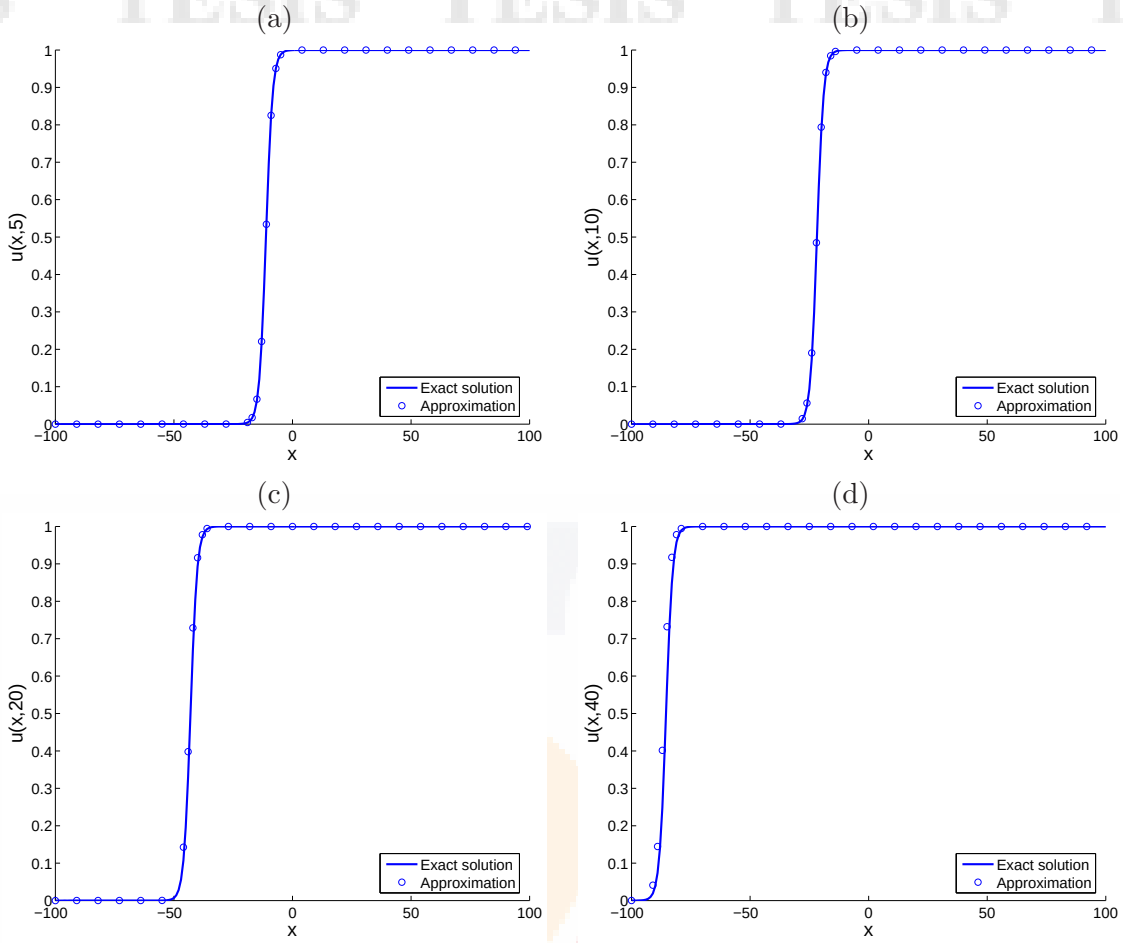

Figure 5.2: Exact and numerical solutions of the model (5.4) with reaction factor (5.2) at four different times, namely $t = 5$, 10, 20 and 40, for an initial profile and initial velocity provided by the equation (5.5) around $t = 0$, with $C_1 = 30$, $C_2 = 20$ and $C_3 = 0$. The following model and computational parameters were employed: $\tau = \alpha = 0$, $\gamma = -1$, $\delta = 1$, $\Delta t = 1 \times 10^{-4}$, $\Delta x = 1$, $\lambda = 0.2$, over the spatial domain $[-100, 100]$.

Proof. The matrix A is an M-matrix by Lemma 41, so that its inverse exists and it is a positive matrix. Moreover, the vector $B_{k_4}\mathbf{u}^k + B_{k_5}\mathbf{u}^{k-1}$ is non-negative, its only zero entries being its first and its last components. We conclude that $\mathbf{u}^{k+1}$ is a vector with positive entries. □

Let δ be a real number such that $\delta \geq 1$, and let τ be a non-negative real number. Let γ and s be real numbers in $(0, 1)$ with $s \leq \gamma$, and let $G : [0, s^{1/\delta}] \times [0, s^{1/\delta}] \to \mathbb{R}$ be the function given by

$$G(x, y) = s^{1/\delta}\left[1 - \frac{\lambda}{2} + \frac{\tau}{\Delta t} - \Delta t(1 - x^\delta)(x^\delta - \gamma)\right] - \left(1 - \lambda + \frac{2\tau}{\Delta t}\right)x - \left(\frac{\lambda}{2} - \frac{\tau}{\Delta t}\right)y. \tag{5.26}$$

The function G is differentiable in the interior of its domain, and it satisfies $G(s^{1/\delta}, s^{1/\delta}) \geq 0$. Moreover, the partial derivatives of G with respect to x and y are

$$\frac{\partial G}{\partial x} = s^{1/\delta}\delta x^{\delta-1}\Delta t\left[2x^\delta - (\gamma + 1)\right] - \left(1 - \lambda + \frac{2\tau}{\Delta t}\right), \tag{5.27}$$

$$\frac{\partial G}{\partial y} = \frac{\tau}{\Delta t} - \frac{\lambda}{2}. \tag{5.28}$$

	Δt			
Time	1×10^{-1}	1×10^{-2}	1×10^{-3}	1×10^{-4}
2.5	1.2089×10^{-2}	1.0405×10^{-3}	3.4436×10^{-4}	3.8019×10^{-4}
5	2.7878×10^{-2}	3.3056×10^{-3}	1.1006×10^{-3}	9.0416×10^{-4}
10	6.1194×10^{-2}	9.5000×10^{-3}	4.7132×10^{-3}	4.2406×10^{-3}
20	1.1860×10^{-1}	2.2285×10^{-2}	1.2862×10^{-2}	1.1926×10^{-2}
40	1.8965×10^{-1}	4.3900×10^{-2}	2.7042×10^{-2}	2.5356×10^{-2}

Table 5.2: Relative errors committed when approximating numerically the exact solution of (5.4) with reaction factor (5.2) at several times, for an initial profile and initial velocity provided by the equation (5.5) around $t = 0$, with $C_1 = 30$, $C_2 = 20$ and $C_3 = 0$. The following model and computational parameters were employed: $\tau = \alpha = 0$, $\gamma = -1$, $\delta = 1$, $\Delta x = 1$, $\lambda = 0.2$, over the spatial domain $[-100, 100]$. Several values of Δt have been chosen.

Evidently, the partial derivative of G with respect to y is negative in $(0, s^{1/\delta}) \times (0, s^{1/\delta})$ if and only if $\lambda > 2\tau/\Delta t$. On the other hand, every x which belongs in $(0, s^{1/\delta})$ satisfies $x^\delta < s \leq \gamma < 1$, so that a sufficient condition for (5.27) to be negative in the interior of the domain of G is that the inequality $s\delta\Delta t[2s - (\gamma + 1)] < 1 - \lambda + 2\tau/\Delta t$ be satisfied. Under these circumstances, the function G is positive in the interior of its domain.

It is interesting to notice that (5.26) may be negative in $(0, s^{1/\delta}) \times (0, s^{1/\delta})$ if $\gamma < s < 1$. However, G is again positive when s is equal to 1, if the conditions derived in the previous paragraph are satisfied.

Proposition 43 (Boundedness)**.** *Let s be a real number such that $0 < s \leq 1$, which satisfies either $s \leq \gamma$ or $s = 1$. Let δ be a real number such that $\delta \geq 1$, let γ and λ both belong in $(0, 1)$, let τ be a non-negative, real number, and assume that $\mathbf{u}^{k-1}$ and $\mathbf{u}^k$ are bounded in $(0, s^{1/\delta})$, for some $k \in \{1, \ldots, M - 1\}$. Suppose that (a) and (b) of Lemma 41, and (c) of Proposition 42 are satisfied. The vector $\mathbf{u}^{k+1}$ is bounded in $(0, s^{1/\delta})$ if the following inequality holds:*

(d) $s\delta\Delta t[2s - (\gamma + 1)] < 1 - \lambda + 2\tau/\Delta t$.

Proof. The vector $\mathbf{u}^{k+1}$ is positive by Proposition 42. Now, let $\mathbf{w}^{k+1} = s^{1/\delta}\mathbf{e} - \mathbf{u}^{k+1}$ and substitute it in (5.22) to obtain $A\mathbf{w}^{k+1} = \mathbf{b}$, where $\mathbf{b}$ is equal to $As^{1/\delta}\mathbf{e} - B_{k_4}\mathbf{u}^k - B_{k_5}\mathbf{u}^{k-1}$. The first and the last components of $\mathbf{b}$ are equal to zero; meanwhile, for every $n \in \{1, \ldots, N - 1\}$, its $(n + 1)$th component assumes the form $G(u_n^k, u_n^{k-1})$, where both u_n^k and u_n^{k-1} belong in $(0, s^{1/\delta})$, and G is the function in (5.26). The hypothesis (c) and the discussion in the previous paragraph yield that $\mathbf{b}$ is a vector all of whose components, except for the first and the last ones, are positive. Consequently, the vector $\mathbf{w}^{k+1}$ is positive or, equivalently, $\mathbf{u}^{k+1} < s^{1/\delta}$. □

5.5 Numerical simulations

In this section, we present some simulations in order to check the performance of our numerical method when it is used to approximate positive and bounded solutions of (5.4). For comparison purposes, our simulations will employ the known, exact solutions presented in Section 5.2.2. We will restrict our attention to relatively wide, bounded domains, and

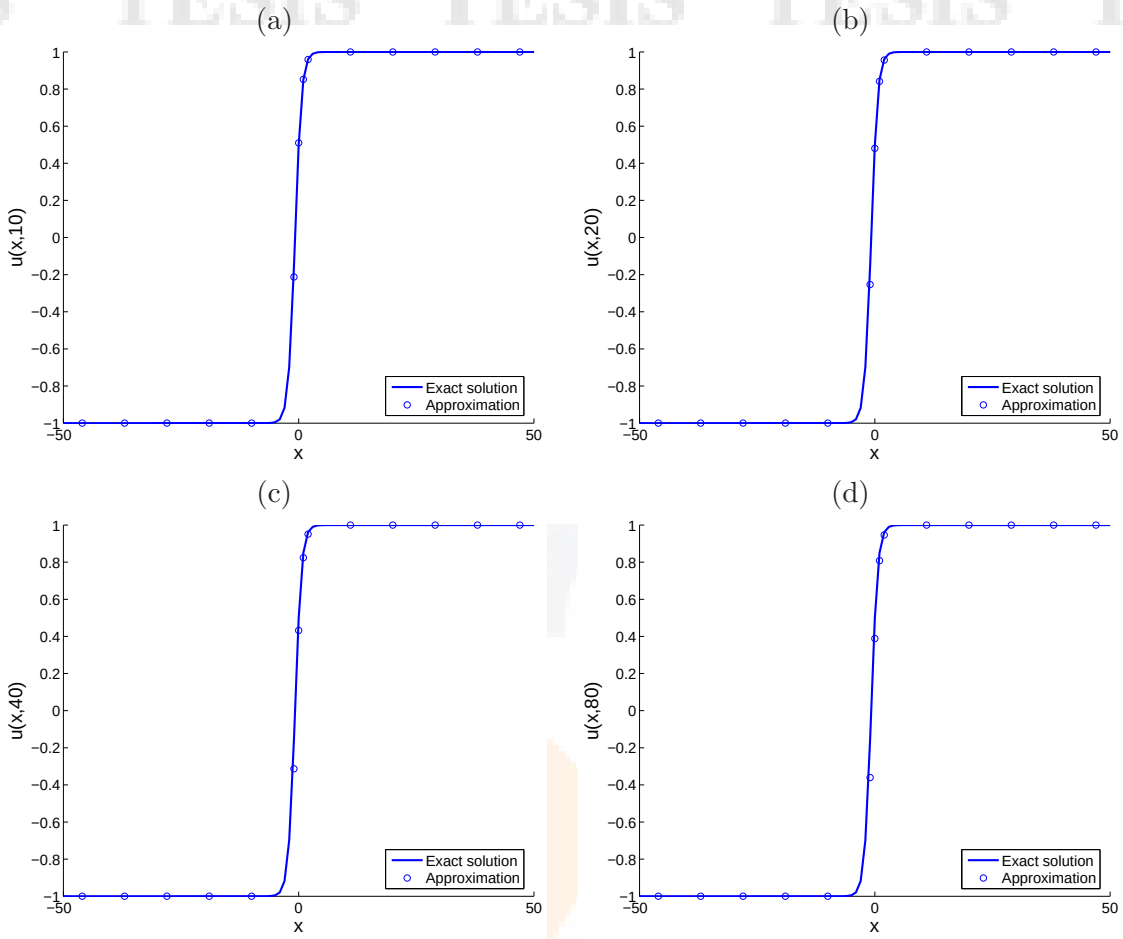

Figure 5.3: Exact and numerical solutions of the model (5.4) with reaction factor (5.2) at four different times, namely $t = 10$, 20, 40 and 80, for an initial profile and initial velocity provided by the equation (5.5) around $t = 0$, with $C_1 = 30$, $C_2 = 20$ and $C_3 = 10$. The following model and computational parameters were employed: $\tau = \alpha = 0$, $\gamma = -1$, $\delta = 1$, $\Delta t = 1 \times 10^{-4}$, $\Delta x = 1$, $\lambda = 0.2$, over the spatial domain $[-50, 50]$.

we will impose homogeneous Neumann boundary conditions on the endpoints of the spatial interval. From a computational perspective, it is important to point out that if u represents the exact solution of interest, then the first two approximations at the times t_0 and t_1 will be given by $u_n^k = u(x_n, t_k)$, for every $n = 0, 1, \ldots, N$ and $k = 0, 1$. Also, it is important to mention that all of our simulations were carried out through an implementation of Thomas' algorithm to solve the tridiagonal system (5.22).

5.5.1 Newell-Whitehead-Segel equations

In the present stage, we consider the model (5.4) when both τ and α are equal to zero, and parameter γ equal to -1. For more accurate comparisons, we let $\|\cdot\|_\infty$ denote the *infinite norm* in $\mathbb{R}^n$, defined by $\|\mathbf{x}\|_\infty = \sup\{|x_i| : i = 1, \ldots, n\}$, whenever $\mathbf{x} = (x_1, \ldots, x_n)$. In these terms, the *relative error* committed when approximating a vector $\mathbf{y} \in \mathbb{R}^n$ by a nonzero vector $\mathbf{x}$, is given by

$$\rho(\mathbf{x}, \mathbf{y}) = \frac{\|\mathbf{x} - \mathbf{y}\|_\infty}{\|\mathbf{y}\|_\infty}. \tag{5.29}$$

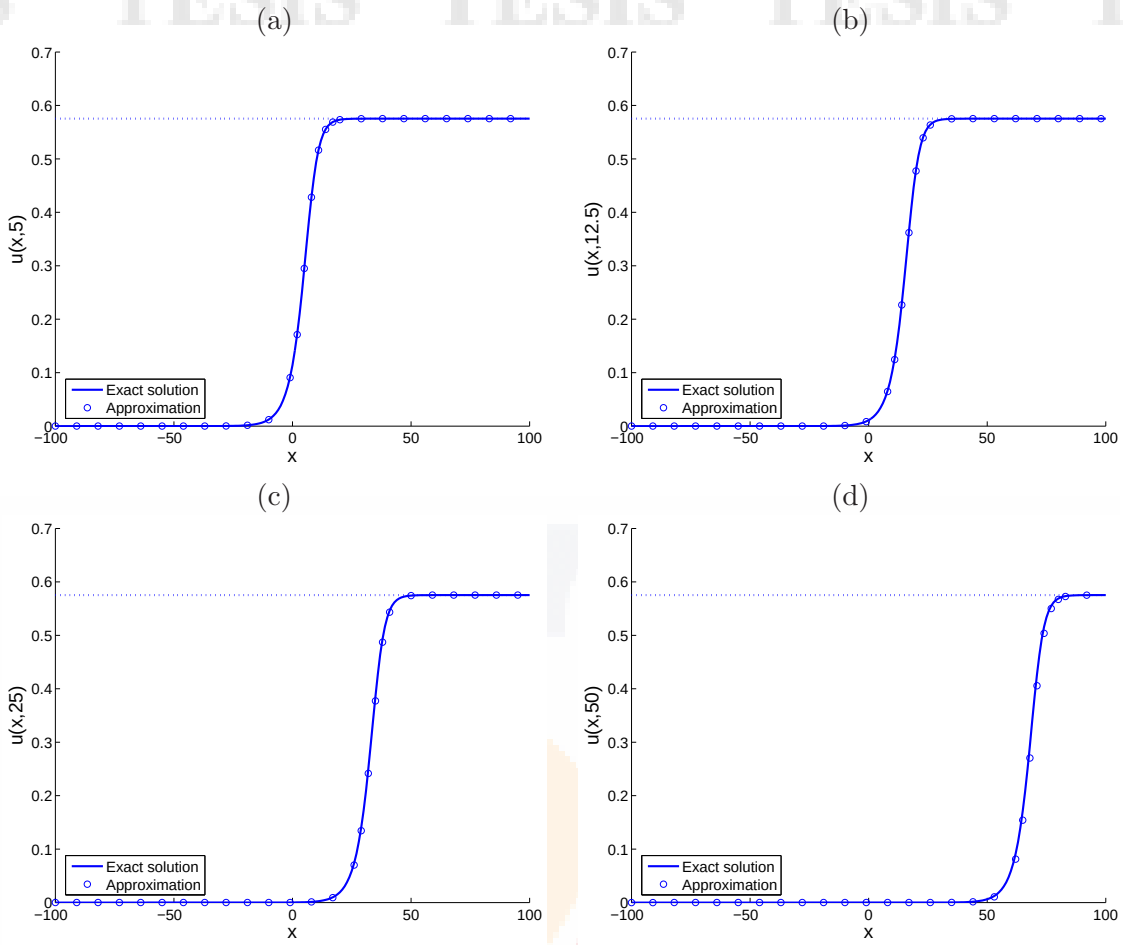

Figure 5.4: Exact and numerical solutions of the model (5.4) with reaction factor (5.2) at four different times, namely $t = 5$, 12.5, 25 and 50, for an initial profile and initial velocity provided by the equation (5.6) around $t = 0$. The following model and computational parameters were employed: $\tau = 0$, $\alpha = 0.05$, $\gamma = 0.38$, $\delta = 1.75$, $\Delta t = 1 \times 10^{-4}$, $\Delta x = 1$, $\lambda = 0.2$, over the spatial domain $[-100, 100]$. The dotted, horizontal line represents the constant $\gamma^{1/\delta}$.

Example 44 (Boundedness in $(0, 1)$)**.** Consider the partial differential equation (5.4) with parameters τ and α both equal to zero, with a reaction factor (5.2) in which γ is equal to -1 and δ is equal to 1. More precisely, we consider a Newell-Whitehead-Segel model over the spatial domain $[-100, 100]$, and we employ the particular solution (5.5) with C_1, C_2 and C_3 equal to 30, 20 and 0, respectively. Computationally, we choose step sizes Δt and Δx equal to 1×10^{-4} and 1, respectively, with λ equal to 0.2. Under these circumstances, Figure 5.2 shows the graphs of the exact solution and the approximation obtained through the finite-difference scheme (5.15) at four different times, namely, 5, 10, 20 and 40. The results evidence a good agreement between the analytical and the numerical solutions. Moreover, the numerical solutions, as the exact ones, remain bounded between 0 and 1 at all times; this is in perfect agreement with the fact that the computational and model parameters satisfy the conditions of Corollary 40. For convenience, we have included Table 5.2, in which we have computed the relative errors committed when approximating the exact solutions of our problem through the finite-difference scheme (5.15), fixing Δx at 1 and decreasing the value of Δt. The results immediately suggest the convergence of our method. □

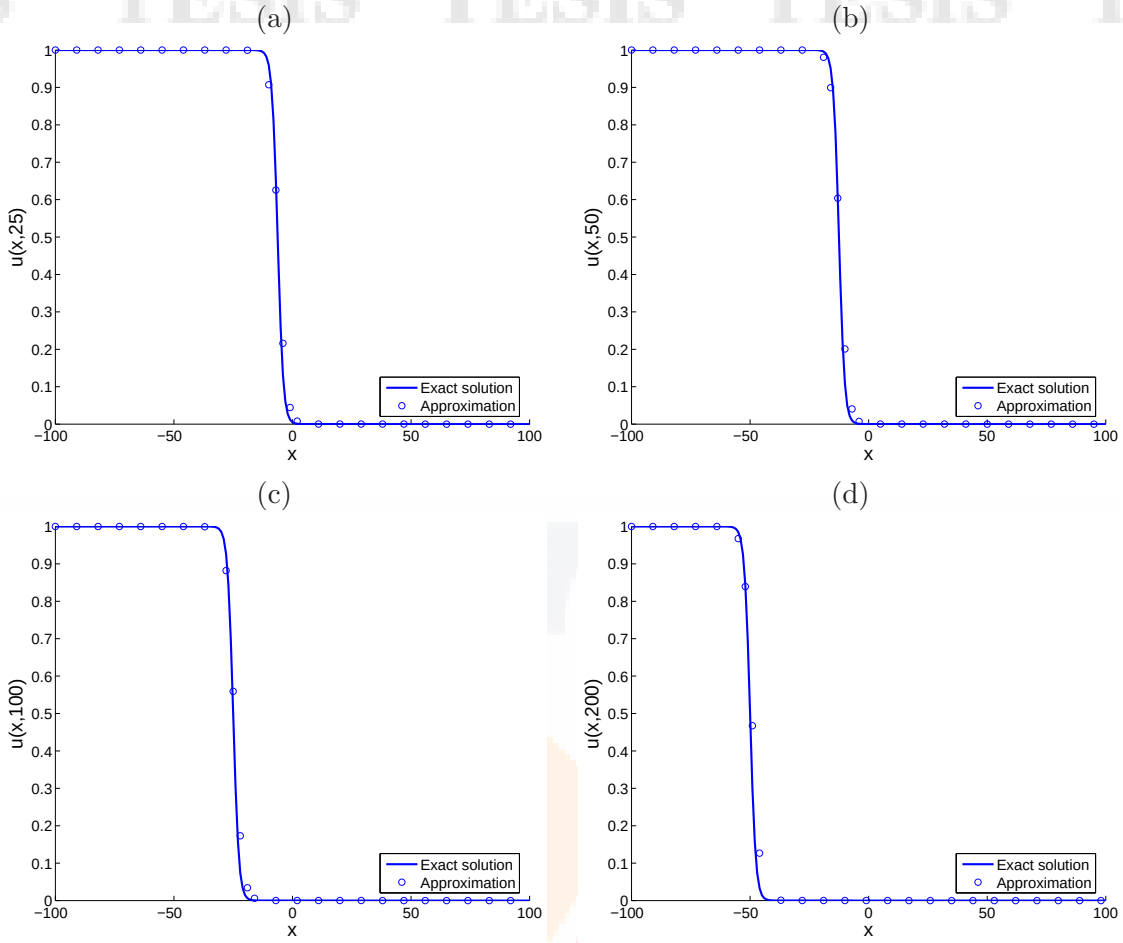

Figure 5.5: Exact and numerical solutions of the model (5.4) with reaction factor (5.2) at four different times, namely $t = 25$, 50, 100 and 200, for an initial profile and initial velocity provided by the equation (5.8) around $t = 0$. The following model and computational parameters were employed: $\tau = 0$, $\alpha = \gamma = 0.5$, $\delta = 1$, $\Delta t = 1 \times 10^{-4}$, $\Delta x = 1$, $\lambda = 0.2$, over the spatial domain $[-100, 100]$.

Example 45 (Boundedness in $(-1, 1)$)**.** Consider exactly the same model studied in Example 44 over the spatial domain $[-50, 50]$, with initial conditions provided by the exact solution (5.5) with C_1, C_2 and C_3 equal to 30, 20 and 10, respectively. Computationally, we let Δt, Δx and λ take on the same values as in the previous example, and consider four different times, namely, 10, 20, 40 and 80. The results of our simulations are presented in Figure 5.3 and, as in Example 44, there exists a good agreement between the numerical and the analytical solutions of the problem under consideration. Moreover, the property of boundedness of the exact solutions is preserved by the computational approximations, in view that the conditions of the Proposition 39 are satisfied. □

5.5.2 Burgers-Huxley equations

In the present section, we consider equations of the form (5.4) with τ equal to zero, and γ in $(0, 1)$.

Example 46 (Boundedness in $(0, \gamma^{1/\delta})$)**.** Consider the model (5.4) with τ equal to 0. For comparison purposes, we use the exact solution (5.6) with parameters α, γ and δ equal to 0.05, 0.38 and 1.75, respectively, so that the analytical solutions are bounded

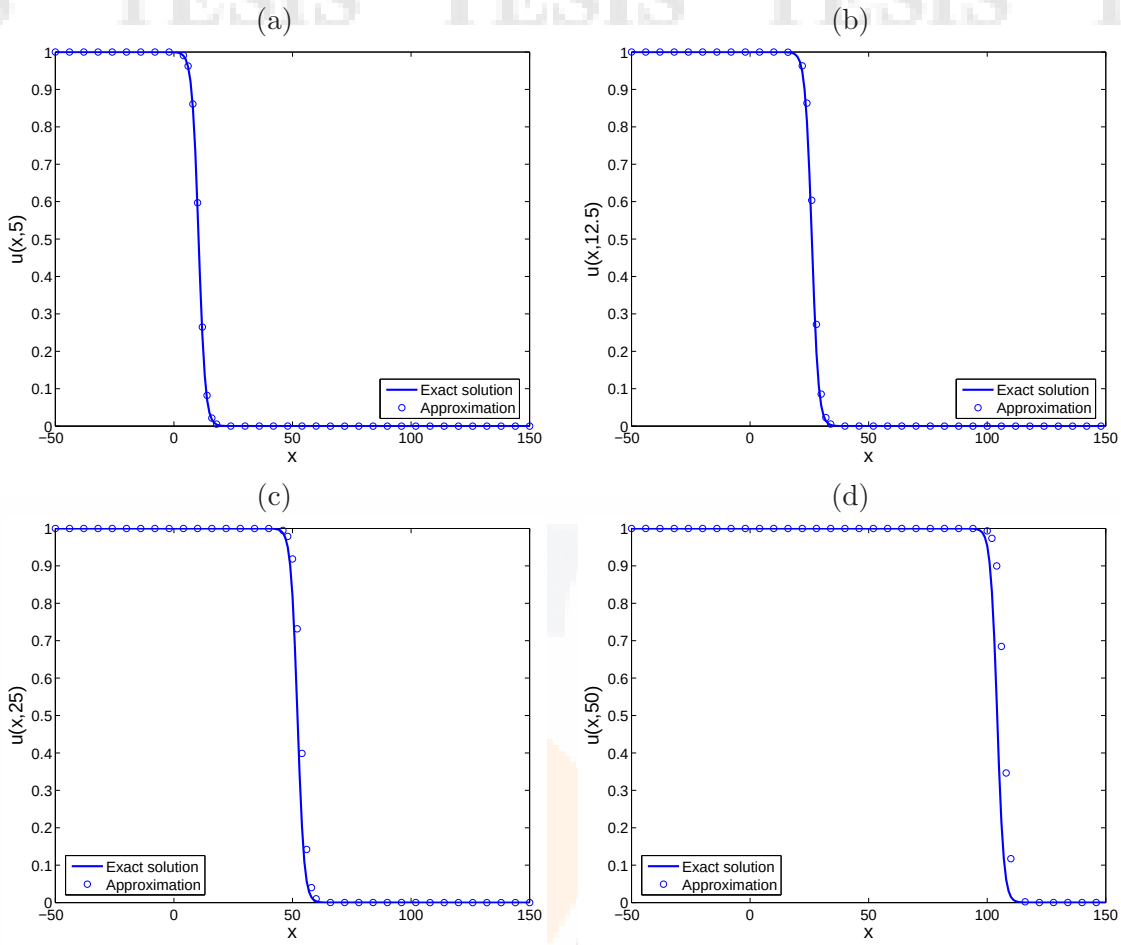

Figure 5.6: Exact and numerical solutions of the model (5.4) with reaction factor (5.2) at four different times, namely $t = 5$, 12.5, 25 and 50, for an initial profile and initial velocity provided by the equation (5.10) with $C_0 = 1$ around $t = 0$. The following model and computational parameters were employed: $\tau = 0.008$, $\alpha = 0$, $\gamma = -1$, $\delta = 1$, $\Delta t = 0.01$, $\Delta x = 1$, $\lambda = 1$, over the spatial domain $[-50, 150]$.

between 0 and $\gamma^{1/\delta}$. Computationally, the parameters Δt, Δx and λ are equal to 1×10^{-4}, 1 and 0.2, respectively, and we use the spatial domain $[-100, 100]$. The exact solutions and the numerical approximations obtained through (5.15) for the times $t = 5$, 12.5, 25 and 50 are shown in Figure 5.4. The graphs evidently show a good agreement between the analytical simulations and the computational estimations. Moreover, the solutions remain bounded within the interval $(0, \gamma^{1/\delta})$. This is in agreement with the fact that the model and computational parameters satisfy the boundedness conditions summarized in Proposition 43. □

Example 47 (Boundedness in $(0, 1)$)**.** Consider the partial differential equation (5.4) with τ equal to zero, and parameters α, γ and δ equal to 0.5, 0.5 and 1, respectively. In this example, we compare the performance of the numerical method (5.15) against the exact solution provided by (5.8), over the spatial domain $[-100, 100]$ at four different times, namely, 25, 50, 100 and 200. The computational parameters are the same as those employed in Example 46. The results are presented in Figure 5.5 where, once again, a good agreement is found between the theoretical and the numerical results. Moreover, one immediately notices that the numerical approximations remain bounded within the

interval $(0, 1)$, a result which is in perfect agreement with the fact that the model and numerical parameters comply with the conditions of Proposition 43. □

5.5.3 Klein-Gordon equation

In this stage, we consider the hyperbolic version of the partial differential equation (5.4) introduced in Section 5.2.2.

Example 48 (Boundedness in $(0, 1)$)**.** We consider now the advectionless form of the partial differential equation (5.4), assuming that τ is a positive constant and that m is equal to 1. We consider a reaction factor (5.2) with γ equal to -1 and δ equal to 1. The resulting model is a nonlinear, damped Klein-Gordon model which, by virtue of the change of variable $\zeta = t/\sqrt{\tau}$, can be rewritten as

$$\frac{\partial^2 u}{\partial \zeta^2} + \frac{1}{\sqrt{\tau}} \frac{\partial u}{\partial \zeta} - \frac{\partial^2 u}{\partial x^2} - u(1 - u^2) = 0. \tag{5.30}$$

The solution of our original problem is given by (5.10) as a function of the pair (x, ζ), for a damping coefficient equal to $1/\sqrt{\tau}$. For simulation purposes, we choose the parameter τ equal to 0.008, and we let Δx and λ be both equal to 1. We have obtained numerical results for values of Δt satisfying the conditions of Corollary 40, and we have obtained good approximations to the exact solution of the problem under consideration, which remain bounded within $(0, 1)$ at all times. In fact, we have also considered values of Δt which just violate property (c) of Proposition 39, and we have found that the numerical results still remain bounded, as Figure 5.6 witnesses. The graphs correspond to the times 5, 12.5, 25 and 50, for values of Δt, Δx and λ equal to 0.01, 1 and 1, respectively. The spatial domain employed is $[-50, 150]$, and the value of the constant C_0 in the particular solution (5.10) is 1. □

Conclusions

Closing remarks

In this work, we have investigated numerically the design of numerical methods to approximate solutions of nonlinear models of mathematical physics and biology. Motivated by the fact that the models of interest possess traveling-waver solutions which are unknown in exact form, we provided a semilinear approach to the problem of approximating consistently the solutions of the considered models, all of which are nonlinear partial differential equations with linear diffusion, and nonlinear reaction and advection. For such partial differential equations, the existence of traveling fronts which are bounded is a well-known fact. Among these models, we made emphasis on the investigation of the following equations and some of their generalizations:

- the classical Fisher-KPP equation
- the Newell-Whitehead-Segel equation,
- the FitzHugh-Nagumo equation,
- the Burgers-Huxley equation, and
- the Burgers-Fisher.

It is important to mention that the traveling-wave solutions considered as bounded profiles (in many cases, non-negative solutions, also), which connect asymptotically two constant solutions of the models investigated. The solutions are monotone in both space and time, and satisfy pertinent symmetry properties. The methods proposed in this work are capable of preserving the boundedness of initial approximations, the non-negativity of the computational solutions, and the skew-symmetry preservation, also. The methods are consistent of second order in space and first order in time.

The methods proposed in this work can be expressed in vector form through the multiplication of a matrix which, under suitable conditions, turns out to be an M-matrix, that is, a strictly diagonally dominant, square, real matrix whose diagonal entries are positive numbers, and whose off-diagonally components are non-positive. As we know, M-matrices are non-singular matrices with the property that all the entries of their inverses are positive, real numbers. This feature of M-matrices guarantees that positive, initial profiles will evolve discretely into positive, new approximations. Moreover, the boundedness of the approximations may be guaranteed via the preservation of the positive character of solutions. Needless to mention that pertinent existence-and-uniqueness results readily follow after these remarks.

From a computational perspective, the methods were implemented in Matlab and, when available, the numerical results were compared against known, exact solutions. The results evince an excellent agreement between the analytical and computational solutions. Moreover, the comparisons show that the methods are indeed second-order approximations

in space nd first-order approximations in time to the exact solutions. Also, the simulations show that the properties of positivity and boundedness are preserved throughout the iterations, even in cases when the analytical conditions for the preservation of positivity and boundedness are broken. These observations suggest that the method is very robust with respect to the preservation of these properties, and further investigation on the matter is motivated by the numerical results.

Perspectives

It is important to mention that, in recent efforts, we have undertaken a nonlinear approach to the problem of approximating traveling-wave solutions of some of the models previously considered. The results (not shown here) evince that the nonlinear approach presents many advantages with respect to the semilinear perspective investigated in this work. Indeed, the properties of positivity, boundedness and skew-symmetry are preserved as in the semilinear case. However, two additional advantages are noticed in this new perspective:

- Firstly, the methods may me conditionally monotone. As consequence, the methods may preserve the temporal and spatial monotonicity of solutions, which are highly desirable characteristics in the approximation of the traveling-wave solutions considered in this work.

- Secondly, the computational implementation requires of Newton's method to solve nonlinear systems of equations. As a consequence, the implementations of the nonlinear methods result in faster techniques which approximate the solutions with a higher degree of accuracy.

Thus, the epilogue of this work opens a new perspective of work: To investigate nonlinear discretizations of the models studied in the present manuscript. The task looks promising, but lies outside the aims of the present work.

Another interesting problem to be tackled in the future is the extension of our results to different methodologies within the area of numerical analysis. Thus, one may inquire about the feasibility of extending this work to the realm of the finite-element methods. From our point of view, the problem is interesting and nontrivial. Indeed, most of the finite-element methods reported in the literature have a high degree of accuracy; however, the possibility of preserving mathematical features of the solutions using this methodology has not been sufficiently exploited. Of course, we hope to investigate this problem in the future.

Bibliography

[1] D. Ağırseven, T. Öziş, An analytical study for Fisher type equations by using homotopy perturbation method, Comput. & Math. Appl. 60 (2010) 602–609.

[2] M. E. Alexander, A. R. Summers, S. M. Moghadas, Neimark-Sacker bifurcations in a non-standard numerical scheme for a class of positivity-preserving ODEs, Proc. R. Soc. A 462 (2006) 3167–3184.

[3] A. Anderson, K. Rejniak, P. Gerlee, V. Quaranta, Microenvironment driven invasion: a multiscale multimodel investigation, J. Math. Biol. 58 (2009) 579–624.

[4] A. J. Arenas, G. González-Parra, B. M. Chen-Charpentier, A nonstandard numerical scheme of predictor-corrector type for epidemic models, Comput. & Math. Appl. 59 (2010) 3740–3749.

[5] A. J. Arenas, J. A. Moraño, J. C. Cortés, Non-standard numerical method for a mathematical model of RSV epidemiological transmission, Comput. & Math. Appl. 56 (2008) 670–678.

[6] D. G. Aronson, H. F. Weinberger, Multidimensional nonlinear diffusion in population genetics, Adv. Math. 30 (1978), pp. 33–76.

[7] M. Berzins, Variable-order finite elements and positivity preservation for hyperbolic PDEs, Appl. Numer. Math. 48 (2004) 271–292.

[8] E. Bonetti, P. Colli, M. Fabrizio, G. Gilardi, Existence and boundedness of solutions for a singular phase field system, J. Diff. Eq. 246 (2009) 3260–3295.

[9] J. H. M. T. Boonkkamp, M. J. H. Anthonissen, The finite volume-complete flux scheme for advection-diffusion-reaction equations, J. Sci. Comput. (2010), online, DOI 10.1007/s10915-010-9388-8.

[10] G. P. Boswell, H. Jacobs, F. A. Davidson, G. M. Gadd, K. Ritz, A positive numerical scheme for a mixed-type partial differential equation model for fungal growth, Appl. Math. Comput. 138 (2003) 321–340.

[11] A. M. Bruckstein, D. Snaked, Skew symmetry detection via invariant signatures, Pattern Recogn. 31 (1998) 181–192.

[12] J. R. Branco, J. A. Ferreira, P. de Oliveira, Numerical methods for the generalized Fisher-Kolmogorov-Petrovskii-Piskunov equation, Appl. Num. Math. 57 (2007) 89–102.

[13] A. G. Bratsos, A fourth order numerical scheme for the one-dimensional sine-Gordon equation, Intern. J. Comput. Math. 85 (2008), pp. 1083–1095.

[14] N. Broekhuizen, G. J. Rickard, J. Bruggeman, A. Meister, An improved and generalized second order, unconditionally positive, mass conserving integration scheme for biochemical systems, Appl. Numer. Math. 58 (2008) 319–340.

[15] R. L. Burden, J. D. Faires, Numerical Analysis, 4th Edition, PWS-KENT Publishing Company, Boston, MA, 1989.

[16] Z. Cen, A second-order finite difference scheme for a class of singularly perturbed delay differential equations, Intern. J. Comput. Math. 87 (2010), pp. 173–185.

[17] B. M. Chen-Charpentier, H. V. Kojouharov, Mathematical modeling of bioremediation of trichloroethylene in aquifers, Comput. & Math. Appl. 56 (2008) 645–656.

[18] J. Cheng, C. W. Shu, A high order accurate conservative remapping method on staggered meshes, Appl. Numer. Math. 58 (2008) 1042–1060.

[19] S. M. Choo, S. K. Chung, Conservative nonlinear difference scheme for the Cahn-Hilliard equation, Comput. & Math. Appl. 36 (1998) 31–39.

[20] S. M. Choo, S. K. Chung, Y. J. Lee, A conservative difference scheme for the viscous Cahn-Hilliard equation with a nonconstant gradient energy coefficient, Appl. Numer. Math. 51 (2004) 207–219.

[21] H. J. Eberl, L. Demaret, A finite difference scheme for a degenerated diffusion equation arising in microbial ecology, Electr. J. Diff. Eq. 15 (2007) 77–95.

[22] H. J. Eberl, D. F. Parker, M. C. M. van Loosdrecht, A new deterministic spatio-temporal continuum model for biofilm development, Comput. Math. Meth. Med. 3 (2001) 161–175.

[23] E. S. Fahmy, Travelling wave solutions for some time-delayed equations through factorizations, Chaos, Solitons & Fractals 38 (2008) 1209–1216.

[24] E. G. Fan, Traveling wave solutions for nonlinear equations using symbolic computation, Comput. & Math. Appl. 43 (2002) 671–680.

[25] Z. Fei, V. M. Pérez-García, L. Vázquez, Numerical simulation of nonlinear Schrödinger systems: A new conservative scheme, Appl. Math. Comput. 71 (1995) 165–177.

[26] Z. Feng, G. Chen, S. Hsu, A qualitative study of the damped Duffing equation and applications, Discr. & Cont. Dynam. Sys — Series B 6 (2006) 1097.

[27] R. A. Fisher, The wave of advance of advantageous genes, Ann. Eugenics 7 (1937) 355–369.

[28] R. FitzHugh, Mathematical models of threshold phenomena in the nerve membrane, Bull. Math. Biol. 17 (1955) 257–278.

[29] J. Fort, V. Méndez, Reaction-diffusion waves of advance in the transition to agricultural economies, Phys. Rev. E 60 (1999) 5894–5901.

[30] J. Fort, V. Méndez, Time-delayed theory of the Neolithic transition in Europe, Phys. Rev. Lett 82 (1999) 867–870.

[31] J. Fort, V. Méndez, Time-delayed spread of viruses in growing plaques, Phys. Rev. Lett. 89 (2002), pp. 178101–178104.

[32] M. Fournié, High order conservative difference methods for 2D drift-diffusion model on non-uniform grid, Appl. Numer. Math. 33 (2000) 381–392.

[33] T. Fujimoto, R. R. Ranade, Two characterizations of inverse-positive matrices: The Hawkins-Simon condition and the Le Chatelier-Braun principle, Electr. J. Linear Alg. 11 (2004) 59–65.

[34] D. Furihata, Finite difference schemes that inherit energy conservation or dissipation property, J. Comput. Phys. 156 (1999) 181–205.

[35] D. Furihata, Finite-difference schemes for nonlinear wave equation that inherit energy conservation property, J. Comput. Appl. Math. 134 (2001) 37–57.

[36] K. P. Hadeler and K. Dietz, Nonlinear hyperbolic partial differential equations for the dynamics of parasite populations, Comp. Math. Appl. 9 (1983), pp. 415–430.

[37] Z. Horváth, Positivity of Runge-Kutta and diagonally split Runge-Kutta methods, Appl. Numer. Math. 28 (1998) 309–326.

[38] C. Huang, Strong stability preserving hybrid methods, Appl. Numer. Math. 59 (2009) 891–904.

[39] H. N. A. Ismail, K. Raslan, A. A. Abd Rabboh, Adomian decomposition method for Burger's-Huxley and Burger's-Fisher equations, Appl. Math. Comput. 159 (2004) 291–301.

[40] L. Jódar, R. J. Villanueva, A. J. Arenas, G. C. González, Nonstandard numerical methods for a mathematical model for influenza disease, Math. & Comput. Simul. 79 (2008) 622–633.

[41] P. M. Jordan, A nonstandard finite difference scheme for nonlinear heat transfer in a thin finite rod, J. Diff. Eq. Appl. 9 (2003) 1015–1021.

[42] P. M. Jordan, On the application of the Cole-Hopf transformation to hyperbolic equations based on second-sound models, Math. Comput. Simul. 81 (2010) 18–25.

[43] P. M. Jordan, A. Puri, Digital signal propagation in dispersive media, J. Appl. Phys. 85 (1999) 1273.

[44] C. Kahl, M. Günther, T. Rossberg, Structure preserving stochastic integration schemes in interest rate derivative modeling, Appl. Numer. Math. 58 (2008) 284–295.

[45] W. E. Kastenberg, P. L. Chambré, On the stability of nonlinear space-dependent reactor kinetics, Nucl. Sci. Eng. 31 (1968) 67–79.

[46] J. Kim, K. Kang, A numerical method for the ternary cahn-hilliard system with a degenerate mobility, Appl. Numer. Math. 59 (2009) 1029–1042.

[47] A. Kolmogorov, I. Petrovsky, N. Piscounov, Étude de l'équations de la diffusion avec croissance de la quantité de matière et son application a un problème biologique, Bull. Univ. Moskou, Ser. Internat. 1A (1937) 1–25.

[48] A. J. Kozakevicius, L. C. C. Santos, ENO adaptive method for solving one-dimensional conservation laws, Appl. Numer. Math. 59 (2009) 2337–2355.

[49] A. E. Kudryavtsev, Solitonlike solutions for a Higgs scalar field, JETP Lett. 22 (1975) 82–83.

[50] Y. N. Kyrychko, M. V. Bartuccelli, K. B. Blyuss, Persistence of travelling wave solutions of a fourth order diffusion system, J. Comput. Appl. Math. 176 (2005) 433–443.

[51] J. A. León, J. Villa, An Osgood criterion for integral equations with applications to stochastic differential equations with an additive noise, Stat. & Prob. Lett. In press, doi:10.1016/j.spl.2010.12.001.

[52] J. E. Macías-Díaz, A numerical method with properties of consistency in the energy domain for a class of dissipative nonlinear wave equations with applications to a Dirichlet boundary-value problem, Z. Angew. Math. Mech. 88 (2008) 828–846.

[53] J. E. Macías-Díaz, On the controlled propagation of wave signals in a sinusoidally forced two-dimensional continuous Frenkel-Kontorova model, Wave Motion 13–23 (2011) 48.

[54] J. E. Macías-Díaz, I. E. Medina-Ramírez, A. Puri, Numerical treatment of the spherically symmetric solutions of a generalized Fisher-Kolmogorov-Petrovsky-Piscounov equation, J. Comput. Appl. Math. 231 (2009) 851–868.

[55] J. E. Macías-Díaz, A. Puri, An energy-based computational method in the analysis of the transmission of energy in a chain of coupled oscillators, J. Comput. Appl. Math. 214 (2008) 393–405.

[56] J. E. Macías-Díaz, A. Puri, A boundedness-preserving finite-difference scheme for a damped nonlinear wave equation, Appl. Numer. Math. 60 (2010) 934–948.

[57] J. E. Macías-Díaz, A. Puri, A numerical method for computing radially symmetric solutions of a sissipative nonlinear modified Klein-Gordon equation, Numer. Meth. Part. Diff. Eq. 21 (2005) 998–1015.

[58] J. E. Macías-Díaz, A. Puri, On some explicit non-standard methods to approximate nonnegative solutions of a weakly hyperbolic equation with logistic nonlinearity, Inter. J. Comput. Math. 88 (2011) 3308–3323.

[59] J. E. Macías-Díaz, J. Ruiz-Ramírez, A non-standard symmetry-preserving method to compute bounded solutions of a generalized newell-whitehead-segel equation, Appl. Numer. Math. 61 (2011) 630–640.

[60] V. Méndez and J. Camacho, Dynamics and thermodynamics of delayed population growth, Phys. Rev. E 55 (1997), pp. 6476–6482.

[61] V. Méndez, J. Camacho, Hyperbolic reaction-diffusion equations for a forest fire model, Phys. Rev. E 56 (1997) 6557–6563.

[62] G. Meral and M. Tezer-Sezgin, Differential quadrature solution of nonlinear reaction–diffusion equation with relaxation-type time integration, Intern. J. Comput. Math. 86 (2009), pp. 451–463.

[63] R. E. Mickens, Discretizations of nonlinear differential equations using explicit nonstandard methods, J. Comput. Appl. Math. 110 (1999) 181–185.

[64] R. E. Mickens, Nonstandard finite-difference schemes for reaction-diffusion equations, Num. Meth. Part. Diff. Eq. 15 (1999) 201–214.

[65] R. E. Mickens, A nonstandard finite-difference scheme for the Lotka–Volterra system, Appl. Numer. Math. 45 (2-3) (2003) 309–314.

[66] R. E. Mickens, Numerical integration of population models satisfying conservation laws: NSFD methods, J. Biol. Dyn. 1 (2007) 427–436.

[67] R. Mickens and P. Jordan, Construction of nonstandard finite difference schemes for $1\frac{1}{2}$ space-dimension-coupled PDEs, Numer. Meth. Part. Diff. Eq. 23 (2007), pp. 211–219.

[68] R. E. Mickens, P. M. Jordan, A positivity-preserving nonstandard finite difference scheme for the damped wave equation, Numer. Meth. Part. Diff. Eq. 20 (2004) 639–649.

[69] R. E. Mickens, P. M. Jordan, A new positivity-preserving nonstandard finite difference scheme for the DWE, Numer. Meth. Part. Diff. Eq. 21 (2005) 976–985.

[70] R. C. Mittal and G. Arora, Efficient numerical solution of Fisher's equation by using B-spline method, Intern. J. Comput. Math. (2010), in press, doi:10.1080/00207160902878555.

[71] S. M. Moghadas, M. E. Alexander, B. D. Corbett, A nonstandard numerical scheme for a generalized Gause-type predator-prey model, Phys. D 188 (2004) 134–151.

[72] S. M. Moghadas, A. B. Gumel, Dynamical and numerical analyses of a generalized food-chain model, Appl. Math. Comput. 142 (2003) 35–49.

[73] R. K. Mohanty, New unconditionally stable difference schemes for the solution of multi-dimensional telegraphic equations, Intern. J. Comput. Math. 86 (2009), pp. 2060–2071.

[74] J. Nagumo, S. Arimoto, S. Yoshizawa, An active pulse transmission line simulating nerve axon, Proceedings of the IRE 50 (1962) 2061–2070.

[75] A. C. Newell, J. A. Whitehead, Stability of stationary periodic structures for weakly supercritical convection and related problems, J. Fluid Mech. 38 (1969) 279–303.

[76] D. Olmos and B. D. Shizgal, Pseudospectral method of solution of the FitzHugh-Nagumo equation, Math. & Comput. Simul. 79 (2009), pp. 2258–2278.

[77] A. Pérez, J. Villa, A note on blow-up of a nonlinear integral equation, Bull. Belg. Math. Soc.-Simon Stevin 17 (2010) 891–897.

[78] A. D. Polyanin, V. F. Zaitsev, Handbook of Nonlinear Partial Differential Equations, 1st ed., Chapman & Hall CRC Press, Boca Raton, Fla., 2004.

[79] H. Ramos and J. Vigo-Aguiar, *A new algorithm appropriate for solving singular and singularly perturbed autonomous initial-value problems*, Intern. J. Comput. Math. 85 (2008), pp. 603–611.

[80] K. Rejniak, R. Dillon, A single cell-based model of the ductal tumour microarchitecture, Comput. Math. Meth. Medic. 8 (2007) 51–59.

[81] J. Ruiz-Ramírez, J. E. Macías-Díaz, On the propagation of binary signals in a two-dimensional nonlinear lattice with nearest-neighbor interactions, J. Nonlinear Math. Phys. 17 (2010) 127–136.

[82] J. A. Saunders, D. C. Knill, Perception of 3D surface orientation from skew symmetry, Vision Res. 41 (2001) 3163–3183.

[83] L. A. Segel, Distant side-walls cause slow amplitude modulation of cellular convection, J. Fluid Mech. 38 (1969) 203–224.

[84] J. Sherratt, S. Gourley, N. Armstrong, K. Painter, Boundedness of solutions of a non-local reaction–diffusion model for adhesion in cell aggregation and cancer invasion, Euro. J. Appl. Math. 20 (2009) 123–144.

[85] J. Shi, S. Wang, Exact multiplicity of boundary blow-up solutions for a bistable problem, Comput. & Math. Appl. 54 (2007) 1285–1292.

[86] M. W. Smiley, An efficient implementation of a numerical method for a chemotaxis system, Intern. J. Comput. Math. 86 (2009) 219–235.

[87] L. Takhtajan, On foundation of the generalized Nambu mechanics, Commun. Math. Phys. 160 (1994) 295–315.

[88] S. Tomasiello, *Numerical solutions of the Burgers–Huxley equation by the IDQ method*, Intern. J. Comput. Math. 87 (2010), pp. 129–140.

[89] M. E. Vázquez-Cendón, L. Cea, Analysis of a new kolgan-type scheme motivated by the shallow water equations, Appl. Numer. Math. in press doi:10.1016/j.apnum.2011.06.002.

[90] R. Verstappen, A. E. P. Veldman, Symmetry-preserving discretization of turbulent flow, J. Comput. Phys. 187 (2003) 343–368.

[91] Y. Wang and S. Li, New schemes for the coupled nonlinear Schrödinger equation, Intern. J. Comput. Math. 87 (2010), pp. 775–787.

[92] X. Y. Wang, Z. S. Zhu, Y. K. Lu, Solitary wave solutions of the generalised Burgers-Huxley equation, J. Phys. A: Math. Gen. 23 (1990) 271.

[93] G. Wu, Uniformly constructing soliton solutions and periodic solutions to Burgers-Fisher equation, Comput. & Math. Appl. 58 (2009) 2355–2357.

[94] L. Zhang, Q. Chang, A conservative numerical scheme for a class of nonlinear Schrödinger equation with wave operator, Appl. Math. Comput. 145 (2003) 603–612.

[95] X. Zhou, Exp-function method for solving Huxley equation, Math. Probl. Eng 2008 (2008) 1–7.

-------- Original Message --------
Subject: Your Submission
Date: 03/09/2013 04:43
From: "Journal CAM" <esubmissionsupport@elsevier.com>
To: jemacias@correo.uaa.mx

Ms. Ref. No.: CAM-D-11-00083
Title: A skew symmetry-preserving computational technique for the positive and the bounded solutions of a time-delayed advection-diffusion-reaction equation
Journal of Computational and Applied Mathematics

Dear Authors,

I am pleased to confirm that your paper "A skew symmetry-preserving computational technique for the positive and the bounded solutions of a time-delayed advection-diffusion-reaction equation" has been accepted for publication in Journal of Computational and Applied Mathematics.

Comments from the Editor and Reviewers can be found below.

Thank you for submitting your work to this journal.

With kind regards,

Yalchin Efendiev
Principal Editor
Journal of Computational and Applied Mathematics

Comments from the Editors and Reviewers: